Step by Step Water Splitting: Heterogeneous Photocatalysis Studies

By

Salimah Alshehri

Thesis submitted to the
Faculty of Graduate and Postdoctoral Studies

University of Ottawa
For MSc degree in chemistry Faculty of Science

Ottawa-Carleton Chemistry Institute

I dedicate this thesis to the strongest person I know: me

Abstract

Due to the environmental problems caused by the steadily increasing usage of fossil fuels, the interest for renewable sources of energy has amplified significantly. Among several possibilities, hydrogen gas is considered to be one of the most promising fuels for the future. If formed from water via photocatalysis it is a desirable, convenient and green improvement in the field of energy. During this work, we have tried to contribute to this important field.

4*wt.*% Au/TiO_2 synthesized by deposition-precipitation with urea was the main photocatalysts used in this project. Other noble metal-loaded (Pt and Ag) titanium dioxide materials were synthesized by deposition precipitation with urea and other methods such as sol gel and sol immobilization. These catalytic systems were studied and their activity compared for hydrogen production from water/methanol mixtures. Sets of monometallic Au, Ag, Pt and bimetallic Au-Pt and Au-Ag supported titanium dioxide were synthesized and tested.

Au/TiO_2 photocatalysts synthesized by deposition precipitation with urea were the best in terms of hydrogen production compared to other photocatalysts. In the evaluation of possible sacrificial molecules, isopropanol was less efficient than methanol. Through the formation of bi-metallic Ag-Au/TiO_2 and Pt-Au/TiO_2 catalysts, the hydrogen production could be further improved.

Finally, Ir supported $\gamma - Al_2O_3$ was investigated for the first time as a heterogeneous catalyst for hydrogen production by photocatalytic dehydrogenation of aqueous *p*-formaldehyde and photoreduction of carbon dioxide.

Acknowledgments

First, completing a master's thesis in a foreign country while being a wife, a mother, is so difficult, it was a long trip full of obstacles and barriers. I want to thank my gad for a group of great people in my life helped make such a success possible. I am deeply grateful to them for making my dream of graduation a reality. For as long as I live, I will be thankful for having them in my life

I would also like to take this opportunity to thank the sponsor of my scholarship **King Abdullah**, who passed away during the time I was studying, for offering the scholarship program which granted me the opportunity to be here. Acknowledgment and thanks are expressed to **Saudi Cultural Bureau** in Canada for their support, assistance and encouragement.

Many thanks go to my supervisor, **Dr. Sandro Gambarotta**. I am very fortunate that he accepted to supervise my thesis. I would like to thank him for his continuous support, his valuables insights, his unlimited patience.

I would also like to thank all my lab mates who have helped guide my project, I am very grateful to **Dr. Nick Alderman Dr. Virginie Peneau, Camilo Viasus, Dr,Indira Thapa, Jacob Sommers, Laura Hull**. I appreciate their skill and knowledge in interaction with students in the lab, presentation seminar and their assistance with the preparation of this thesis.

Thank you to Dr. **Dr. Glenn A. Facey** for trining and helping me with NMR analysis**.** Also, many thanks go to **Dr. Yun Liu** for your training and help with my TEM and EDS needs.

I would also like to express my deepest gratitude to my awesome parents, **Safia & Ali**; without them in my life I wouldn't be who I am. Their love, care, encouragement, and support have always reached me, wherever I was. "Thank you" will not be enough, even if I said it to them every second of the rest of my life.

Moreover, I dedicate this thesis to my soul mate and the love of my life, my husband, **Maeed** Thank you for holding my hand from the beginning of my study abroad until I reached this stage of prosperity. Thank you for your love, support, motivation, understanding and cooperation. I really appreciate your endless efforts to share responsibility with me to help me reach my goals.

I also dedicate this thesis to the best things that ever happened to me, my lovely kids, **Hamed & Hind.** You are my precious inspiration. When I see your smile, when I hold you, when I hug you, I feel that I have the whole world in my hands. Without you in my life I would not think about the future and I would not be encouraged to make it brighter by completing such work.

I would like to express my genuine thanks to all my siblings (**Sharifa, Hasan, Layla, Huda, Hind, and cutest little brother Hassan)**. Even though you are far away, your encouragements reach my heart. I am so grateful to have you in my life, and I hope to be a part of your accomplishments as well.

I would like to thank my friends in Canada who have eased the difficulty of being far away from home by providing me with love, laughter, cheer, and help, in sickness and in health. Throughout this long journey, you have been like sisters to me, especially, **Muneerah** and **Hessa**.

Table of Contents

List of Tables

List of Figures

List of Abbreviations

Acac	Acetylacetone
CB	Conduction band
DPU	Deposition precipitation with urea
EDS	Energy dispersive spectroscopy
Eg	Energy/Band gap
ΔH	Enthalpy (KJ/mol)
H•	Hydrogen radical
OH•	Hydroxyl radical
h+	Hole
GC	Gas chromatography
p-FA	Paraformaldehyde
SEM	Scanning electron microscopy
STH	Solar-to-hydrogen
TCD	Thermal conductivity detector
TEM	Transmission electron microscopy
TOF	Turnover frequency

TON	Turnover number
VB	Valence band
WOC	Water oxidation catalyst
wt%	Weight percent (% m/m)
λ	Wave length

Chapter 1

Introduction

1. General Introduction

Global demand and consumption of energy has been increasing significantly in recent years due to rapid economic growth in both industrialized and developing countries. The world's largest source of energy currently is the combustion of carbon-based fossil fuels such as petroleum, natural gas and coal. Together, these fuels account for more than 80 % of the global energy production, according to an estimate of 2008.[1, 2] However, this type of energy production affords many harmful components, such as sulphur oxides, nitrogen oxides, heavy metals, and, of course, carbon dioxide, which is by far the major component of greenhouse gases. Recently, and due to pressing environmental issues, research activity increasingly focused on producing inexpensive and clean energy from renewable sources alternative to fossil fuels. These studies targeted water, wind, the sun, and biomass as potential sources of alternative and clean energy.[2,3] Although these energy sources have been known in the past, their use has remained limited due to several formidable challenges.

1.1 Hydrogen as future fuel

Hydrogen is an important fuel with great potential for future applications because it is the simplest and most abundant element in the universe. It has a high-energy content and the highest energy-to-mass ratio of any chemical. Yet, it is an encouraging option for replacing fossil fuels.[4]

Table 1.1. summarizes the most relevant physical and chemical properties of hydrogen compared to some of the fossil fuels currently in use. The energy of each fuel can be represented by the value of heat produced from the complete combustion.[5] In addition to providing the most of energy, hydrogen combustion generates only water as a product.

While elemental hydrogen does occur naturally in small amounts, it is largely available combined with other elements. Water, of course, would be the perfect source of hydrogen as long as an inexpensive way for its extraction in an industrial scale could be found.

Fuel	**Density (g/l)**	**Lower heating Value(MJ/Kg)**	**Carbon Percentage %**
Crude Oil	845	42.8	85.0
Natural Gas	0.654	50.1	75.0
Conventional Gasoline	737	43.7	85.5
Conventional Diesel	856	41.8	87.0
Hydrogen	0.0818	121.0	0

Table 1.1. The energy content of different fuels.

1.2 Hydrogen production methods

Being an explosive gas, it is unlikely that hydrogen can be directly used for transportation purposes or as a household energy supply. However, it can be safely used in power and industrial plants requiring large amount of energy (e.g. steel factories, power plants, etc.) where all the necessary safety devices may be readily in place. Therefore, the development of the production and storage of hydrogen rapidly becomes of strategic importance in the economy of the industrialized world. Today hydrogen is already being produced in large amounts for industrial

and commercial purposes.[6] Preparation of ammonia through the Haber process is one of the main uses, but there are several large scale catalytic hydrogenation reactions which also rely on the availability of this gas. Of course, the current usage would be just a small fraction of the amount needed for hypothetical energy production on global scale.[6]

Currently, hydrogen can be extracted from various sources using catalytic methods. The most common and commercially convenient methods are the steam reforming of natural gas, partial oxidation of hydrocarbons, and coal gasification.[7] Although well refined, these processes all produce CO_2 as a byproduct.

1.2.1 Steam Reforming of Natural Gas

Steam reforming of natural gas is a process in which methane reacts with steam to generate mixture of carbon dioxide and hydrogen according to the overall equation.[7]

$$CH_4 + 2H_2O \leftrightarrow CO_2 + 4H_2 \qquad \Delta H = 165 kJ/mol$$

Alternatively:

$$CH_4 + H_2O \leftrightarrow CO + 3H_2 \qquad \Delta H = 206.2 kJ/mol$$

followed by water-gas shift reaction:

$$CO + H_2O \rightarrow CO_2 + H_2 \qquad \Delta H = -41.2 kJ/mol$$

is a possible alternative.

The reactions are carried out at pressures above 20 bar, and temperatures in the range of 760-815 $^{\circ}C$ in the presence of a catalyst.

1.2.2 Partial Oxidation of Hydrocarbons

Partial oxidation method is a H_2 extraction technique where hydrocarbons are converted into a blend of H_2, CO, CO_2 via reaction with steam and oxygen. This process occurs at high pressure, with or without catalysts depending on the feedstock selected. This method can be applied to any hydrocarbon[7].

$$C_nH_m + n/2\ O_2 \rightarrow nCO + m/2\ H_2 + heat$$

$$C_nH_m + nH_2O + heat \rightarrow nCO + (n+m/2)\ H_2$$

$$CO + H_2O \rightarrow CO_2 + H_2$$

1.2.3 Coal Gasification

The gasification of coal is one possibility of extracting hydrogen from water. The reaction of coal with oxygen and steam under high pressures and temperatures affords syn-gas, a mixture of carbon mono- and dioxide and hydrogen.

$$CH + O_2 + H_2O \rightarrow CO + CO_2 + H_2 + \text{other species}$$

are appropriate for a hydrogen-based and environmentally clean economy, due to the employment of carbon, ultimately ending as carbon dioxide.[7,8]

1.3 Hydrogen as a clean fuel

As a part of a global research endeavor for decreasing dependence on fossil fuels, scientific research has focused on the generation of hydrogen from renewable resources such as biomass and water through carbon-free processes. Table1.2. summarizes the advantages and disadvantages of hydrogen production and storage.

Table 1.2. The Benefits and drawbacks of hydrogen production.

Benefits	**Drawbacks**
• Environmentally friendly • Available and renewable • High energy content • Low maintenance	• Low hydrogen production efficiencies • Costly to generate • Difficult to store • Explosive.

The only genuine possibility of obtaining hydrogen in large scales without releasing undesirable byproducts, is of course using water as starting material in a process which is called: "reverse hydrogen combustion".

$$H_2O \rightarrow H_2 + 1/2\ O_2$$

$$\Delta H^\circ = 241.93 \text{ kJ/mol}$$

$$\Delta G^\circ = 228.71 \text{ kJ/mol}$$

Extraction of hydrogen from water, also commonly named as "water splitting", is thermodynamically uphill and requires a large energy input. This could be achieved with several techniques. Thermal and solar conditions are the most straightforward but are not particularly attractive given the extreme temperatures to be used, in turn posing severe engineering problems. Electrochemical conditions are not attractive either due to slow production rates and the requirement for cumbersome apparatus. Therefore, the best alternative is to input energy under the form of light.

The field of heterogeneous photocatalysis has become an attractive technology during the past four decades due to its applications which include water and air purification, and chemical synthesis.[10,11]

Recently, interest in heterogeneous photocatalysis has focused on the use of semiconducting materials. This technology has been researched widely for hydrogen production because it is inexpensive, environmentally friendly and potentially efficient. The next chapter will elaborate in more detail the usage and review the concerning literature.

In the enormous family of available photocatalysts based on semiconducting materials, titanium dioxide is particularly popular due to its versatility, stability and promising light-harvesting characteristics.[12,13]

In terms of photocatalytic hydrogen production, many studies have been carried out to synthesize effective photo-catalysts which are inexpensive and environmentally friendly.[14,15] One of the techniques to improve the performances of these systems is the employment of sacrificial

reagents such as alcohols and hydrocarbons, typically to facilitate the parallel oxidation process.[16] In fact, the release of oxygen during water splitting is always the most difficult and challenging part of the process and often results in catalyst decomposition. However, should sacrificial reagents be used, important requirements for them are being inexpensive, easy to find and renewable.

1.4 Thesis Objective

A large amount of research has addressed the enhancement of photocatalyst activity for visible light H_2 production.[18,19,20] This thesis focuses on the activity of Au/TiO_2 photocatalysts for the formation of hydrogen from water in the presence of sacrificial reagents (methanol, isopropanol).

The aims of this research are highlighted into two sections:

- A variety of gold loaded TiO_2 photocatalysts (1,2,4 wt.% Au) were prepared and their activity for dehydrogenation of water/alcohols mixture studied. In addition, photocatalysts contain bimetallic systems supported by TiO_2 were synthesised by different methods to study the effect of preparation methods on the hydrogen productivity. Also, parameters such as methanol volume, catalyst loading, different gold loads on titanium dioxide, and different pH for the reaction were evaluated.
- The productivity of hydrogen in the presence of isopropanol as a sacrificial reagent compared to methanol on several mono and bimetallic supported TiO_2 was also evaluated.

Finally, the dehydrogenation of *p*-formaldehyde and photoreduction of carbon dioxide with Ir/$\gamma - Al_2O_3$ were studied.

1.5 Thesis Outline

The first paragraph of each chapter includes a detailed summary.

Chapter 1 is a general introduction.

Chapter 2 is a literature review.

Chapter 3 overviews the preparation methods, characterization techniques and photocatalytic reactors used during this study.

Chapter 4 reports the results of our study of the dehydrogenation of methanol and isopropanol on Au/TiO_2 P25 and the factors that affect the activity of hydrogen formation. Amount of hydrogen and by-products are described.

Chapter 5 is a study on the dehydrogenation of *p*-formaldehyde and photoreduction of carbon dioxide on Ir/ $\gamma - Al_2O_3$, and studies the factors that affect the activity of reaction.

Chapter 6 overviews the conclusions of this thesis work. Some recommendations are provided for future work.

1.6 References

(1) Moriarty, P.; Honnery, D. *Renewable and Sustainable Energy Reviews***2012**, *16*, 244–252.

(2) Asif, M.; Muneer, T. *Renewable and Sustainable Energy Reviews***2007**, *11*, 1388–1413.

(3) Vezirolu, T.; Barbir, F. *International Journal of Hydrogen Energy***1992**, *17*, 391–404.

(4) Wietschel, M.; Ball, M. *The Hydrogen Economy* **2009**, 613–639.

(**5**) Hussain, M. M.; Dincer, I. *Electric and Hybrid Vehicles* **2010,** 275–286**.**

(6) Kikuchi, R. *Environmental Impact Assessment Review***2006**, *26*(2), 206–218.

(7) Twigg, M. V. *Catalyst handbook*; Manson, **2008**.

(8) Ogden, J. M. *Annual Review of Energy and the Environment* **1999**, *24*(1), 227–279.

(9) Sakintuna, B.; Lamaridarkrim, F.; Hirscher, M. *International Journal of Hydrogen Energy* **2007,** *32*(9), 1121–1140**.**

(10) Mills, A.; Hunte, S. L. *Journal of Photochemistry and Photobiology A: Chemistry***1997**, *108*(1), 1–35.

(11) Davis, A. P.; Huang, C. *Water Research* **1990,** *24*(5), 543–550.

(12) Sasahara, A.; Tomitori, M. *The Journal of Physical Chemistry C* **2016**, *120*(38), 21427–21435.

(13) Yang, H.; Guo, L.; Yan, W.; Liu, H. *Journal of Power Sources* **2006,** *159*(2), 1305–1309.

(14) Hernández-Alonso, M. C. A. D. D.; Fresno, F.; Suárez, S.; Coronado, J. M. *Energy & Environmental Science* **2009,** *2*(12), 1231.

(15) Mills, A.; Lee, S.-K. *Journal of Photochemistry and Photobiology A: Chemistry* **2002,** *152*(1-3), 233–247.

(16) Maeda, K.; Domen, K. *Chemistry of Materials* **2010,** *22*(3), 612–623.

(17) Rossetti, I. *ISRN Chemical Engineering* **2012,** *2012*, 1–21

(18) Zhao, W.; Ai, Z.; Dai, J.; Zhang, M. *PLoS ONE* **2014**, *9*(8).

(19) Priebe, J. B.; Radnik, J.; Lennox, A. J. J.; Pohl, M.-M.; Karnahl, M.; Hollmann, D.; Grabow, K.; Bentrup, U.; Junge, H.; Beller, M.; Brückner, A. *ACS Catalysis* **2015**, *5*(4), 2137–2148.

(20) Yang, X.; Wu, L.; Du, L.; Li, X. *Catalysis Letters* **2015**, *145*(9), 1771–1777

Chapter 2

Literature Review

2. Introduction

Fossil fuels supply about 88 percent of the world's energy. Although this natural resource has allowed the tremendous progress of our civilization, it has also led to the release of large amounts of greenhouse gases, such as carbon dioxide (CO_2) and methane (CH_4), with devastating impact on our environment. In addition, the consumption of fossil fuels is rapidly escalating a global energy crisis since the depletion of this natural resource is foreseeable in a not distant future. Large cost increases are therefore to be expected.[1] Thus, the need for alternative fuels, including the development of renewable sources such as wind and solar is particularly pressing.[2]

Recently, hydrogen has become the focus of interest in the search for a suitable and clean energy fuel. It is therefore ironic that approximately 95% of the current hydrogen supply is still obtained from fossil origins, with only 5% from renewable sources. The production of hydrogen via photocatalytic decomposition of water could be the solution. The utilization of TiO_2 as a photocatalyst is a promising technology because of low-cost and clean hydrogen formation. This chapter describes the basic applications of photocatalysis for hydrogen production.[2,3]

2.1 Photocatalysis

The term "photocatalysis" originates from two Greek words: the prefix "photo" meaning light, and the word "catalysis" meaning decompose.[4] In a proper scientific definition, it is referred to a process in which light (ultraviolet, visible or infrared) activates a substance or semiconductor. A photocatalyst is defined as a material which, upon irradiation, accelerates a reaction without being itself involved in the stoichiometry of the chemical transformation.

Today, photocatalysis has become one of the most important technologies in the industrialized world. This spans from genuine photochemical reactions to photocatalytic activation, which can be carried out either homogeneously or heterogeneously. Although, both homogeneous and heterogeneous photocatalysis are technologies of widespread potential, heterogeneous photocatalysis has become a more extensively researched area during the past decade. This is mainly because of its potential application in water-air purification, energy production and organic synthesis including carbon-carbon or carbon-heteroatom formation.[5,72]

2.2 Heterogeneous Photocatalysis

In the most general term, the role of a semiconductor heterogeneous photocatalyst is to accelerate a photoreaction in the presence of solid materials. However, it can also be used to harvest radiant energy and transfer it to the reagents. A third possibility is for the photocatalyst to generate reactive species upon irradiation and permitting, for example, photochemical oxidation and reduction reactions on the surface of the semiconductor photocatalyst.[5,6] Today, the most pressing applications of heterogeneous photocatalysis are for water splitting and air/water

purification.[6]

The significance of photocatalysis became apparent in 1972 with Fujishima and Honda seminal work on the decomposition of water into hydrogen and oxygen (water splitting or hydrogen reverse combustion) while irradiating TiO_2 with UV light.[6] Today, photocatalytic hydrogen production from water splitting is being widely targeted by researchers around the world. Photocatalytic water splitting processes involve the use of light, semiconductor catalysts and, possibly, an organic sacrificial reagent.[6,7]

2.2.1 Photocatalysts (Photocatalytic Semiconductors)

Photocatalysts are solid semi-conducting materials which accelerate chemical reactions without being consumed. As a result of the absorption of photons, electron from the valence band are promoted to the conduction band. The HOMO-LUMO separation, or band-gap in this case, is the factor determining the potential made available to the particular redox transformation promoted by the photocatalyst. It also determines the frequency of the photon being absorbed (see Figure 2.1.).[9] Photocatalytic activity of the semiconductors is affected by many factors including: structure, particle size, surface properties, presence of additives and preparation techniques.[8]

Metal oxide semiconductors, as shown in Table 2.1., commonly display photocatalytic properties and are particularly desirable because of their photo-corrosion resistance, wide band gap energy, and stability.[9]

Semiconductor	Band Gap Energy	Wavelength(nm)
TiO_2 (rutile)	3.0	413
TiO_2 (anatase)	3.2	388
ZnO	3.2	388
ZnS	3.6	335
CdS	2.4	516
Fe_2O_3	2.3	539
WO_3	2.8	443
$SrTiO_3$	3.4	365

Table 2.1. Band Gap Energies and Corresponding Radiation Wavelength Required for the Semiconductors.[9]

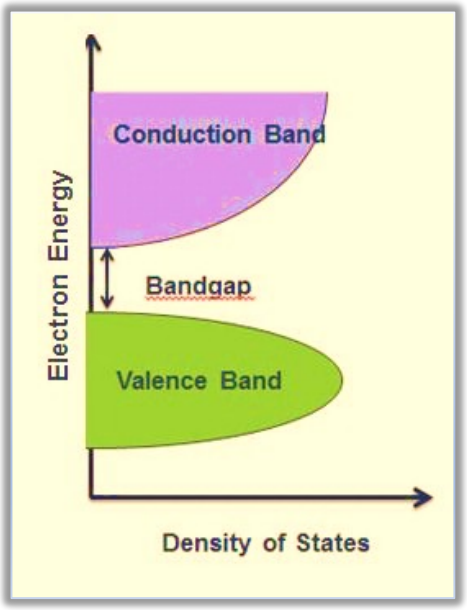

Figure 2.1. Energy band scheme for a solid semiconductor.

2.2.1.1 Titanium Dioxide (TiO_2)

Among the many existing photosemiconductors, titanium dioxide is a material of prominent practical importance. Industrially, it is produced from limonite ($FeTiO_3$), which is a common mineral found in large deposits in several parts of the globe. Its main application remains as a white pigment, used in a wide range of products such as paper, rubber, plastics and cosmetics. Photo-stability, low cost, non-toxicity and ability to enhance the oxidation of organic compounds, altogether, make TiO_2 a versatile and intensively studied photocatalyst.[10,11]

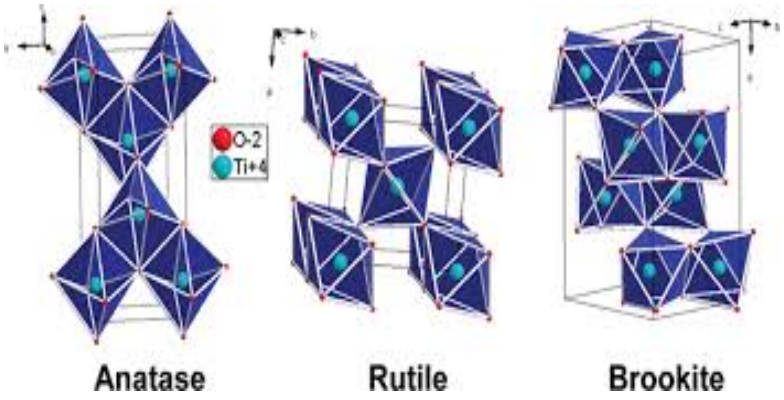

Figure 2.2. The structures of (a) anatase, (b) rutile and (c) brookite TiO_2.

Titanium dioxide is found in three different crystallographic structures: anatase, rutile and brookite, depicted in Figure 2.2. The brookite structure is less important for photocatalysis because of the difficulty obtaining it in the pure form. Anatase is the most common structure used in photocatalytic applications under UV light. Rutile is instead the most stable structure, since the other two forms convert into it when heated or processed at temperatures higher than 600°C. Photo-

activation under solar irradiation conditions is limited since only 4-5% of the sunlight that reaches the earth's surface is in the near-UV light range, where the band gap of this material is located.[12] The most common physical properties of these types of TiO_2 structures are summarized in Table 2.2 .[13]

Structures Name	Crystalline Form	Density g/cm^3	Refractive Index	Melting Point	Boiling Point
Rutile	Tetragonal System	4.27	2.72	1825	-
Anatase	Tetragonal System	3.90	2.52	Transformation to Rutile	2927
Brookite	Orthogonal System	4.13	2.63	Transformation to Rutile	

Table 2.2. The properties of three structures of titanium dioxide.[13]

During photocatalytic oxidation reactions of titanium dioxide, electrons from the valence band of TiO_2 are pushed into the conduction band by UV light. In doing so, a displacement of charge is created with an accumulation of negative charge in the conductive band and the creation of positive charge in the valence band. This is commonly described as the formation of e^-_{CB}/h^+_{VB} pairs. These pairs may migrate within the compound. When they reach the surface of the nanocrystal, redox reactions may be triggered according to the redox potential as determined by the band gap and as required by the target molecule Figure 2.3.[15]

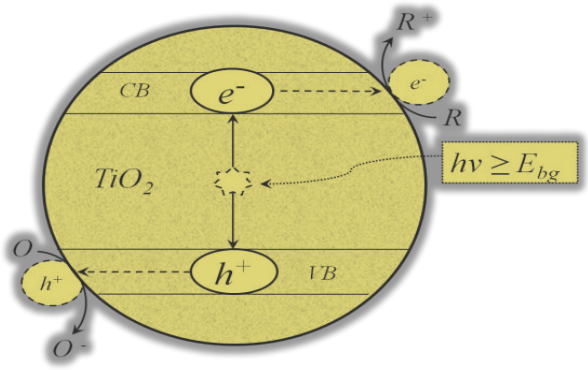

Figure 2.3. Schematic of titanium dioxide particle (TiO_2) photocatalytic activation reaction process.

2.2.2 Photocatalytic Hydrogen Generation Method

There are many different semiconducting materials available, but only a handful are suitable for use in photocatalytic water splitting. Due to its stability and availability, TiO_2 appears to be the most suitable.[8,16,17] With a potential for the VB holes of +1.23, TiO_2 may generate oxygen or hydroxyl radicals ($^{\bullet}OH$) from water. The potential of the CB electron of − 0.52 V, is also sufficiently negative to reduce protons and evolve hydrogen from water. As mentioned before, a good semiconductor photocatalyst should be able to catalyze reactions, be activated by sunlight, be photo-stable, easy to produce and be cost effective.[9,10] TiO_2 is near to being an ideal photocatalyst, comprising almost all the above properties. The only drawback is that, like other wide-band gap semiconductors, it does not absorb visible light, making it inefficient in sunlight. There are many methods to increase the effectiveness of TiO_2 in absorbing the light in the visible region, such as doping with metal or non-metal elements, and loading different ratios of metal onto the surface of titanium dioxide, such as noble metals like Au, Pt, Ag.[19,20,21,22]

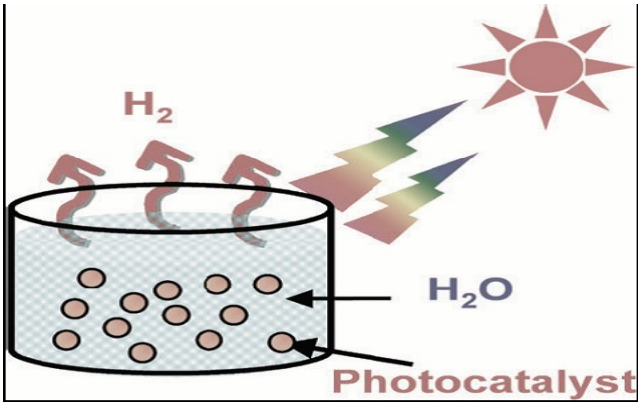

Figure 2.4. Photocatalytic water splitting by a powder photocatalyst.[8]

2.2.2.1 Metal-containing Titanium Dioxide

As mentioned above, the photocatalytic effectiveness of titanium dioxide has been enhanced by the loading of different precursors (metals), including Pt, Au, Pd, Rh, Ni, Cu, and Ag on the surface via different deposition methods, such as doping, precipitation, and impregnation. [19,23,24] These synthetic methods are discussed in more detail in section 2.6.

The extent of metal loading and the deposition methods have different effects on the rate of photocatalytic hydrogen formation. The improved photocatalytic activity is due to a more efficient transfer of the electrons from the photocatalyst to the acceptor.[25] With this regard, many studies have established that when the metals are deposited onto the surface of semiconductors, the Fermi level shifts to negative energy potentials. This shift helps to enhance the interfacial charge transfer, and this point will be discussed in more detail in section 2.5.1. In essence, the Fermi Levels of noble metals are lower than the corresponding levels of TiO_2. Therefore, the photo-excited electrons transfer from the conduction band (CB) of titanium dioxide to the noble metal present

on the TiO_2 surface, leaving photo generated holes on the valence band (VB) unchanged Figure 2.5.[25,26] The possibility of adjusting the actual band gap through the deposition of the appropriate metal is one of the reasons for the versatility of metal-doped titanium dioxide, making these materials popular for a wide range of applications spanning from photocatalytic hydrogen production to organic pollutants decomposition.[27]

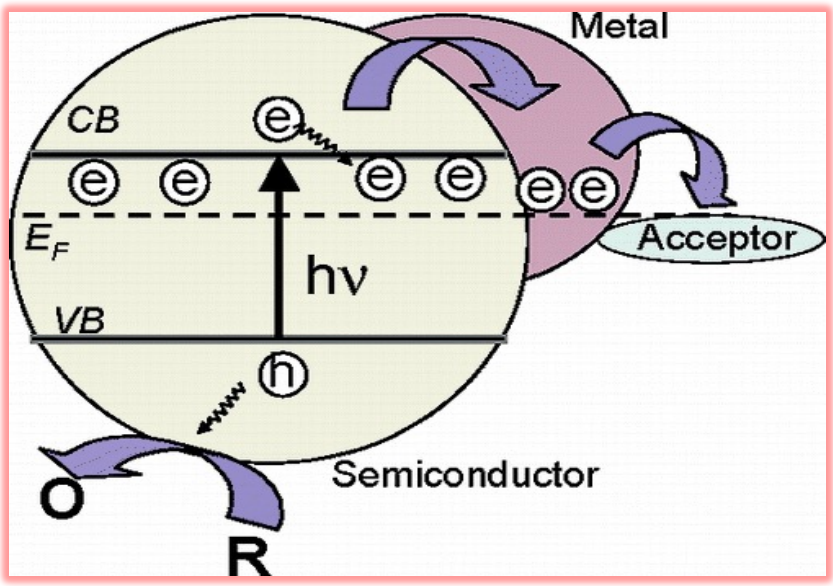

Figure 2.5. Photocatalytic activation TiO_2 by noble metal.[26]

2.2.2.2 Addition of Sacrificial Reagents

In the overall water splitting reaction, the most challenging stage is not the reduction of protons to hydrogen gas but the oxidation of water to oxygen. Oxygen is a very reactive species and, therefore, it might easily trigger unwanted transformations, including irreversible catalyst decomposition. Moreover, the rapid recombination of CB electrons and VB holes, makes the efficiency of water splitting quite poor while using TiO_2 photocatalysts in pure water. One way

around this problem consists of the use of sacrificial agents as easier targets for the oxidative semi-reaction. In fact, sacrificial reagents are commonly encountered in many photocatalytic reaction systems for hydrogen evolution. Alcohols such as methanol, ethanol, and isopropanol have been reported to greatly enhance the photocatalytic activity. [28,29,30,31] These sacrificial reagents occupy the holes and undergo a photoexcitation reaction, thereby acting as good hole scavenger and slowing or even preventing the electron–hole recombination. By contrast, they facilitate the promotion of the excited electron into the conduction band to participate to the reduction of hydrogen ions.[31,32] Different alcohols such as methanol and ethanol have been tested and found to be effective sacrificial reagents in improving hydrogen production.[24,29,30,34] Many studies have demonstrated methanol as the best sacrificial reagent, and it has been the sacrificial agent of preference for this work. Other alcohols such as isopropanol have been probed nonetheless.

The equation below shows the dehydrogenation of methanol in the presence of water. Out of three moles of hydrogen produced, only one is derived from water while, regrettably, CO_2 is also formed. Table 2.3. reports the byproducts encountered when various alcohols are used as the sacrificial agent.[28]

$$CH_3OH + H_2O \rightarrow 3H_2 + CO_2$$

Table 2.3. The gases produced from different alcohols**.**

Alcohol	**Gases Products**	**Alcohol**	**Gases Products**
Methanol	H_2, CO_2	1,2-Propanediol	H_2, CO_2, CH_4
Ethanol	H_2, CO_2, CH_4	1,3-Propanediol	H_2, CO_2
1-Propanol	H_2, CO_2, C_2H_6	1,3-Butanediol	H_2, CO_2
2-Propanol	H_2, CO_2, CH_4	2,3-Butanediol	H_2, CO_2, CH_4
1-Butanol	H_2, CO_2, C_3H_8	1,2,4-Butanetriol	H_2, CO_2
2-Butanol	H_2, CO_2, C_2H_6, CH_4		

Since 2010 several scientific works appeared in the literature describing the successful low-temperature hydrogen production from methanol in aqueous solutions.[71] Earlier reports described catalytic systems producing hydrogen below 100 ℃ by using heterogeneous catalysts in the presence of photo-activators.[72] Table 2.4. gives some examples**.**

Table 2.4. Hydrogen generation via heterogeneous photocatalysts in water using methanol as a sacrificial agent.

Catalyst	**Light source**	**TOF (h^{-1})**	**Temperature**	**Reference**
0.1 % Au/TiO_2 (Anatase)	Hg	1.34	RT	73
0.1 % Au/TiO_2 (Rutile)	Hg	1.05	RT	73
1% Pt/TiO_2	150 W UV	1.01	RT	74
Ag_2O Pt/TiO_2	Sunlight	5.35	RT	75

Bi_2S_3/TiO_2	UV(365 nm)	0.136	RT	76
Nano $Pt/TBACa_2Nb_3O_{10}$	300 W Xe	24.6	30	77
Bulk $Pt/TBACa_2Nb_3O_{10}$	300 W Xe	1.81	30	77
0.5 % $Pt/NaTaO_3$	150 W Hg	0.038	25	78
0.5 % $Pt/CeNaTaO_3$	150 W Hg	0.012	25	78
0.5 % $Pt/YbNaTaO_3$	150 W Hg	0.140	25	78
0.5 % $Pt/LaNaTaO_3$	150 W Hg	0.106	25	78

As mentioned previously, the dehydrogenation of methanol by using different metal-doped titanium dioxide is now established. Examples of metals used include gold, platinum, and silver. The role of the dopant is to reduce the band gap of the catalysts and prevent charge recombination. Ohtani investigated the deposition of gold on titanium dioxide photocatalysts.[73] While irradiating a catalyst with a 0.1 wt.% doping of Au on anatase TiO_2 and using a Hg lamp, previous research has obtained an optimal rate of hydrogen from the dehydrogenation of methanol of 570 μmol h^{-1} g^{-1} [37].

Meanwhile, Puzenat *et al*. studied the activity of Pt/TiO_2 for hydrogen production by coupling methanol dehydrogenation and a proton exchange membrane PEM fuel cell .[74] They performed the reactions with a 15 W UVA lamp for both photo-deposition of Pt onto the surface of TiO_2 and hydrogen evolution. Although the TOF was low for the catalytic cycle ($1.01h^{-1}$), the activity of the fuel cell continued with no poisoning effect for over 100 h under continuous removal of O_2 by N_2 carrier gas.

Compounds with semiconducting properties can also be combined with TiO_2 obtaining result similar to those achieved with the deposition of metals. Again, the role of these materials is to tune the band gap and prevent charge recombination via electron or hole injection into TiO_2 by the second semiconductor. In 2010, Subrahmanyam *et al*. investigated the deposition of Ag_2O onto anatase TiO_2 for catalytic activity in water and methanol solutions under sunlight irradiation.[75] The result was a respectable TOF of 5.35 h^{-1}, with no sign of catalyst failure within 24 hours. These authors also reduced Ag on TiO_2 via the deposition method but with limited success.

In 2012, Kang and Kim tested the activity of Bi_2S_3-deposited TiO_2 for dehydrogenation of methanol under irradiation with UV light (365 nm), but the activity was also modest (TOF = 0.136 h^{-1}).[76]

In 2012, Osterloh *et al*. compared the photocatalytic activity for water reduction and oxidation performance of nanoparticles (~1 nm thick) of Pt loaded on $TBACa_2Nb_3O_{10}$ micro particles (~250 nm thick), a layered niobate shown in figure 2.5.[77] In this system, the niobates are modified with photodeposited Pt and IrOx nanoparticles to work as active sites for H_2 and O_2 production, respectively. The activity of nanostructure was TOF = 24.6 h^{-1}, while, the bulk structure activity was TOF = 1.82 h^{-1}.

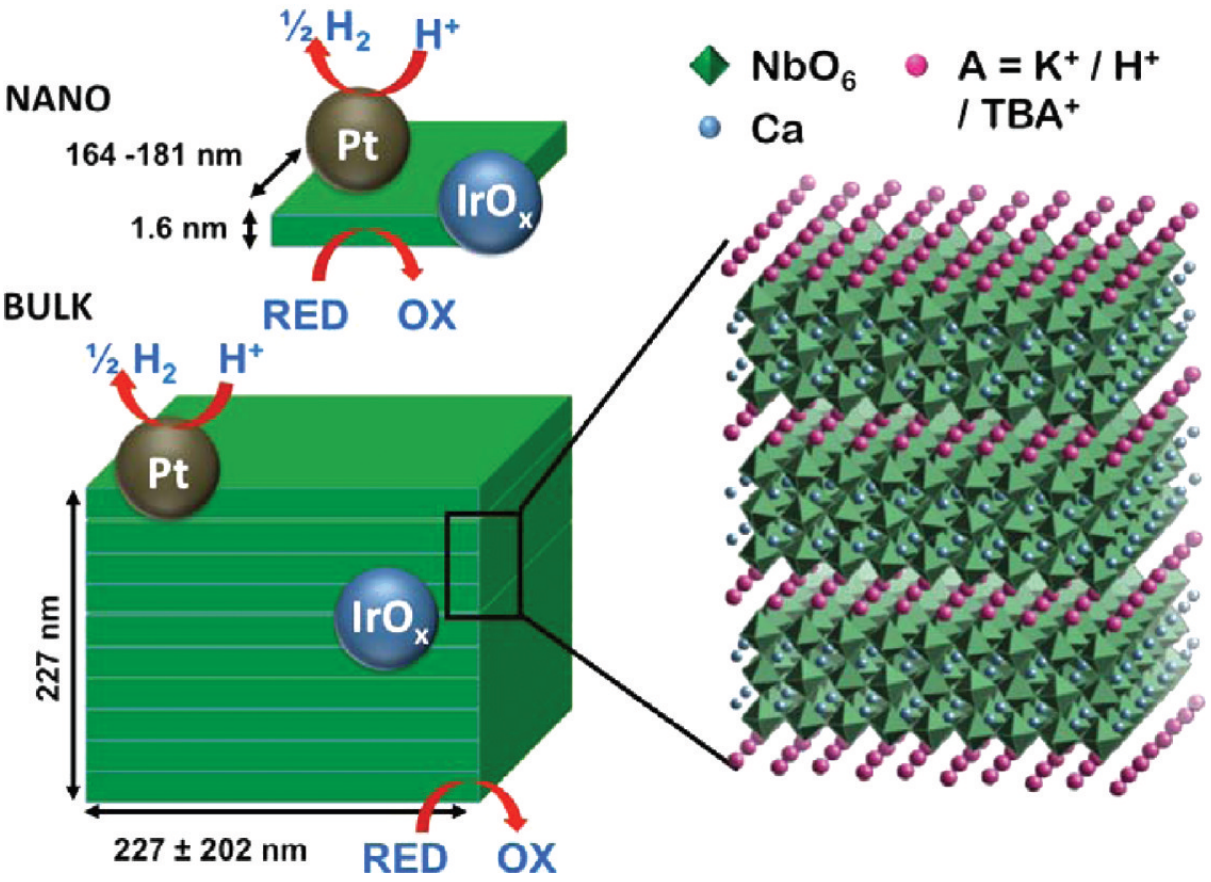

Figure 2.6. Hydrogen production by bulk and nano-scale niobate catalysts.[77]

More recently, de la Pena *et al,* studied the activity of $MNaTaO_3$ (M = Ce, Yb, La) catalysts, which were synthesized by a solid-state method, followed by photo-deposition of 0.5% Pt.[77] The results showed that the Yb-containing material was the most active (TOF = 0.140 h^{-1}). The increased activity was ascribed to the fact that it has a higher absorbance than La and the undoped metal. On the other hand, Ce doped $NaTiO_3$ catalysts possesses the greatest absorbance in the visible region but the structure of the catalyst is converted from orthorhombic to monoclinic, thus dropping its activity.

There are several structural aspects that should be considered to determine the alcohols that are dehydrogenated. Namely they are 1) the hydrogen atom must be in the alpha position and 2) alkyl

groups attached to alcohols must produce the corresponding alkanes. Methylene groups between alcohols must be oxidized to carbon dioxide.[28,36]

Formaldehyde has also successfully been used as a sacrificial agent. Solid *p*-formaldehyde contains 6.7 wt. % of hydrogen while in the hydrated form (methanediol) the hydrogen content rises to 8.4 wt.% [79]. The result of dehydrogenation of a *p*-formaldehyde solution in water is 2 moles of H_2 and 1 mole of CO_2, while dehydrogenation of anhydrous formaldehyde generates only one mole of H_2 and 1 mole CO. For the use in fuel cells, this reaction should be avoided because of the poisoning effect of carbon monoxide.[79]

The first study showing formation of hydrogen from formaldehyde with alkaline solutions appeared in 1887.[80] More recently, the reaction was explained as being produced by an intermediate of the Cannizzaro reaction interacting with water to generate formate and release hydrogen while in the presence of high concentration of sodium hydroxide and low concentrations of formaldehyde. Figure 2.7. illustrates the generated Cannizzaro intermediate.[81,82]

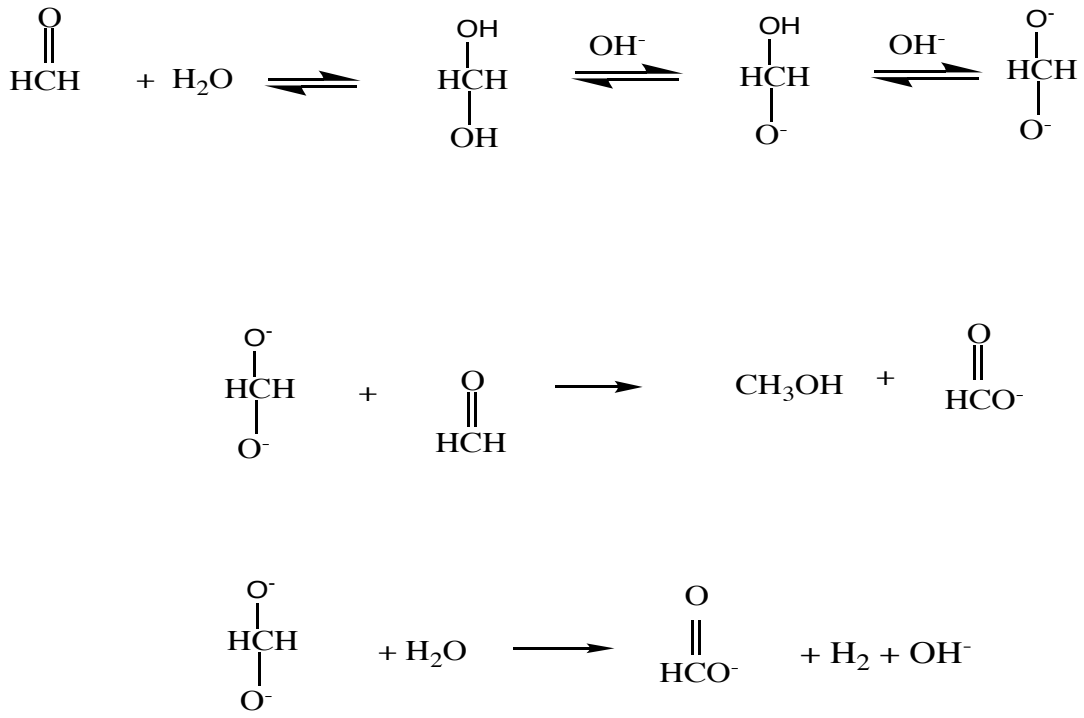

Figure 2.7. Schematic representation of the Cannizzaro mechanism.

Ray *et al*, have studied the activity of 0.25% Pt/TiO_2 photocatalysts for hydrogen production using formaldehyde as a sacrificial reagent in acidic, neutral and basic conditions.[85] The group found that under acidic conditions, dehydrogenation of formaldehyde was lower compared to neutral and basic conditions. This study was the first example of photocatalytic dehydrogenation of formaldehyde under acidic conditions.

In 2015, the Jia group studied the activity of Cu doped $LaCoO_3$ photocatalysts for dehydrogenation of formaldehyde solutions.[88] They found that Cu doped perovskites have a large amount of oxygen vacancies that help prevent electron-hole recombination. The activity of this catalyst is enhanced by biomass residues on the surface of the photocatalysts. Moreover, reducing

the band- edge plays an important role for increasing the activity of catalysts. Figure 2.8. shows possible formation of M-LaCo0.7Cu0.$_3$O$_3$.[88]

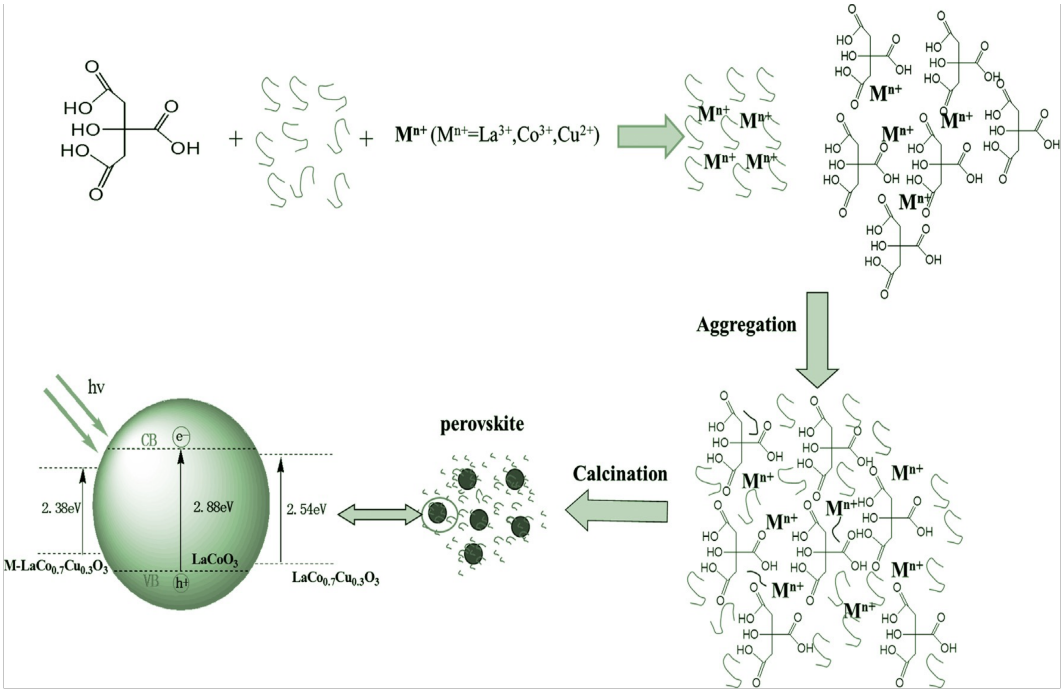

Figure 2.8. Schematic pathway of formation M-LaCo0.7Cu0.$_3$O$_3$.

2.3 Challenges and Requirements for Water Splitting

In general, sunlight is the simplest and more economical energy source, and because of its wide spectrum, could be very desirable for commercial applications. Photocatalytic water splitting using sunlight is a challenging task with several problems to be overcome. It should be reminded that transforming water into elemental oxygen and hydrogen requires a large input of energy (495 kJ/mole).[37] Given his thermodynamic scenario, water splitting can be only achieved at temperatures in the range of 1800 K with a change of free energy turning into zero. At this very high temperatures, the reaction mixtures are in fact under plasma-type of conditions rendering product separation almost impossible.[38]

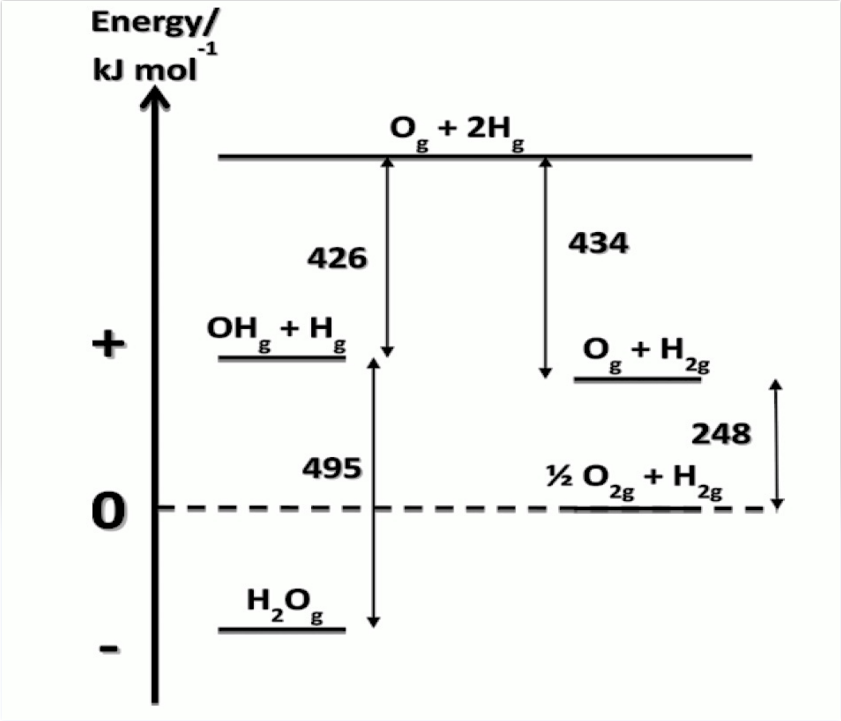

Figure 2.9. Born-Haber cycle for water dissociation to hydrogen and oxygen.

Therefore, irradiation remains the only viable possibility for achieving water splitting. A comparison of the irradiation spectra for different types of lamps is illustrated in Figure 2.10. One should notice that the mercury lamp, 400 W Hg arc lamp and the ballasted mercury lamp have strong Hg emission lines. The most attractive characteristic of the Hg radiation is the presence of intense emission lines at wavelengths that can be of interest for different applications such as photocatalytic processes. Although of convenient usage, none of the artificial light sources has the same spectral distribution as sunlight.

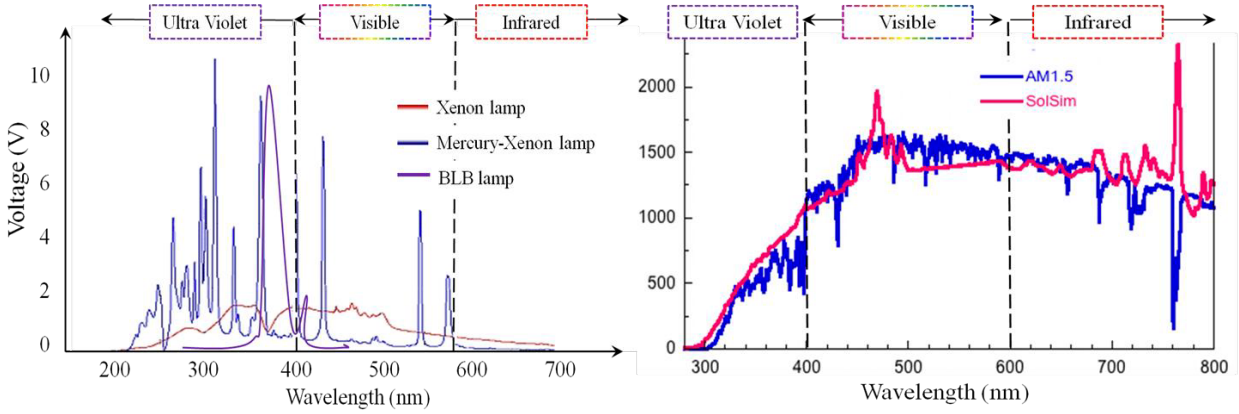

Figure 2.10. Spectrums for different light sources.

2.4 Basic Principle of Photocatalytic Water Splitting

The water splitting reaction, shown in equation 1, is an uphill reaction due to the large positive value of the Gibbs free energy involved.[39,40] If the reaction is promoted by light, as in a photocatalytic process, the wavelength of photons need to be a least 1100 nm.

$$H_2O \xrightarrow{h\nu} 1/2\ O_2 + H_2 \qquad \Delta G = 237\ \text{kJ/mol} \quad (1)$$

The photocatalytic process involves the three main steps shown in Figure 2.11.

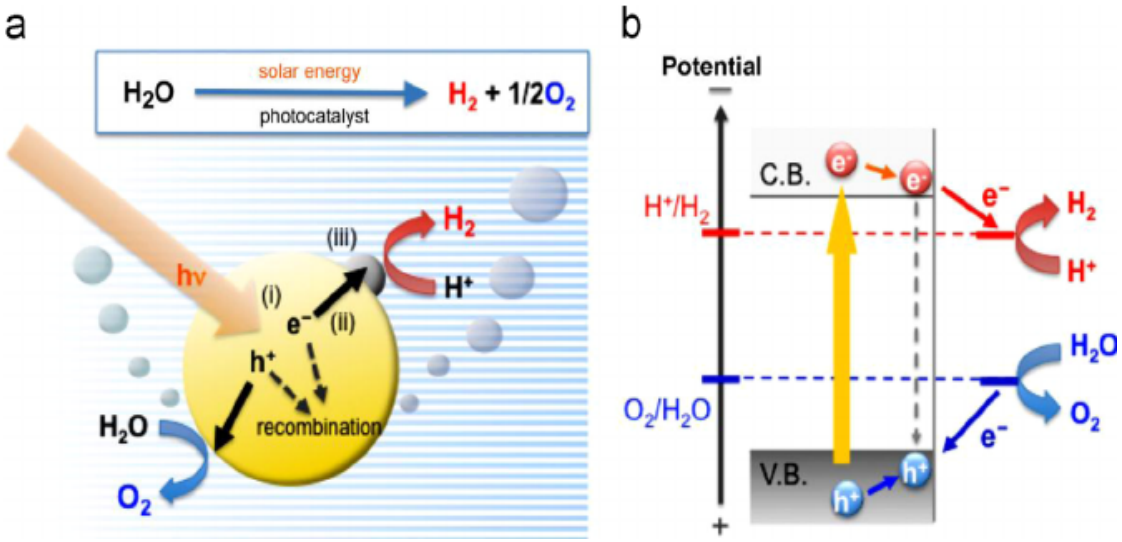

Figure 2.11. Schematic illustration of water-splitting photocatalysis .[70]

In the first step of the process, the photo-semiconductor absorbs suitable photons to generate electron-hole pairs Figure 2.11. The electron is excited to the conduction band while a hole remains in the valence band. This excitation occurs when the energy of incident photons is higher than the energy of the band gap of the semiconductor. The theoretical minimum energy required for water splitting is 1.23 eV, which equates a wavelength shorter than 1100 nm.[41]

The second step of the photocatalytic reaction is the migration of electrons and holes to the surface positions of the photocatalyst where the two redox processes of water splitting may occur. A significant challenge for the photocatalytic reaction is to favor this step while disfavoring or delaying the rapid electron/hole recombination. Approximately 90% or more of the photo-generated electron/hole pairs recombine within 10 ns from the excitation time, leading to the limitation of the rate of quantum yield to less than 10%. This recombination rate was determined for TiO_2 photocatalysts by transient photoluminescence spectroscopy. There are some factors that

help to minimize the charge recombination, such as using crystalline materials which provide separation centers in the photocatalyst. In addition, a small particle size provides a higher surface area with larger distribution of reactive sites thus lowering the possibility of recombination.[41]

In the final step, after the electron/hole pairs successfully migrate to the surface of the photo semiconductors and interact with surface active sites, the redox reaction may occur with electrons reducing H^+ to hydrogen and holes oxidizing water to oxygen Figure 2.11.[41,70]

2.5 Gold Metal Modified Titanium Dioxide Photocatalysts

Recently, elemental gold has increasingly attracted attention in the realm of heterogeneous catalysis due to its ability to catalyze a wide range of chemical reactions.[43].In contrast to the inert nature of the bulk metallic gold/Au nanoparticles (1-5 nm in diameter), especially when distributed on the surface of oxide supports, display significant catalytic properties for different type of reactions .[43,44] In particular, gold nanoparticles supported on titanium dioxide (TiO_2) can enhance the oxidation of carbon monoxide to carbon dioxide at low temperature (–233 °C).[44] The modification of the titanium dioxide surfaces with different noble metal nanoparticles, such as Au, Pt, and Pd, is used to activate titanium dioxide towards hydrogen formation.[45] The interest in gold supported titanium dioxide is mainly due to its high photocatalytic hydrogen production rates under both UV and visible light.[46]

2.5.1 Interfacing Gold Nanoparticles with TiO_2

The interplay between noble metal nanoparticles, such as gold, and the surface of titanium dioxide results in important materials which can enhance hydrogen production.[46] Figure 2.12 depicts the energy levels for gold and titanium dioxide when not in contact (left side) and when in contact (right side).[28]Gold nanoparticles and titanium dioxide both have uniform charge distributions and are electrically neutral with respect to one another. The Fermi level of Au nanoparticles = 0.45 V vs. SHE is lower than in pure TiO_2.[28,48] The work functions of Au and TiO_2, which are the energies required to remove an electron from the solid to the point in the vacuum above the surface, are represented by ΦM and ΦS respectively. As also shown, the work function depends on the position of the Fermi level. The work function of Au nanoparticles are larger than for Ti.[49]

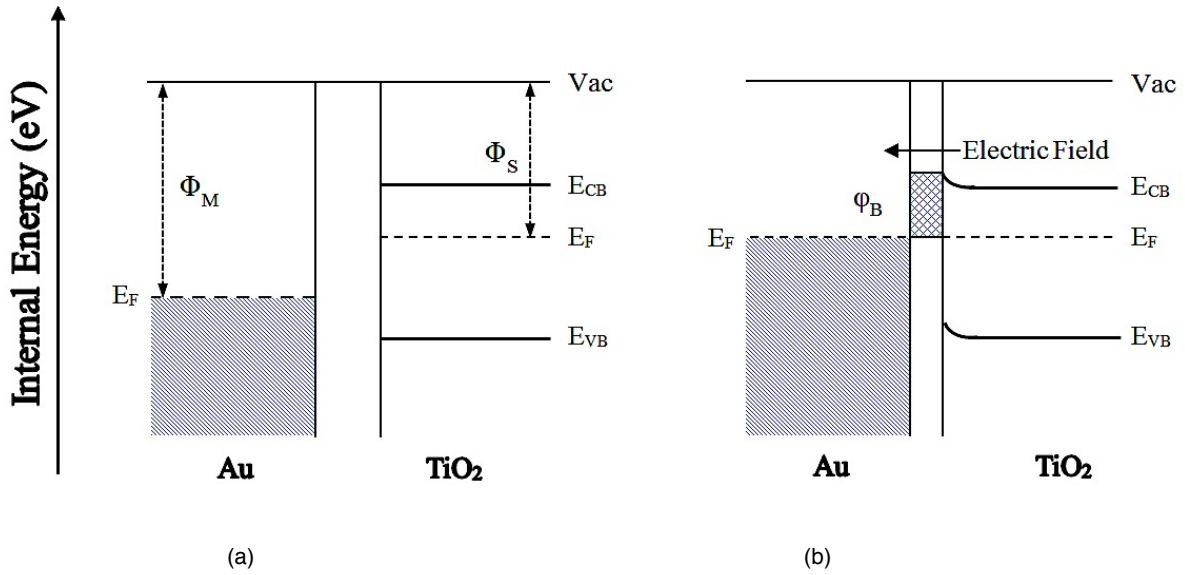

Figure 2.12. Diagram (a) illustrates the gold and TiO_2 surface when they are not in contact. Diagram (b) shows the contact between gold and TiO_2.

Figure 2.12 illustrates the electrical charge redistribution as gold nanoparticles on the surface of titanium dioxide .[47] Because of the higher work function of Au, electrons migrate from the surface of titanium dioxide to the Au nanoparticles. The gold nanoparticles now contain a net negative charge while titanium dioxide has gained a net positive charge. The surface space charge region is depleted of charge carriers. [28,47,48] As shown in Figure 2.12, in the inner space charge region, and due to the flow of charge, the bands of the semiconductor bend up in response to the electric field created across the space charge layer. The difference in work functions of the two species affect the degree of bending. The interfacial region is called the Schottky barrier φB.[50] When charge can flow in only one direction, electrons are effectively channeled to the Au nanoparticles following irradiation. Therefore, Au nanoparticles act as both electron traps, reducing charge recombination in TiO_2, and as cathodic sites where protons generated from water or alcohol photooxidation are reduced to molecular H_2 ($2H^+ + 2^{e-} \rightarrow H_2$). Not all noble metals are able to form a rectifying contact. If ΦM is smaller than ΦS, or in the case that impurities exist at the interface (i.e. a metal oxide), the rectifying nature of the contact may be broken.[49] A non-rectifying contact is referred to as an Ohmic contact which forms between Au nanoparticles and TiO_2 because of an abundance of impurities at the interface.[28,48] When Au particles are distributed on the surface of titanium dioxide, electrical charges also redistribute. The semiconductor acquires negative charge relative to the Au nanoparticles due to the high work function of Au, and the transfer of electrons continues until the Fermi levels equilibrate. Consequently, Au acquires a net negative charge while the semiconductor obtains a net positive charge. As shown in Figure 2.12, the bands of the semiconductor within the space charge layer curve up to the electric field made across the space charge layer. The degree of the curving is related to the difference in the work function of these species. Metal-semiconductor interfacial region establishes energy barrier which are known as a

Schottky barrier. When the barrier is rectifying, electrons are transferred to the Au nanoparticles following irradiation. Thus, Au nanoparticles act as electron traps, minimizing charge recombination in TiO_2 and act as cathodic sites where protons are reduced to molecular H_2 ($2H^+ + 2e- \rightarrow H_2$).[86]

2.6 Deposition of Au on The Surface of Titanium Supports

There are three main methods to synthesize gold-supported titanium dioxide surfaces, such as incipient wetness, deposition precipitation with urea, and immobilisation.

2.6.1 Impregnation to Incipient Wetness

The impregnation by the incipient wetness technique is the most popular method to deposit metals on the surface of titanium dioxide because of its simplicity. This method consists of the treatment of the metal oxide support, such as titanium dioxide, with an aqueous solution of the metal sources ($HAuCl4.3H_2O$, $PdCl_3$, $AgCl_3$) followed by drying and calcination.[51,52] This technique is particularly successful when the volume of metal precursor equals the pore volume of the support. This is called the incipient wetness amount as the solution enters the pores by capillarity. The loading of the noble metal is adjusted through the concentration of the metal precursor solution used. The sample is dried to remove the water followed by calcination at high temperature, around 500 °C, to remove all the volatiles from the surface. In addition to its simplicity, this method has the advantages of maximizing the amount of metal loading on the surface support and being reproducible. However; there are also some disadvantages. With this

preparation method, it is difficult to control the particle size. Also, small amounts of Cl cannot be removed from the surface which leads to poisoning for many reactions.[52,85]

2.6.2 Deposition Precipitation Method

Deposition precipitation with urea is the best synthetic method for gold supported titanium dioxide surfaces. For many catalytic reactions, supported gold catalysts are more active when metal gold particles are smaller than 5 nm .[53]The deposition precipitation method involves the precipitation of the gold precursor ($HAuCl_4.3H_2O$) on the surface of titanium dioxide.[54] At room temperature, the suspension of the support in aqueous solution contains metal salt and water with urea acting as delay-base. However, hydrolysis starts over 70°C within seven hours as shown in equation 2.6. In turn, this affords small gold nanoparticles (3 nm or less).

$$CO(NH_2)_2 + 3H_2O \rightarrow CO_2 + 2NH^{4+} + 2OH^- \qquad (2.6)$$

After seven hours, the pH is increased from 3 to 7. Then the solution is washed with water followed by drying in vacuum. The last step is the calcination of the powder in air at 300°C for one hour. In addition, when the time of deposition-precipitation decreases, the size of the gold nanoparticles decreases. The difference between the deposition-precipitation method with urea and the previous method is that it leads to small nanoparticles with a longer separation time.[68] Furthermore, unlike the typical deposition-precipitation, the gold in solution is deposited only onto the support. Therefore, it makes it very easy to synthesize samples with comparable gold loading and different particles sizes by simply controlling the precipitation time.[55,56,58]

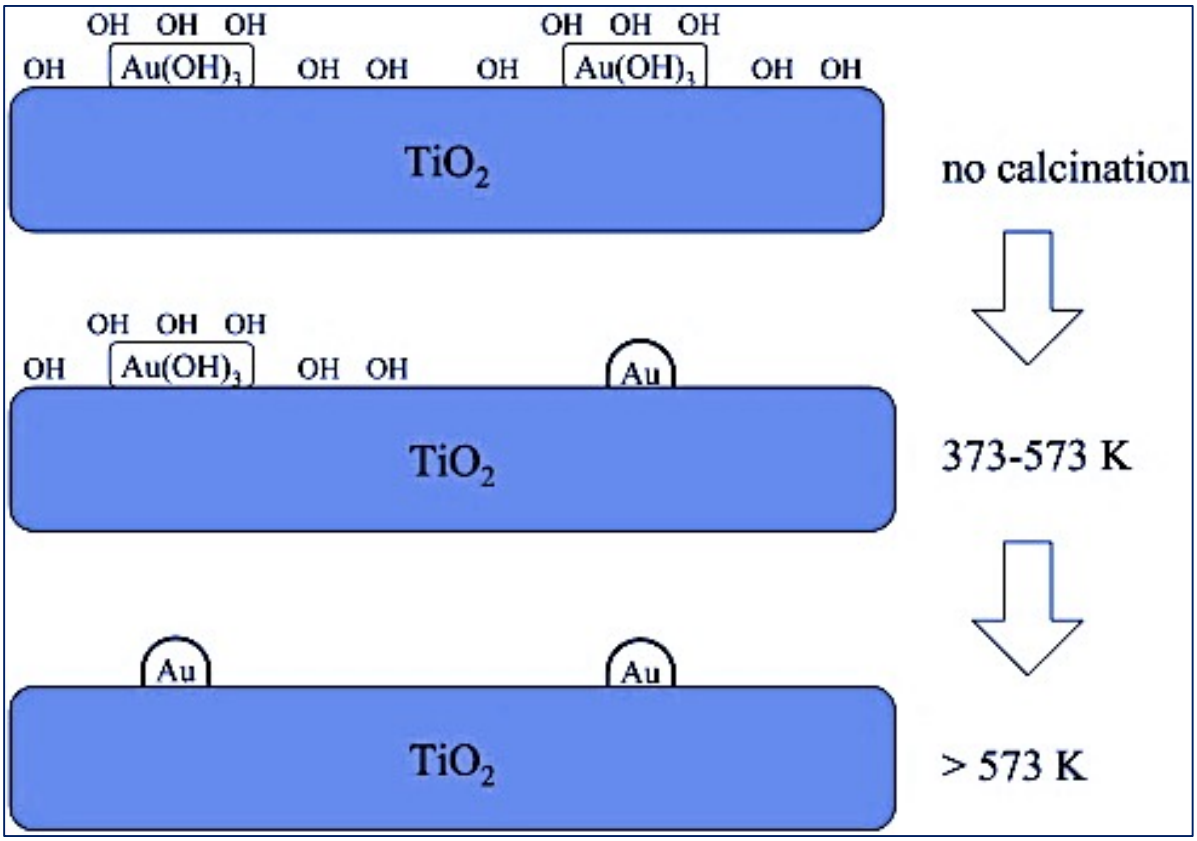

Figure2.13. Schematic of conversion of $Au(OH)_3$ species supported on TiO_2 into Au-TiO_2 during calcination .[57]

2.6.3 Sol Immobilisation

This type of preparation method is a basic method to produce a metal nanoparticle on the surface of a support. Recently, this method has become a popular synthetic method due to the ability to produce nanoparticles in the range of 2-4 nm. Also, this method is relatively inexpensive and simple.[59,60] The first step of sol immobilisation consists of preparing a solution of Au precursor ($HAuCl_4.3H_2O$) and a protecting agent such as polyvinyl alcohol with appropriate concentrations in water. Then, after the addition of a reducing agent such as $NaBH_4$, the Au precursor is reduced,

and the currently formed NP capped by using the protecting agent. The role of poly-vinyl alcohol (PVA) is that of a steric stabiliser.[62] It is believed that PVA binds to the gold NPs through the hydroxyl groups with the polymer generating a physical barrier which helps to prevent NP growth. $NaBH_4$ is the most common reducing agent used in the sol immobilisation method because it has sufficient reducing power to help to transform $HAuCl_4$ into Au metal. Figure 2.14 shows the schematic representation of the sol immobilisation technique. The next step after the colloid is formed is to immobilise the NPs by adding titanium dioxide as support to the solution using sulphuric acid, followed by calcination to remove the protecting agent. [60,61]

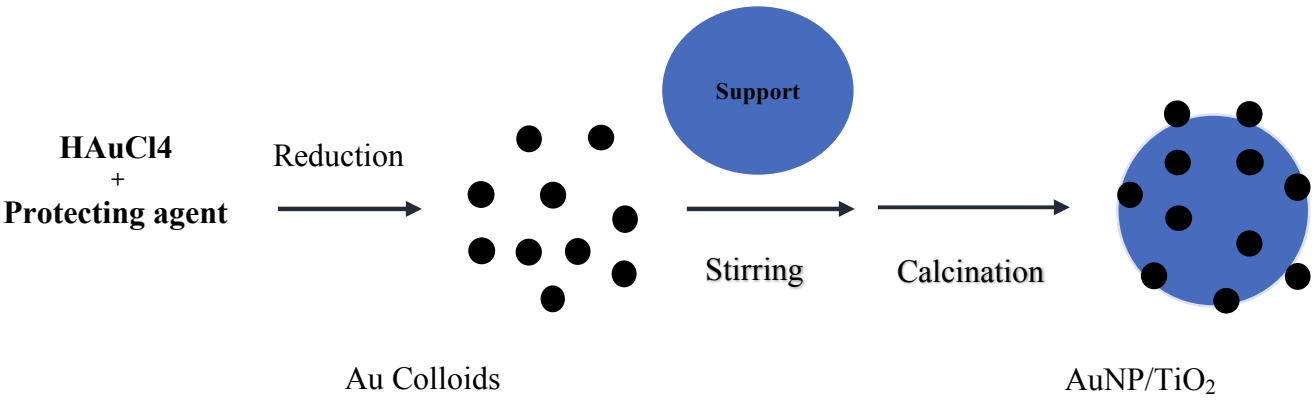

Figure 2.14. Schematic illustration of Au sol –immobilization.[61]

The sol-immobilization method has some advantages, including producing narrow particle size distribution (2-4 nm of Au), and being reproducible, simple and inexpensive. Moreover, it can be used with a wide range of noble metals such as Au, Pd, Pt and Ag. [64,65,66] The only drawback of this method is that it is not suitable for all supports. Also, after the deposition, some protecting ligands may remain on the surface of the NP thus affecting the activity .[67,68]

2.7 References

(1) Moriarty, P.; Honnery, D. *Renewable and Sustainable Energy Reviews***2012**, *16*(1), 244–252.

(2) Schiermeier, Q.; Tollefson, J.; Scully, T.; Witze, A.; Morton, O. *Nature***2008,** *454*(7206), 816–823.

(3) Vezirolu, T.; Barbir, F. *International Journal of Hydrogen Energy***1992,** *17*(6), 391–404.Serpone, N. *Journal of Advanced Oxidation Technologies***1997**, *2*(1).

(4) Mills, A.; Hunte, S. L. *Journal of Photochemistry and Photobiology A: Chemistry***1997**, *108*(1), 1–35.

(5) Honda, K.; Fujishima, A.; *Naturel* **1972**, *238*, 37-38.

(6) Bowker, M.; Morton, C.; Kennedy, J.; Bahruji, H.; Greves, J.; Jones, W.; Davies, P.; Brookes, C.; Wells, P.; Dimitratos, N. *Journal of Catalysis* **2014,** *310*, 10–15.

(7) Kudo, A.; Miseki, Y. *Chem. Soc. Rev.***2009,** *38*(1), 253–278.

(8) Jing, D.; Guo, L.; Zhao, L.; Zhang, X.; Liu, H.; Li, M.; Shen, S.; Liu, G.; Hu, X.; Zhang, X. *International Journal of Hydrogen Energy***2010,** *35*(13), 7087–7097.

(9) Lazar, M.; Varghese, S.; Nair, S. *Catalysts***2012,** *2*(4), 572–601**.**

(10) Gaya, U. I.; Abdullah, A. H. *Journal of Photochemistry and Photobiology C: Photochemistry Reviews* **2008,** *9*(1), 1–12.

(11) Carp, O.; Huisman, L.; Reller, A. *Progress in Solid State Chemistry* **2004,** *32*(1-2), 33–177. Chen, X.; Mao, S. S. *ChemInform***2007**, *38*(41).Choi, K.; Woo, S.; Park*, C. H. *New Physics: Sae Mulli* **2015,** *65*(2), 121–128.

(12) Bagheri, S.; Julkapli, N.; Hamid, S. B. *Electron Microscopy in Heterogeneous Catalysis*.

(13) Maeda, K. *Journal of Photochemistry and Photobiology C: Photochemistry Reviews***2011,** *12*(4), 237–268.

(14) Hara, M.; Domen, K. *The Journal of Physical Chemistry B* **2004,** *108*(49), 19078–19078.

(15) Tang, J.; Durrant, J. R.; Klug, D. R. *Journal of the American Chemical Society***2008,** *130*(42), 13885–13891.

(16) Zaleska, A. *Recent Patents on Engineering***2008,** *2*(3), 157–164.

(17) Kennedy, J.; Jones, W.; Morgan, D. J.; Bowker, M.; Lu, L.; Kiely, C. J.; Wells, P. P.;

(18) Dimitratos, N. *Catalysis, Structure & Reactivity* **2014,** *1*(1), 35–43.

(19) Galińska, A.; Walendziewski, J. *Energy & Fuels* **2005**, *19*(3), 1143–1147.

(20) Melvin, A. A.; Illath, K.; Das, T.; Raja, T.; Bhattacharyya, S.; Gopinath, C. S. *Nanoscale***2015**, *7*(32), 13477–13488**.**

(21) Nadeem, M. A.; Majeed, I.; Waterhouse, G. I. N.; Idriss, H. *Catalysis, Structure & Reactivity***2015,** *1*(2), 61–70.

(22) Sang-Aroon, W.; Arsana, P.; Bubpa, C. *Journal of Applied Sciences***2012**, *12*(17), 1809–1816.

(23) Ibhadon, A.; Fitzpatrick, P. *Catalysts***2013**, *3*(1), 189–218.

(24) Subramanian, V.; Wolf, E. E.; Kamat, P. V. *Journal of the American Chemical Society***2004**, *126*(15), 4943–4950**.**

(25) Lee, S.-Y.; Park, S.-J. *Journal of Industrial and Engineering Chemistry***2013,** *19*(6), 1761–1769**.**

(26) Bahruji, H.; Bowker, M.; Davies, P. R.; Pedrono, F. *Applied Catalysis B: Environmental***2011**, *107*(1-2), 205–209.

(27) Shen, M.; Henderson, M. A. *The Journal of Physical Chemistry Letters***2011,** *2*(21), 2707–2710**.**

(28) Nuhu, A.; Soares, J.; Gonzalez-Herrera, M.; Watts, A.; Hussein, G.; Bowker, M. *Topics in Catalysis***2007,** *44*(1-2), 293–297.

(29) Guzman, F.; Chuang, S. S. C.; Yang, C. *Industrial & Engineering Chemistry Research***2013,** *52*(1), 61–65.

(30) Jafari, T.; Moharreri, E.; Amin, A.; Miao, R.; Song, W.; Suib, S. *Molecules***2016,** *21*(7), 900.

(31) Millard, L.; Bowker, M. *Journal of Photochemistry and Photobiology A: Chemistry***2002,** *148*(1-3), 91–95.

(32) Yang, Y.; Chang, C.; Idriss, H. *Applied Catalysis B: Environmental***2006,** *67*(3-4), 217–222.

(33) Caravaca, A.; Jones, W.; Hardacre, C.; Bowker, M. *Proceedings of the Royal Society A: Mathematical, Physical and Engineering Science***2016,** *472*(2191), 20160054.

(34) Ismail, A. A.; Bahnemann, D. W. *Solar Energy Materials and Solar Cells***2014,** *128*, 85–101.

(35) Bowker, M. *Green Chemistry***2011,** *13*(9), 2235.

(36) Kogan, A. *International Journal of Hydrogen Energy***1997,** *22*(5), 481–486.

(37) Chiarello, G. L.; Paola, A. D.; Palmisano, L.; Selli, E. *Photochem. Photobiol. Sci.***2011,** *10*(3), 355–360.

(38) Huang, J.-H.; Wong, M.-S. *Thin Solid Films***2011**, *520*(5), 1379–1384.

(39) Hernández-Alonso, M. C. A. D. D.; Fresno, F.; Suárez, S.; Coronado, J. M. *Energy & Environmental Science***2009,** *2*(12), 1231.

(40) Prati, L.; Villa, A. *Catalysts***2011,** *2*(4), 24–37.

(41) Jiang, Z.; Yang, Y.; Shangguan, W.; Jiang, Z. *The Journal of Physical Chemistry C* **2012**, *116*(36), 19396–19404.

(42) Haruta, M.; Kobayashi, T.; Sano, H.; Yamada, N. *Chemistry Letters***1987**, *16*(2), 405–408.

(43) Rajeshwar, K. *Journal of Applied Electrochemistry***2007,** *37*(7), 765–787.

(44) Connelly, K.; Wahab, A. K.; Idriss, H. *Materials for Renewable and Sustainable Energy***2012**, *1*(1).

(45) Linsebigler, A. L.; Lu, G.; Yates, J. T. *Chemical Reviews***1995,** *95*(3), 735–758.

(46) Zhang, Z.; Yates, J. T. *Chemical Reviews***2012,** *112*(10), 5520–5551.

(47) C. *Recent Patents on Engineering***2010,** *4*(3).

(48) Baliga, B. J. *Advanced power rectifier concepts*; Springer: New York, **2009**.

(49) Bowker, M.; Nuhu, A.; Soares, J. *Catalysis Today***2007,** *122*(3-4), 245–247.

(50) Bahruji, H.; Bowker, M.; Davies, P. R.; Morgan, D. J.; Morton, C. A.; Egerton, T. A.; Kennedy, J.; Jones, W. *Topics in Catalysis***2014**, *58*(2-3), 70–76.

(51) Song, S.; Sheng, Z.; Liu, Y.; Wang, H.; Wu, Z. *Journal of Environmental Sciences***2012**, *24*(8), 1519–1524.

(52) Nadeem, M. A.; Majeed, I.; Waterhouse, G. I. N.; Idriss, H. *Catalysis, Structure & Reactivity***2015,** *1*(2), 61–70.

(53) Prati, L.; Villa, A. *Gold catalysis: preparation, characterization, and applications*; Pan Stanford Publishing: Singapore, **2016.**

(54) Zanella, R.; Giorgio, S.; Henry, C. R.; Louis, C. *The Journal of Physical Chemistry B***2002**, *106*(31), 7634–7642.

(55) Zwijnenburg, A.; Goossens, A.; Sloof, W. G.; Crajé, M. W. J.; Kraan, A. M. V. D.; Jongh, L. J. D.; Makkee, M.; Moulijn, J. A. *The Journal of Physical Chemistry B***2002**, *106*(38), 9853–9862.

(56) Seoudi, R.; Said, D. A. *World Journal of Nano Science and Engineering***2011,** *01*(02), 51–61.

(57) Dimitratos, N.; Lopez-Sanchez, J. A.; Morgan, D.; Carley, A.; Prati, L.; Hutchings, G. J. *Catalysis Today***2007**, *122*(3-4), 317–324.

(58) Dimitratos, N.; Villa, A.; Prati, L.; Hammond, C.; Chan-Thaw, C. E.; Cookson, J.; Bishop, P. T. *Applied Catalysis A: General***2016,** *514*, 267–275.

(59) Cybulski, A.; Moulijn, J. A.; Stankiewicz, A. I. *Novel concepts in catalysis and chemical reactors: improving the efficiency for the future*; Wiley-VCH: Weinheim, **2010.**

(60) Prati, L.; Martra, G. *Gold Bulletin***1999**, *32*(3), 96–101.

(61) Lopez-Sanchez, J. A.; Dimitratos, N.; Hammond, C.; Brett, G. L.; Kesavan, L.; White, S.; Miedziak, P.; Tiruvalam, R.; Jenkins, R. L.; Carley, A. F.; Knight, D.; Kiely, C. J.; Hutchings, G. J. *Nature Chemistry***2011,** *3*(7), 551–556.

(62) Priebe, J. B.; Radnik, J.; Lennox, A. J. J.; Pohl, M.-M.; Karnahl, M.; Hollmann, D.; Grabow, K.; Bentrup, U.; Junge, H.; Beller, M.; Brückner, A. *ACS Catalysis***2015,** *5*(4), 2137–2148.

(63) Cihlar, J.; Bartonickova, E.; Cihlar, J. *Journal of Sol-Gel Science and Technology***2013,** *65*(3), 430–442.

(64) Prati, L.; Villa, A. *Catalysts***2011,** *2*(4), 24–37.

(65) Sankar, M.; He, Q.; Morad, M.; Pritchard, J.; Freakley, S. J.; Edwards, J. K.; Taylor, S. H.; Morgan, D. J.; Carley, A. F.; Knight, D. W.; Kiely, C. J.; Hutchings, G. J. *ACS Nano***2012,** *6*(8), 6600–6613.

(66) Zanella, R.; Delannoy, L.; Louis, C. *Applied Catalysis A: General***2005,** *291*(1-2), 62–72.

(67) Abe, R. *Journal of Photochemistry and Photobiology C: Photochemistry Reviews***2010,** *11*(4), 179–209.

(68) Chiarello, G. L.; Aguirre, M. H.; Selli, E. *Journal of Catalysis***2010**, *273*(2), 182–190.

(69) Ma, Y.; Guan, G.; Shi, C.; Zhu, A.; Hao, X.; Wang, Z.; Kusakabe, K.; Abudula, A. *International Journal of Hydrogen Energy***2014**, *39*(1), 258–266.

(70) Kowalska, E.; Rau, S.; Ohtani, B. *Journal of Nanotechnology***2012,** *2012*, 1–11.

(71) Rodriguez, J.; Thivel, P.-X.; Puzenat, E. *International Journal of Hydrogen Energy***2013**, *38*(15), 6344–6348.

(72) Lalitha, K.; Reddy, J. K.; Sharma, M. V. P.; Kumari, V. D.; Subrahmanyam, M. *International Journal of Hydrogen Energy***2010,** *35*(9), 3991–4001.

(73) Kim, J.; Kang, M. *International Journal of Hydrogen Energy***2012**, *37*(10), 8249–8256.

(74) Sabio, E. M.; Chamousis, R. L.; Browning, N. D.; Osterloh, F. E. *The Journal of Physical Chemistry C***2012**, *116*(4), 3161–3170.

(75) Jana, P.; Montero, C. M.; Pizarro, P.; Coronado, J.; Serrano, D.; Oshea, V. D. L. P. *International Journal of Hydrogen Energy***2014,** *39*(10), 5283–5290.

(76) Heim, L. E.; Schlörer, N. E.; Choi, J.-H.; Prechtl, M. H. G. *Nature Communications***2014**, *5*.

(77) Loew, O. *Berichte der deutschen chemischen Gesellschaft***1887,** *20*(1), 144–145.

(78) Ashby, E. C.; Doctorovich, F.; Liotta, C. L.; Neumann, H. M.; Barefield, E. K.; Konda, A.; Zhang, K.; Hurley, J.; Siemer, D. D. *Journal of the American Chemical Society***1993,** *115*(3), 1171–1173.

(79) Kapoor, S.; Naumov, S. *Chemical Physics Letters***2004**, *387*(4-6), 322–326.

(80) Li, Y.; Chen, T.; Wang, T.; Zhang, Y.; Lu, G.; Bi, Y. *International Journal of Hydrogen Energy***2014,** *39*(17), 9114–9120.

(81) Hu, H.; Jiao, Z.; Ye, J.; Lu, G.; Bi, Y. *Nano Energy***2014**, *8*, 103–109.

(82) Delannoy, L.; Hassan, N. E.; Musi, A.; To, N. N. L.; Krafft, J.-M.; Louis, C. *The Journal of Physical Chemistry B***2006**, *110*(45), 22471–22478.

(83) Chen, J.; Cen, J.; Xu, X.; Li, X. *ChemInform***2016,** *47*(13).

(84) Chowdhury, P.; Malekshoar, G.; Ray, M. B.; Zhu, J.; Ray, A. K. *Industrial & Engineering Chemistry Research***2013,** *52*(14), 5023–5029.

(85) Wang, L.; Pang, Q.; Song, Q.; Pan, X.; Jia, L. *Fuel***2015**, *140*, 267–274.

Chapter 3

Experimental

3. Introduction

The first section of this chapter describes the materials and preparation methods of catalysts that were used for this study. The deposition–precipitation with urea method was the main method used. The second section details all the various characterization techniques used. The final section describes the experimental set up and details of how reactions were performed.

3.1 Material used

Titanium (IV) oxide, anatase and rutile powder, titanium tetra-isopropoxide, urea 99.5% pellets, gold(III) chloride trihydrate [$HAuCl_4.3H_2O$], chloroplatinic acid hexahydrate [$H_2PtCl_6 \cdot 6H_2O$], silver nitrate [$AgNO_3$], sodium borohydride[$NaBH_4$], and polyvinyl alcohol], ammonia, methanol, ethanol, and isopropanol, sulfuric acid, sodium hydroxide, ammonium acetate, glacial acetic acid, acetyl acetone purchased from sigma Aldrich.

3.2 Catalysts Preparation Methods

There are several types of catalysts that were used in this study synthesised according to three different preparation techniques. The semiconductor photocatalyst titanium dioxide P25 (70% anatase and 30% rutile) was used as a support for gold, silver and platinum which were synthesized by deposition precipitation with urea (DPU).[1,2]

3.2.1 Synthesis of 4 wt% M -TiO_2 via Deposition–Precipitation with Urea

The deposition–precipitation of Au, Ag and Pt with urea was carried out according to the procedure described by Zanella *et al* for the preparation of gold supported titanium dioxide.[1] Under stirring, 2.5 g of titanium oxide was added to a solution of 250 ml of water containing one of each metal precursor: (108 mg of Gold(III) chloride trihydrate, or 113 mg of chloroplatinic acid hydrate, 64 mg of silver nitrate), and 6.3 g of urea. The suspensions of TiO_2 particles were heated to 85 ^oC for eight hours, and filtered under vacuum. The resulting material was collected, washed repeatedly with milli Q water, dried for two days at room temperature and calcined at 300 ℃ for one hour to thermally reduce metal cations to the zero-valent state metal (0).[1,11].

3.2.2 Synthesis of Au-TiO_2 with Different Weight Loading of Au via DPU

Changing the desired weight loading of gold on the titanium dioxide surface was accomplished by adding the desired amount of titanium oxide to the gold precursor. In brief, specific volumes of the gold stock solution (i.e., 25, 50,100 mL - to get final gold loadings of 1, 2, 4 wt.%, respectively) were added to milli-Q water to reach a total volume of 250 mL. As mentioned above, the solutions were added to 250 ml round bottomed flasks. Then 6.3 g of urea and 2 g of titanium dioxide TiO_2 support were added to each of the Au^{3+} solutions. The suspensions were stirred and heated for eight hours at 80^oC. After 8 hours, the yellow Au^{+3} impregnated P25 TiO_2 powders were collected by filtration under vacuum, and washed repeatedly with milli-Q water to remove Cl^- ions. The samples were dried at 70 ℃ overnight and calcined at 300 ℃ for 2 h. The calcination at 300 ℃ reduces surfacial Au(III) to metallic gold (Au^0). After calcination, the

color of the Au/P25 TiO_2 photocatalysts were purple because of the localized surface Plasmon resonance of supported Au nanoparticles. [2,3,4]As shown in Figure 3.1., the color darkens with the loading increase.

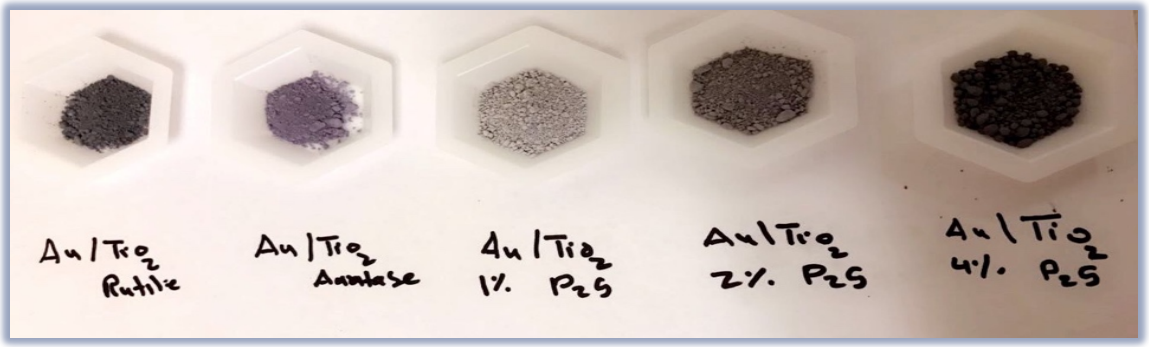

Figure 3.1. Au-TiO_2 with different weight loading of Au via deposition–precipitation method with urea.

3.3 Catalyst preparation: Other methods

3.3.1 Sol Gel Method

In this project, several metals (Au, Ag, Pt, Mn, W, Co, Cu, Ce, La, Fe, Ni) doped titanium dioxide were prepared using sol gel methods. The details of this method are as follows.

3.3.1.1 Synthesis of Metals Doped Titanium Dioxide (TiO_2)

Figure 3.2. describes the steps in preparing different metals (Au, Ag, Pt, Mn, W, Co, Cu, Ce, La, Fe, Ni) with each of them doped into TiO_2 by using their salts as precursor. The solutions were prepared by taking the required amount of each metal salt ($AlCl_3$, $HAuCl_4.3H_2O$, $AgNO_3$, $PtCL_3$, $Fe(NO_3)_3$, $Mn(C_5H_7O_2)_3$, CeNO3, $(CH_3CO_2)_7Cr_3(OH)_2 \cdot 6H2O$, WO_3, $RuCl_3$, $(CH_3CO_2)_2Co$,

$La(NO_3)_3$, $Fe(NO_3)_3$, $Ni(OCOCH_3)_2 \cdot 4H_2O$) and dissolving it in deionized water. Then, under vigorous stirring, the metal salt solution and ammonia solution were added dropwise to the titanium tetra-isopropoxide solution. The mixture was stirred for two hours at room temperature, then heated for 24 hours at 80℃. The precipitate was filtered and washed with water to remove any contamination and salts, and left to dry at 100℃ for 24h, followed by calcination at 450 ℃ for 3 hours.[5]

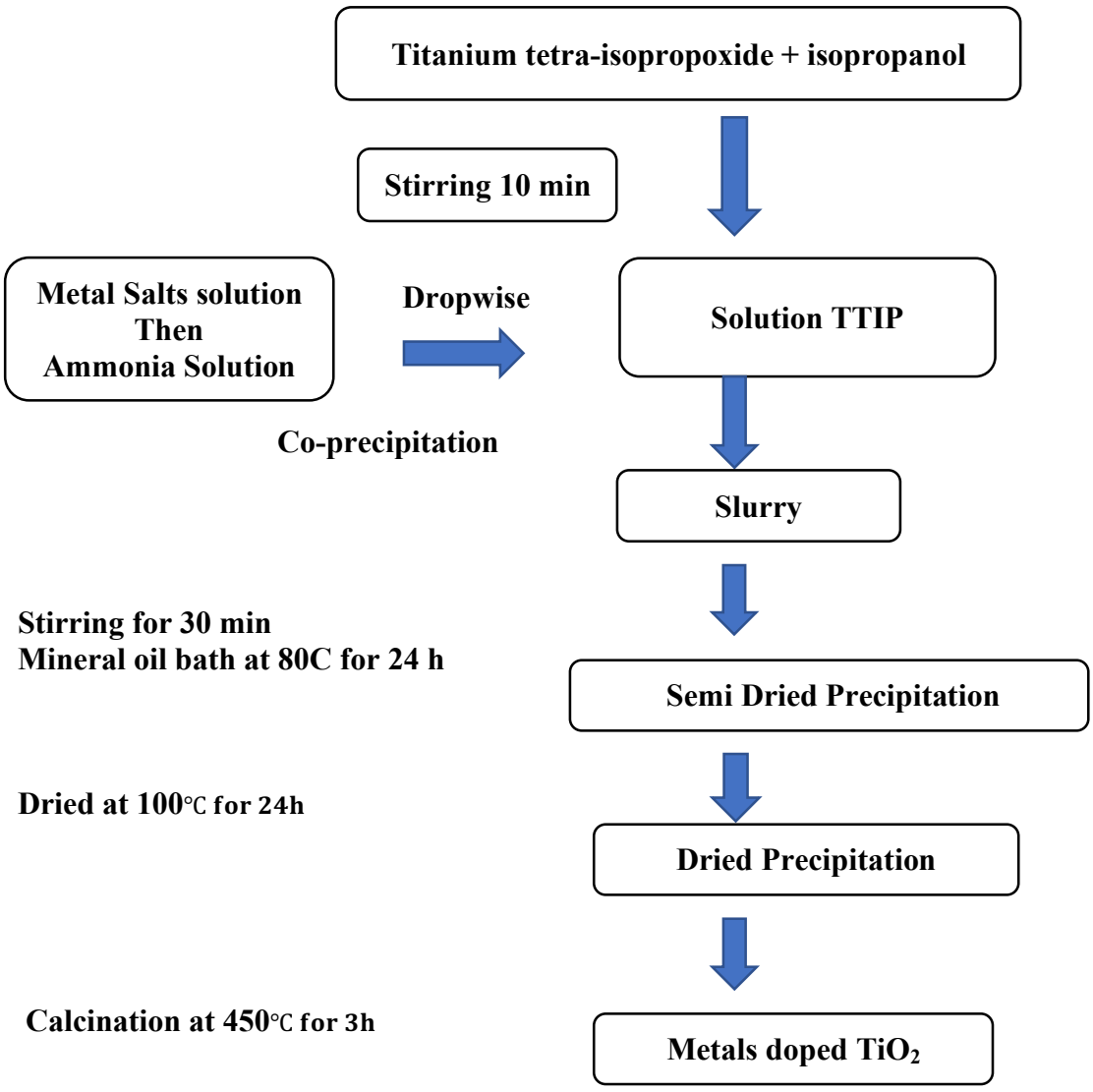

Figure 3.2. Synthesis steps to support metals on TiO_2.

3.3.2 Sol Immobilization

The sol immobilization method was used in this project to synthesize monometallic Au, Pt, Ag, and bimetallic Ag-Au, and Pt-Au supported on titanium dioxide P25.

3.3.2.1 Synthesis of Monometallic Au, Pt, Ag Using Sol Immobilization Method

Au/TiO_2 Ag/TiO_2 and Pt/TiO_2 were prepared by using the following procedure. Polyvinyl alcohol (PVA) was added to aqueous solutions (1.36 M) of $HAuCl_4{\cdot}3H_2O$, $AgNO_3$ and $H_2PtCl_6.xH_2O$. Subsequently, a solution of $NaBH_4$ was prepared and added to form a sol. After the sol formation (30 minutes), the colloid was immobilized by adding (2.5 g) TiO_2 powder (acidified to pH 1 by sulphuric acid) under vigorous stirring conditions. After 2 h, the slurry was filtered, the catalyst was washed thoroughly with distilled water to remove all the soluble species, such as NaCl, and then dried at 120℃ overnight.

3.4 Characterization of Au Supported Titanium Dioxide Photocatalyst

Different techniques were employed to analyze and determine the physical and chemical properties of 4% gold-supported titanium dioxide, including Transmission Electron Microscopy Analysis (TEM), Energy Dispersive X-Ray Analysis (EDX) and Diffuse Reflectance UV-Vis Spectroscopy.

3.4.1 Transmission Electron Microscopy (TEM)

The images were taken on JEOL: JEM-2100FETEM operated at 200 keV with a LaB_6 filament. TEM microscopy contains a column under vacuum in the region of 1 x 10^{-5} mbar to let the electron beam travel without interference from air molecules. The filament is located at the top, and accelerates an electron beam down the column with energy 200 keV.[7] As shown in Figure 3.3., this beam is focused by an electromagnetic lens system with two condenser lenses. The focused beam then passes through a specimen of thickness 100 nm or less for high resolution imaging. When the beam passes through the sample, some electrons will interact resulting in some being absorbed or scattered. This will occur in areas that have heavy atoms or when the sample is thick. After the beam exits the sample, a set of projection lenses spreads the beam onto a fluorescent viewing screen. This provides a rough image, through a lead glass viewing window, of electrons hitting the screen and emitting fluorescent photons in the visible range. This image is used as an aid during beam focusing. Under the fluorescent screen, there is a charge couple device (CCD) camera which converts the electron intensity at a given coordinate into a digital image.[8]

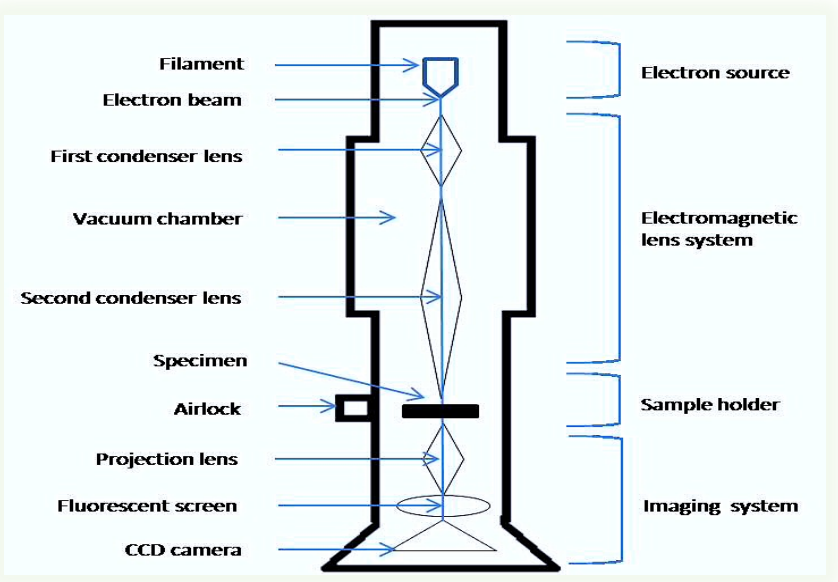

Figure 3.3. Schematic set up of TEM column.

3.4.1.1 TEM Sample Preparation

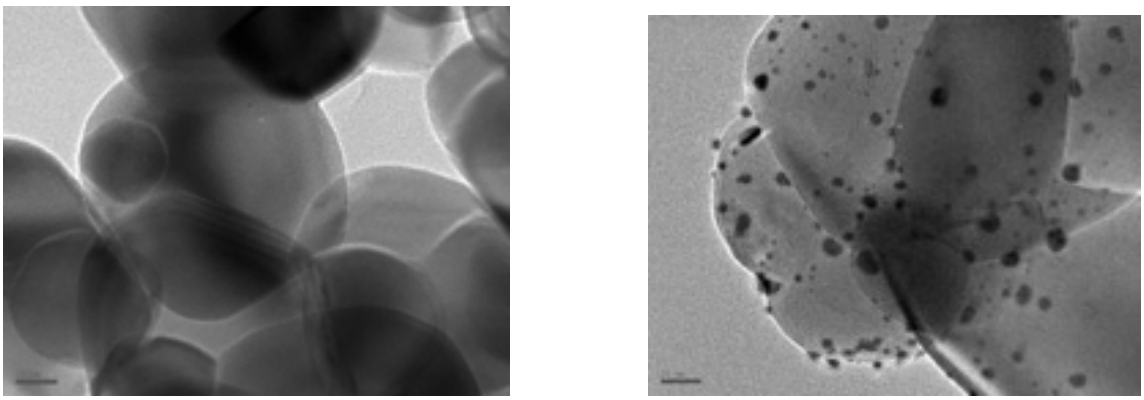

a) P25 TiO_2 **b)** P25 TiO_2 – Au loaded

Figure 3.4. Transmission electron microscopy images for P25 TiO_2 and P25 TiO_2-Au loaded.

Figure 3.4. shows that the deposition–precipitation method with urea is a reliable technique for gold loading onto a titanium dioxide surface.

3.4.2 Energy Dispersive X-Ray Analysis (EDX)

Energy Dispersive X-Ray Analysis (EDX) is an analytical method used for determining the elements composing a sample. It is usually coupled with a transmission electron microscope [TEM] or a scanning electron microscope [SEM]. During EDX analysis, the sample is bombarded with an electron beam inside the electron microscope, the electrons collide with the sample atoms, freeing them in the process. A position vacated by an ejected inner shell electron is eventually occupied by a higher energy electron from an outer shell. For this to happen, the transferring outer electron must give up some of its energy by emitting an X-ray.[10]

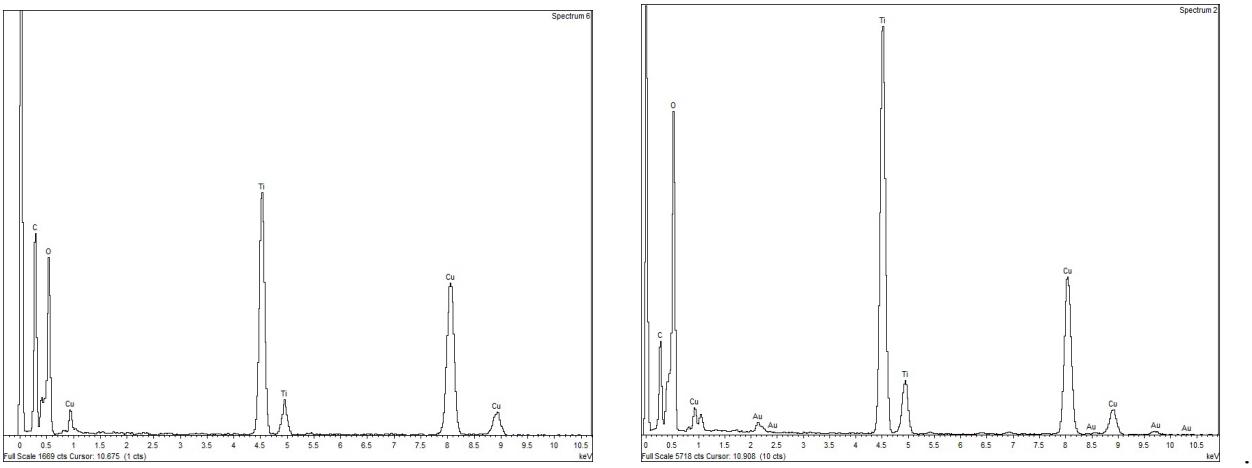

a) EDX spectrum of P25 TiO_2 **b)** EDX spectrum of Au /P25TiO_2

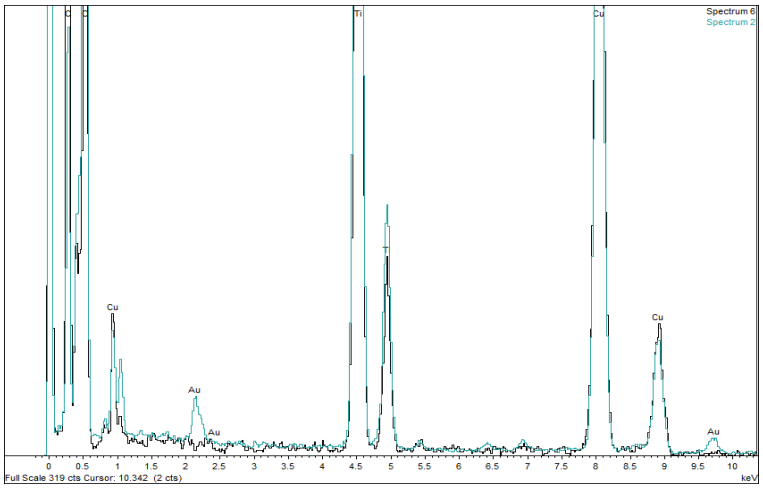

Figure 3.5. c) EDX spectrum 4 wt. % Au TiO_2 P25.

In this project, Energy Dispersive X-Ray Analysis (EDX) of the composites was used to confirm the presence of 4% wt. Au on the surface of the titanium dioxide (TiO_2). The Au containing sample shows signals at both 2keV (M Line) and 10keV (L Line).

3.4.3 Diffuse Reflectance UV-Vis Spectroscopy

Ultraviolet – visible spectroscopy refers to absorption or reflectance spectroscopy in the 200 – 800 nm region. For liquids, photons in this energy range can initiate transitions from ground state to the excited states of electrons in molecules. During this project, UV-Vis spectroscopy was used to determine the band gap and the wavelength of the semiconductor materials of titanium dioxide used before and after the deposition of metal nanoparticles since gold addition enhances irradiation absorption in the visible range. Figure 3.6. shows the effect of gold loading on the titanium dioxide band gap energy. From this analysis, we can see that gold doping on TiO_2 P25 introduces additional electron energy levels (Fermi Levels) into the conduction band, resulting in the reduction of the energy band gap level from 3.20 to 2.50 eV.[11]

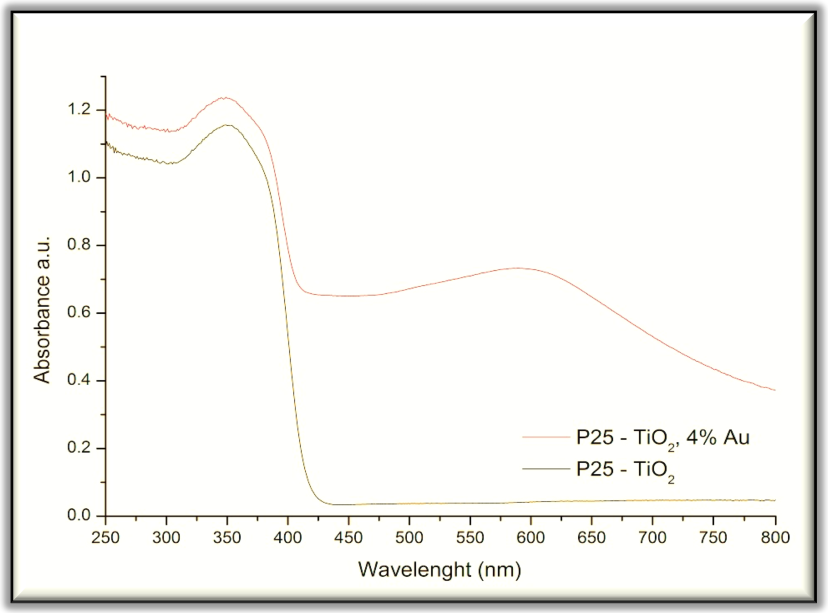

Figure 3.6. Optical absorption spectra of P25 (TiO_2) and gold loaded TiO_2.

3.5 Photoreactor Set-up

The quartz glassware, which contained water and a sacrificial agent such as methanol, isopropanol, and a photocatalyst, Figure 3.7. was used as a reactor. The photon source in this reaction was a Hg- 400 W Arc lamp. The equipment used to measure the amount of hydrogen produced was a gas chromatograph (GC), as shown in Figure 3.7. The photo reactor was housed in a foil box to protect personnel from the harmful radiation produced by the lamp.

3.6 Sample Reactor

Figure 3.7. is a schematic of a photoreactor for hydrogen production reactions at room temperature. The reactor for all liquid phase reactions was a 250-mL bottle flask. The reaction mixture contained 0.200 g of the catalyst added in a solution of 100 ml of water and 100 µl of MeOH. The solutions were purged with argon for 30 minutes before irradiation. The reactor was placed in front of the light for irradiation. Every 50 minutes, 200 µl of sample gas was taken for five hours by using GC syringe. Experiments were repeated three times to account for experimental errors.

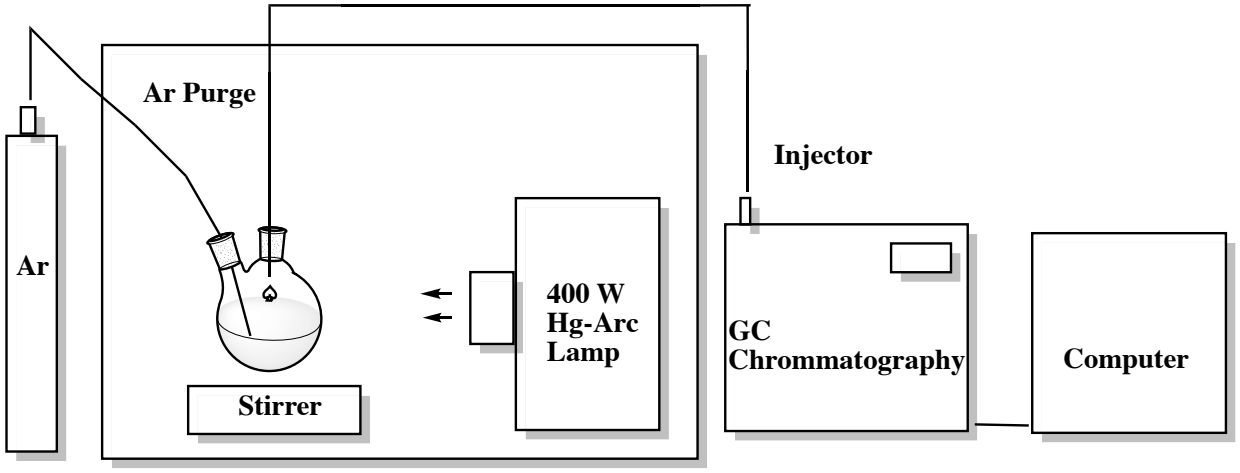

Figure 3.7. Sample photoreactor for hydrogen production from sacrificial reagent/water mixture.

3.7 Light Source

In this project, the photon source was a 400 W mercury arc lamp whose main lines follow the trend of sunlight Figure 3.8.

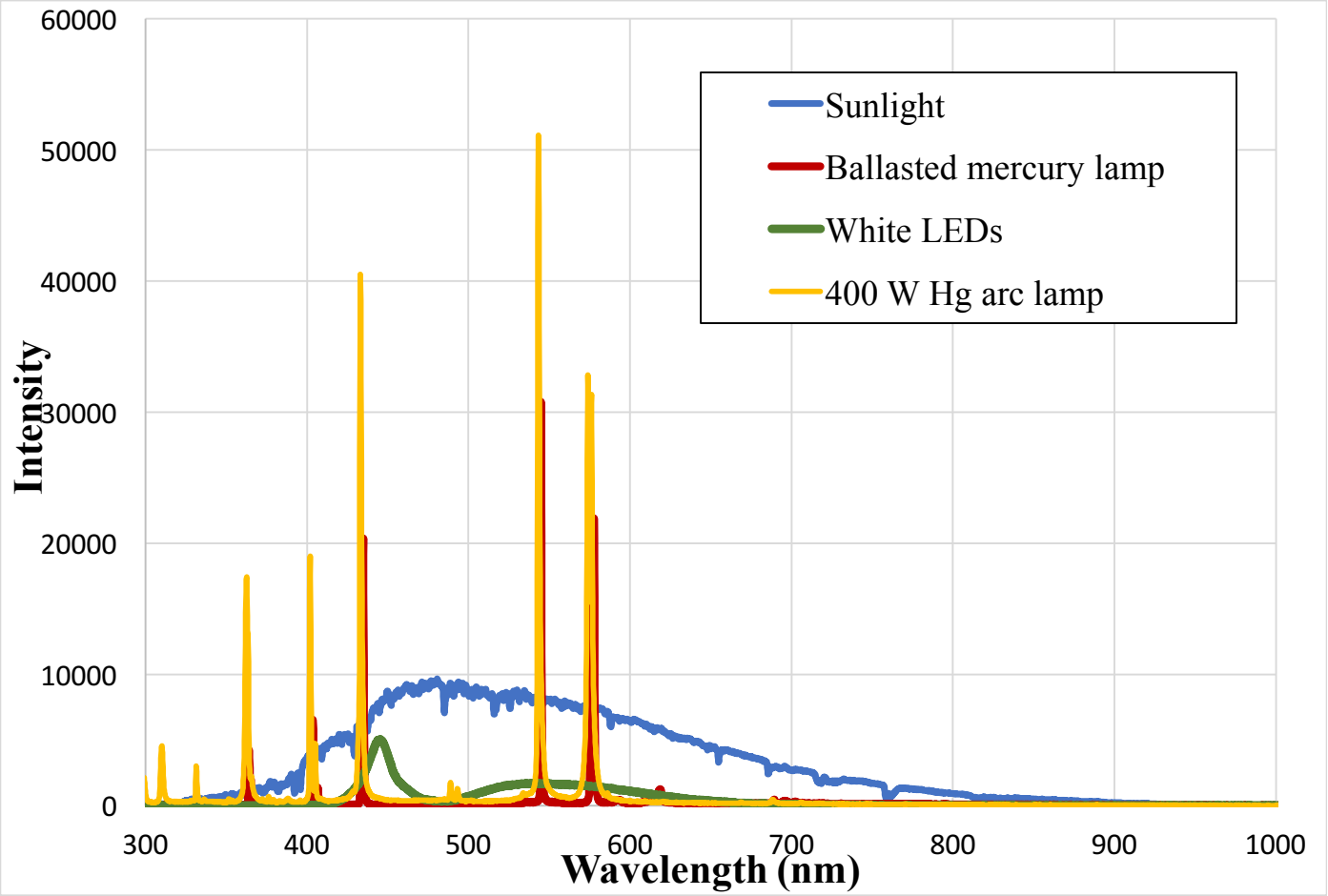

Figure 3.8. Wavelength of Mercury arc lamps used for photocatalytic reactions.

3.8 Analytical Methods

In this project, liquid and gas products were analysed and quantified using Gas Chromatography (GC), and UV-1100 spectrophotometry. GC analysis was performed to detect hydrogen generated during photocatalytic reactions by Agilent 7820A GC gas and liquid.

Every fifty minutes, 200 μl of gas was taken from samples by using a gas tight syringe and was injected into a gas chromatograph to identify the gaseous products during the photocatalytic reaction using a Thermal Conductivity Detector with argon as the carrier gas.

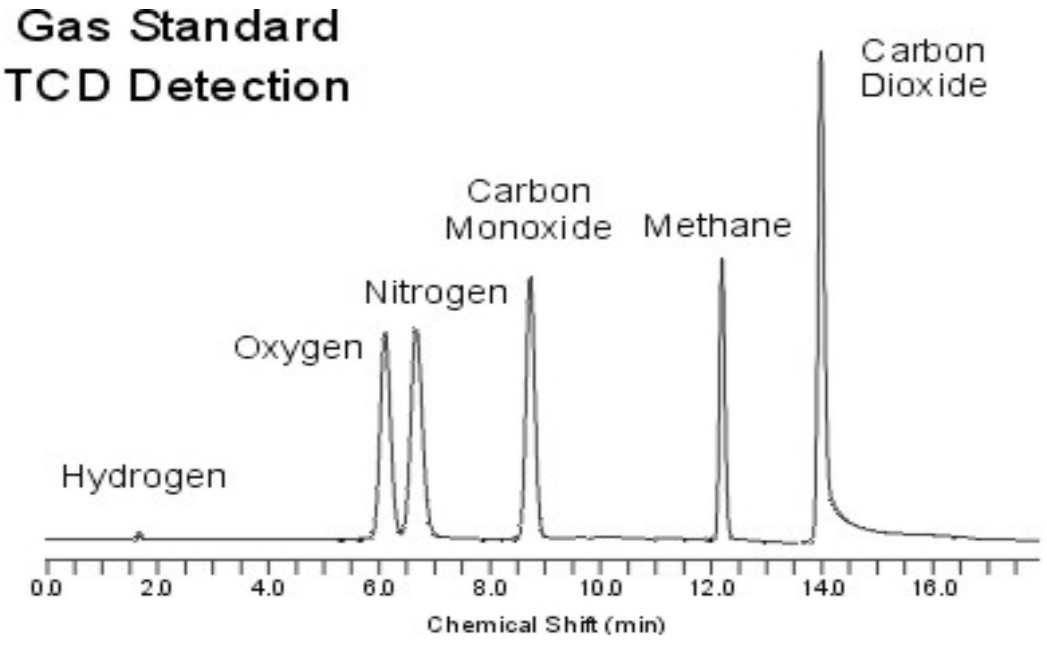

Figure 3.9. Example of analysed gases by GC chromatography.

3.8.1. Hydrogen Calibration:

The volume of gas produced during the reaction was analyzed by GC, and quantified by comparison with a calibration curve Figure 3.10.

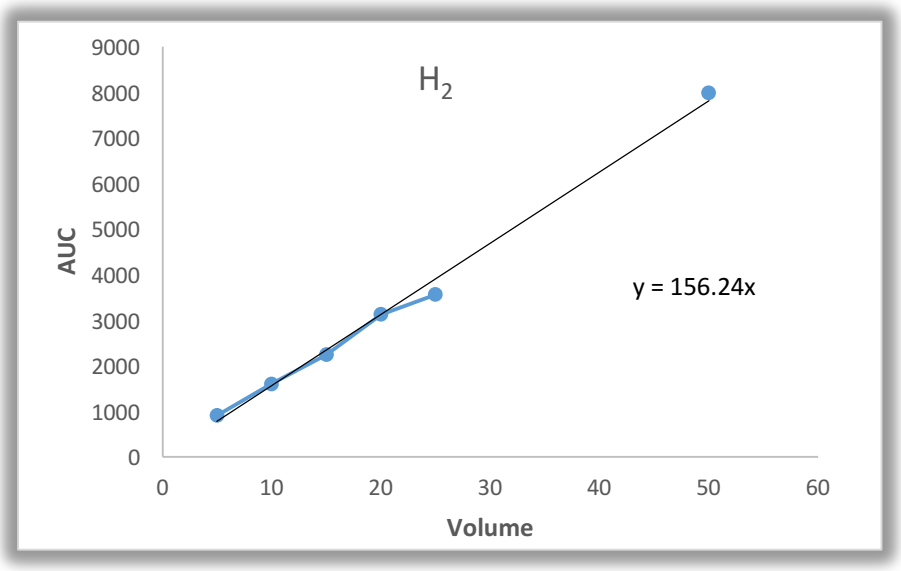

Figure 3.10. Calibration plot for hydrogen.

3.9 References

(1) Jovic, V.; Chen, W.-T.; Sun-Waterhouse, D.; Blackford, M. G.; Idriss, H.; Waterhouse, G. I. *Journal of Catalysis***2013,** *305*, 307–317.

(2) Zanella, R.; Giorgio, S.; Henry, C. R.; Louis, C. *The Journal of Physical Chemistry B* **2002**, *106*(31), 7634–7642.

(3) Hugon, A.; Delannoy, L.; Louis, C. *Gold Bulletin***2008,** *41*(2), 127–138.

(4) Oros-Ruiz, S.; Zanella, R.; López, R.; Hernández-Gordillo, A.; Gómez, R. *Journal of Hazardous Materials***2013**, *263*, 2–10.

(5) Kennedy, J.; Jones, W.; Morgan, D. J.; Bowker, M.; Lu, L.; Kiely, C. J.; Wells, P. P.; Dimitratos, N. *Catalysis, Structure & Reactivity***2014**, *1*(1), 35–43.

(6) Signoretto, M.; Menegazzo, F.; Michele, A. D.; Fioriniello, E. *Catalysts* **2016,** *6*(6), 87.

(7) Agilent | Chemical Analysis, Life Sciences, and Diagnostics http://www.agilent.com/en-us/products/gas-chromatography/gc-systems/7820a-gc (accessed Jun 5, **2017**).

(8) Zanchetta, C.; Patton, B.; Guella, G.; Miotello, A. *Measurement Science and Technology***2007**.

(9) Clement, R. E.; Fowlis, I. *Gas chromatography*; Wiley, **1995**.

(10) Snow, N. H.; Slack, G. C. *TrAC Trends in Analytical Chemistry***2002,** *21*(9-10), 608–617.

(11) Murdoch, M.; Waterhouse, G. I. N.; Nadeem, M. A.; Metson, J. B.; Keane, M. A.; Howe, R. F.; Llorca, J.; Idriss, H. *Nature Chemistry***2011.**

Chapter 4

Hydrogen formation from alcohol /water mixtures

4. Introduction

In this chapter, experiments of hydrogen production using a mixture of water/alcohols (methanol, isopropanol, namely) using Au/TiO_2 as a photocatalyst will be described. Methanol is used as a more promising feedstock compared to other alcohols, such as ethanol, due to its higher hydrogen content and the fact that it is one of the easiest alcohols to be obtained.[1] The set-up for these reactions is shown in Chapter 3 Figure 3.6.1. Methanol can be dehydrogenated with water at room temperature and pressure by using Au/TiO_2 photocatalysts, affording hydrogen gas and different organic products according to the sequence of reactions reported in Figure 4.1. Several parameters were investigated to study their effect on hydrogen productivity. These factors include the presence of different metals on titanium dioxide, various loading of gold, different TiO_2 supports, effect of pH changes, different methanol concentrations, and various 4 wt.% Au/TiO_2 catalyst loadings. During the photocatalytic dehydrogenation of water/methanol mixtures, different intermediate species such as formaldehyde were identified. Dehydrogenation of water using isopropanol as a sacrificial reagent instead of methanol was also analyzed. Finally, the impact of bimetallic $Au\text{-}M/TiO_2$ (M: Pt, Ag) nanoparticles on the hydrogen production was examined.

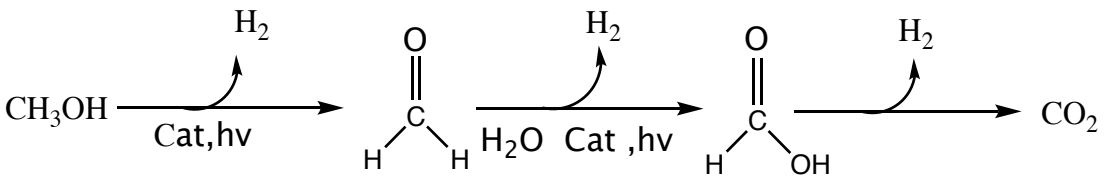

Figure 4.1. Schematic process steps for dehydrogenation of water /methanol mixture.

4.1 Photocatalytic Reaction Mechanism

As mentioned in previous chapters, photocatalysts can convert the energy of sunlight into chemical energy. Although TiO_2 can be excited in the UV range, it displays *per se* a very low activity for hydrogen production. The enhancement of activity can be achieved once noble metals are deposited onto its surface.[1]

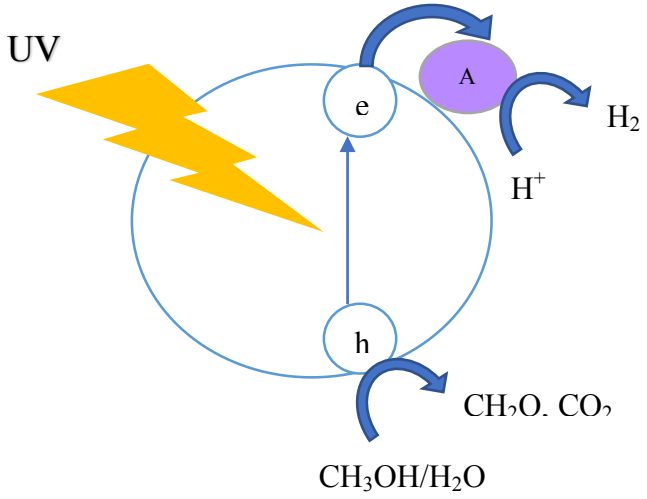

Figure 4.2. Photocatalytic hydrogen production via dehydrogenation of methanol/water mixture using Au/TiO_2.[3]

Figure 4.2 shows the mechanism of dehydrogenation of water/methanol mixtures via Au/TiO_2. The mechanistic steps may be summarized as follows. Firstly, UV light promotes electrons to the conduction band of titanium dioxide, thus forming electron-hole pairs. Secondly, the positive

charge of the holes performs water oxidation with release of O_2 and parallel formation of protons. In the third stage, the electrons in the conduction band are transferred to the gold nanoparticles which, by acting as a nano-electrode, reduces hydrogen ions to H_2. In addition, the hole may also oxidize methanol to formaldehyde (4) and eventually to carbon dioxide by releasing even larger amounts of H_2 as shown in equations (5-7). The overall sequence of events composing the photocatalytic reaction is shown in equation (8). [2,3]

$$TiO_2 + 2hv \rightarrow TiO_2\ (2e^- + 2h^+) \quad (1)$$

$$2h^+ + H_2O \rightarrow \tfrac{1}{2}\ O_2 + 2H^+ \quad (2)$$

$$2H^+ + 2e^- \rightarrow H_2 \quad (3)$$

$$2h^+ + CH_3OH \rightarrow 2H^+ + CH_2O \quad (4)$$

$$CH_3OH \leftrightarrow CH_2O + H_2 \quad (5)$$

$$CH_2O + H_2O \leftrightarrow CH_2O_2 + H_2 \quad (6)$$

$$CH_2O_2 \leftrightarrow CO_2 + H_2 \quad (7)$$

$$CH_3OH + H_2O \leftrightarrow CO_2 + 3H_2 \quad (8)$$

4.2. Effect of different metals

Many studies into the effect of different metal supported titanium dioxide for hydrogen production from water/methanol mixtures have been published in the literature.[4,5,6,7] The results pointed out that gold and platinum provide the best activity for hydrogen production.

Figure 4.3. shows comparative hydrogen production for Au, Ag and Pt supported on TiO_2. As shown, gold had the highest activity compared to the other metals with 24 μmole of hydrogen produced compared to 9 μmole and 6 μmole for platinum and silver respectively.

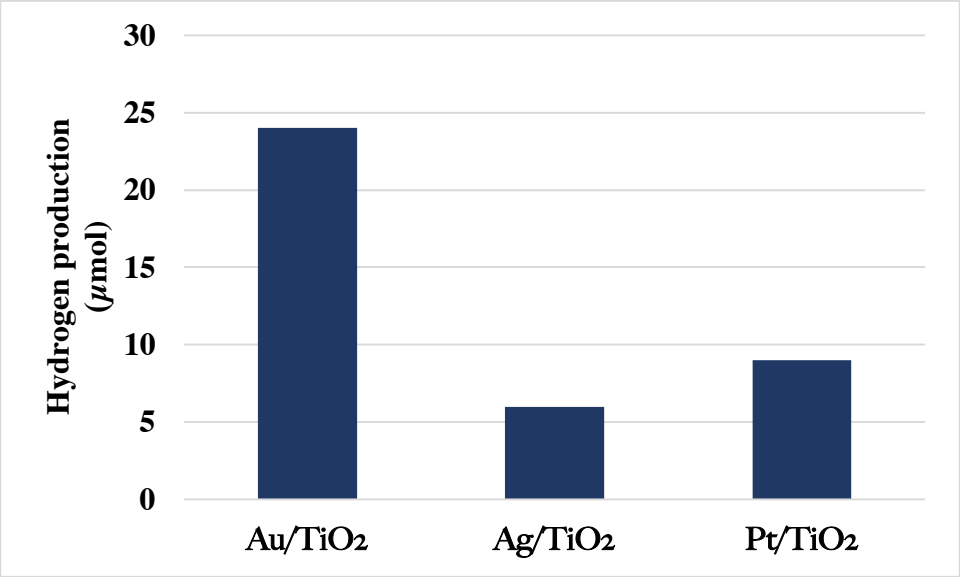

Figure 4.3. The effect of noble metals-loaded TiO_2 prepared via DPU on hydrogen formation. Reaction conditions: Room Temperature, (50 ml H_2O /1mL MeOH mixture),100 mg of catalyst, irradiated with 400 W arc Hg lamp for five hours.

In a seminal study, Brückner and his group indicated that the activity of gold supported titanium dioxide for hydrogen production depends on structural variations introduced by the method adopted for Au deposition.[8] To assess this point, several metals were deposited on TiO_2 using the sol-gel method. TiO_2-P25 (mixture of 70% anatase and 30% rutile) was used as a support. Hydrogen formation was recorded as a function of time Figure 4.4.

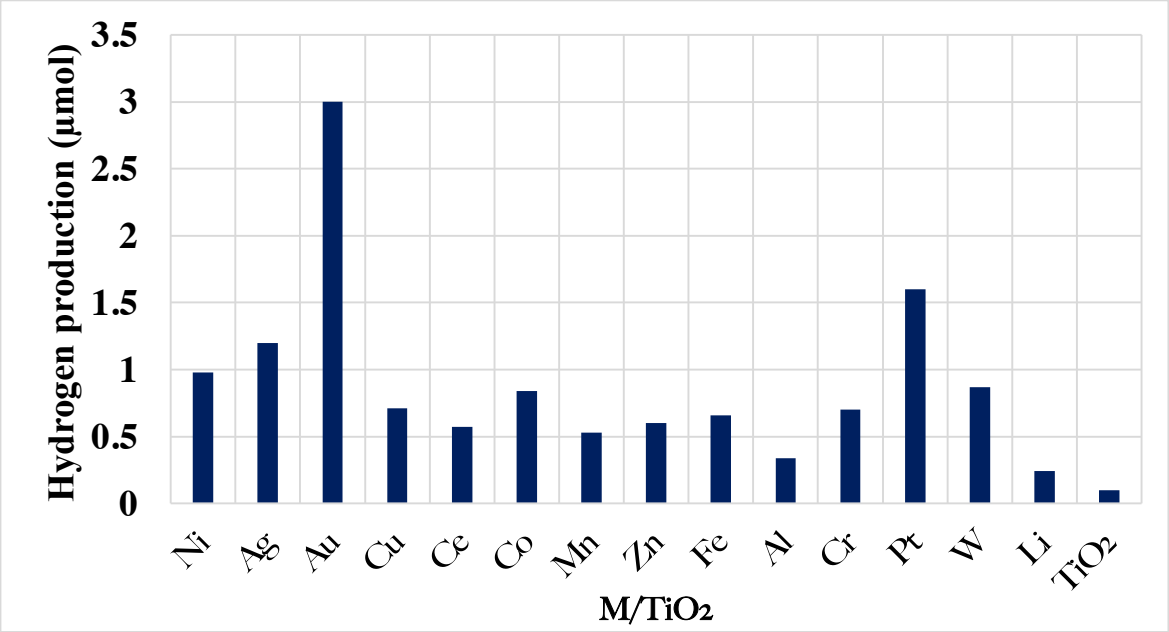

Figure 4.4. The effect of various metal doped TiO_2 prepared via sol gel on the volume of hydrogen generation, Reaction conditions: Room Temperature, (50 ml H_2O /1 mL MeOH mixture) ,100 mg of catalyst, irradiated with 400 W arc Hg lamp for five hours.

As shown in figure 4.4., the noble metal nanoparticles gold, platinum and silver display the best activity. The amount of hydrogen generated by pure TiO_2 was negligible. The three best metals (Au, Ag and Pt) were also deposited using urea instead of the sol-gel technique. Figure 4.5 shows the comparison clearly indicating that the deposition via urea treatment produces by far the most performing catalyst. The reaction of urea with the Au starting salt is described below.

In a standard experiment, suspensions of the starting materials were stirred and heated at 80°C. After eight hours, and due to the presence of chloro-auric acid, the pH of the solution was lowered to 1.3. The titanium dioxide isoelectric point is 6, and the surface is protonated ($TiOH_2^+$) at pH = 3.[2] This results in the adsorption of $AuCl_4^-$ from the solution on to the surface of the titanium dioxide affording Ti-O-$AuCl_3$ units. The steps of decomposition of urea are as follows:

1. The decomposition of urea produces OH^- ions when the temperature is raised to 80^oC.

$$CO(NH_2)_2(aq) + 3H_2O \rightarrow 2NH_4^+(aq) + CO_2(g) + 2OH^-(aq)$$

2. The pH will consequently increase from 3 to 9 thus enhancing ligand exchange reactions on the TiO_2 surface.

$$TiOH_{(s)} + AuCl_3(OH)^-_{(aq)} \leftrightarrow TiOAuCl_{3(ads)} + H_2O + Cl^-_{(aq)}$$

3. Chloride ions are replaced by hydroxyl groups after the eight-hour reaction.

$$Au(OH)nC_{l4}{}^- (n = 1\text{-}3) \rightarrow Au(OH)_{3(s)} \rightarrow Au_2O_{3(s)}$$

4. Dispersion of Au^{3+} on the surface of TiO_2 occurs due to the change in pH.

By using the deposition precipitation method, the active components remain on the surface of TiO_2 and none of them are buried within it. The advantage of using thermal decomposition of urea is that hydroxyl ions are formed slowly through the liquid phase and their concentration is very low due to being consumed rapidly, thereby preventing the precipitation away from the surface of support.

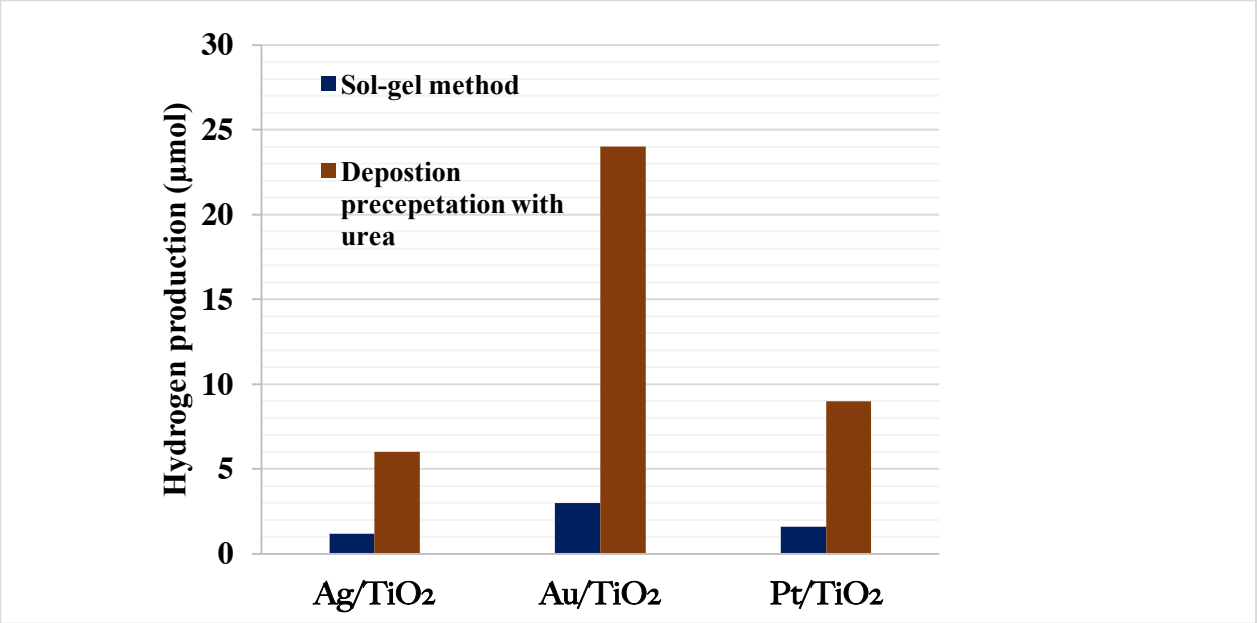

Figure 4.5. The effect of preparation methods of noble metals supported TiO_2 on the volume of hydrogen generation.

4.3 Photocatalytic hydrogen production from various gold loading on TiO_2

Different gold loadings on the surface of titanium dioxide have been examined. Samples of 1, 2 and 4 wt.% Au on titanium dioxide were prepared by adding different amounts of gold stock solution of $HAuCl_4.3H_2O$ (1.1 mM) to milli-Q water. After the addition of urea and TiO_2, the suspensions were stirred and heated at 80 ℃ for 8 hours. The Au(III) containing TiO_2 powders were collected by vacuum, dried for 2 days at 20 ˚C, and then calcined at 300 ˚C for 1 h to thermally reduce surface Au(III) cations to Au(0).

As mentioned before, during the deposition-precipitation with urea, the pH increases gradually over time. Before the decomposition of urea, the low pH indicates the presence of very few OH sites. During the decomposition of urea, the pH gradually increases leading to an increment of the

number of OH sites on the surface of TiO_2. This allows the formation of Au complex surface units and the growth of colloid on the surface of TiO_2. Figure 4.6 shows the TEM images of 1,2,4 *wt.*% Au supported TiO_2. It can be observed that most of the Au particles are located on the surface of TiO_2. The corresponding formation of hydrogen is shown in Figure 4.6, the optimal weight loading was 2 wt.% .

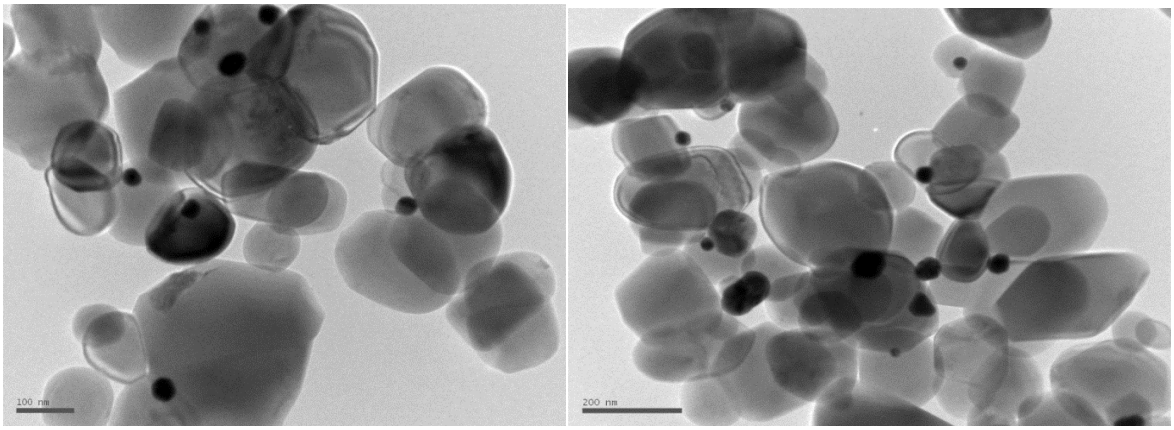

a) 4 *wt.*% Au /TiO_2

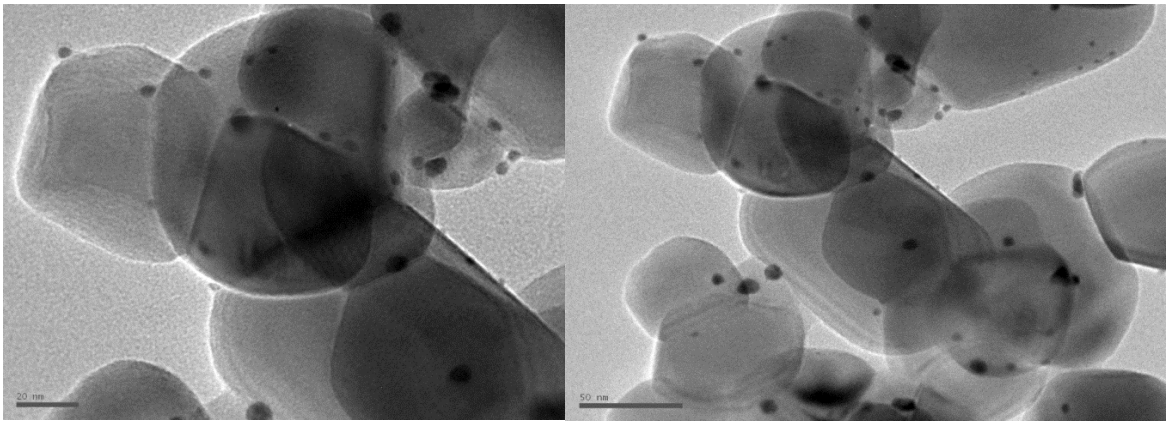

b) 2 *wt.*% Au /TiO_2

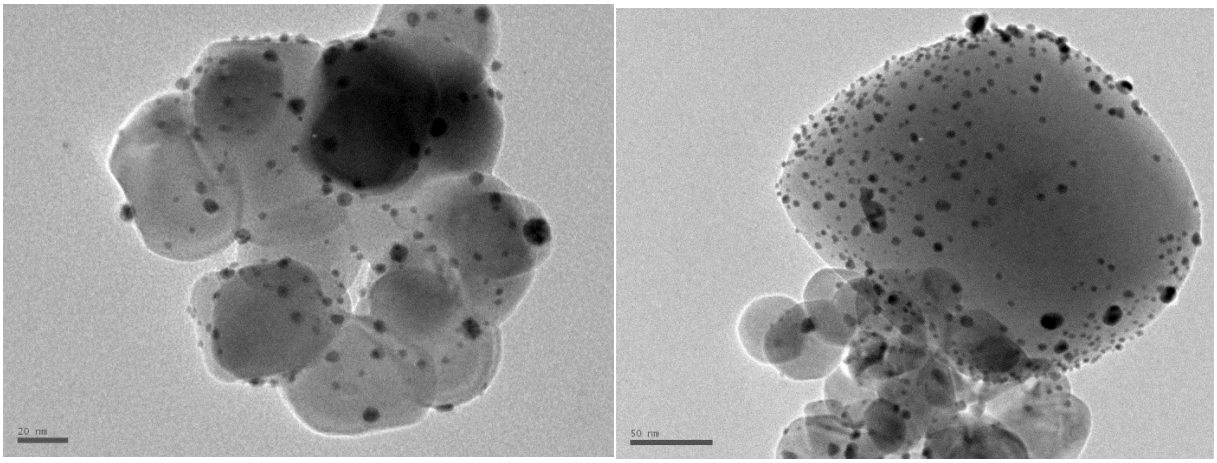

a) 1 *wt.*% Au /TiO_2

Figure 4.6. TEM images of various Au deposited on the surface of TiO_2.

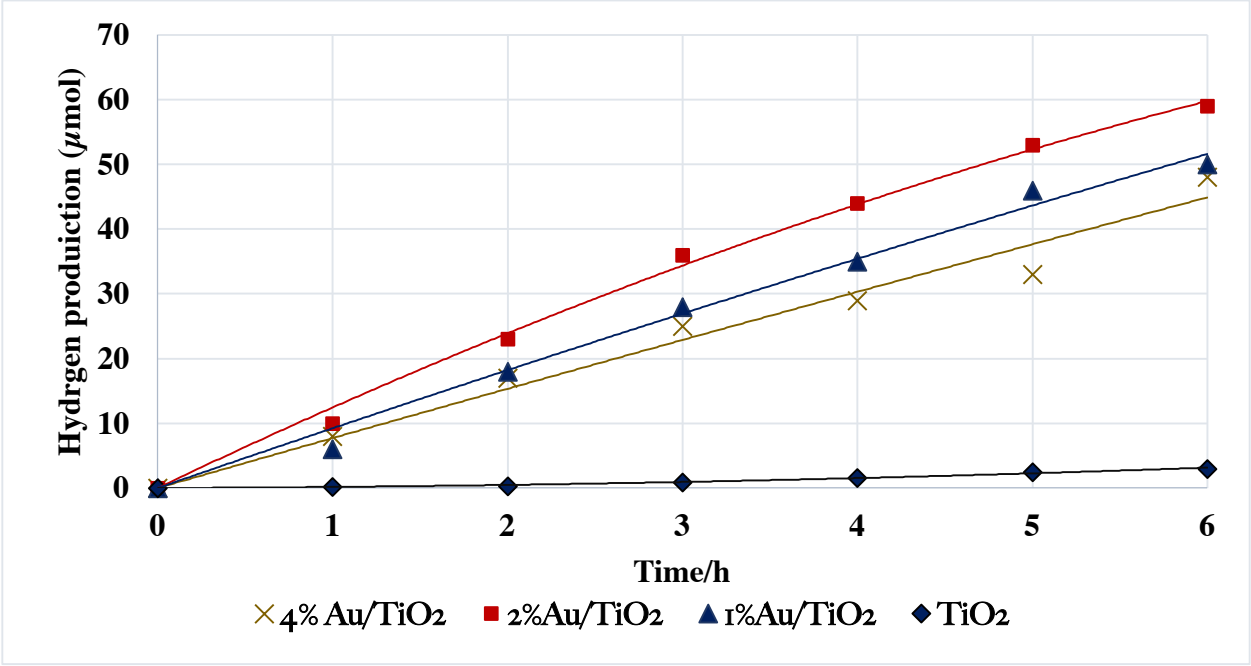

Figure 4.7. Hydrogen production from water/methanol using various Au loading.

4.4 Effect of different TiO_2 supports on the photocatalytic hydrogen production from methanol/water mixture over 4 wt.% Au/TiO_2

In this study, we have focused on Au/TiO_2 4%wt. because it showed the ability to dehydrogenate methanol to formaldehyde and eventually to carbon dioxide during photocatalytic hydrogen production. Instead, with other 1- and 2 % wt. loadings, no products were detected during hydrogen production. Gold nanoparticles 4 %wt. were supported on three different titanium dioxide structures, rutile, anatase, and P25 (which is a mixture of 70:30 anatase: rutile). The deposition was performed via the urea precipitation method and the samples tested to compare the photocatalytic activities. Figure 4.8 shows anatase as the best photocatalyst. This is probably due to a combination of reasons, such as the presence of a wider band gap, longer charge-carrier lifetime, longer exciton diffusion length, and higher charge-carrier mobility.

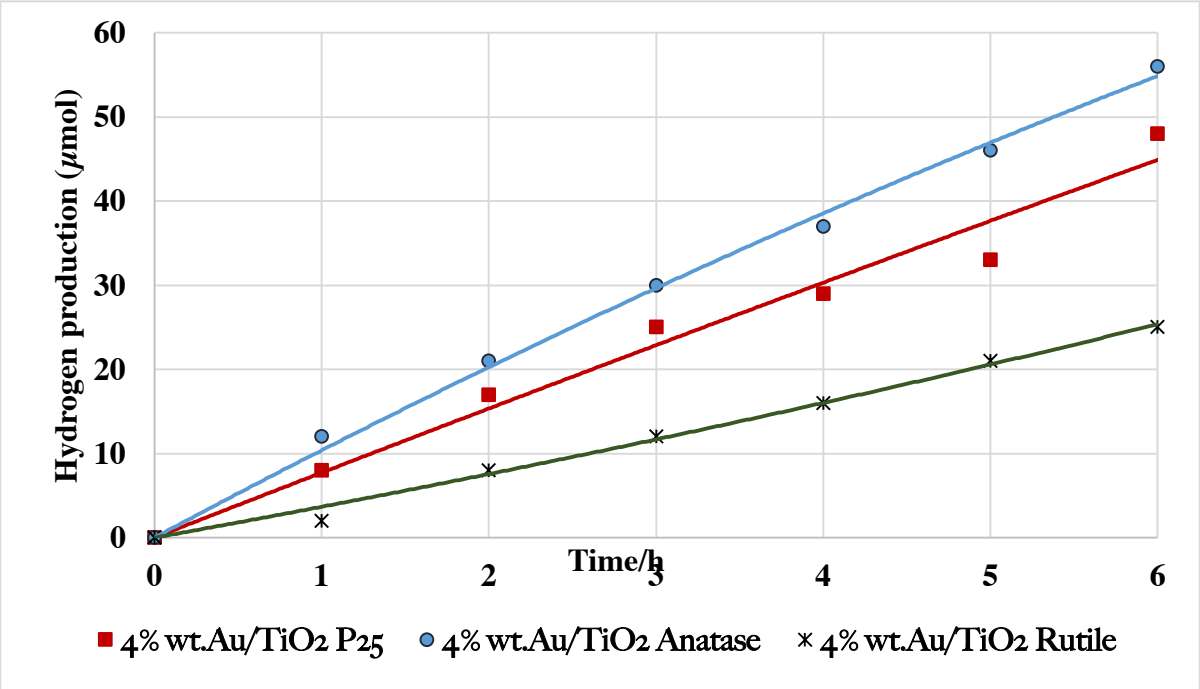

Figure 4.8. Hydrogen production from methanol/water over different TiO_2 structures with Au.

4.5 Effect of pH on the production of hydrogen

The reaction environment affects the activity of photocatalytic hydrogen production from water/methanol mixtures. The experiments were performed at room temperature and pressure. The initial pH (approximately 10) remained unchanged during the entire experimental run. Figure 4.9. and 4.10. show the amount of hydrogen produced with and without NaOH as base. The results indicate that at the alkaline conditions are slightly beneficial to hydrogen evolution. In addition, reactions in alkaline conditions continuously produced hydrogen for more than ten days (figure 4.10.). After ten days, the volume of hydrogen gradually decreased. At this stage. the color of the photocatalyst changed to dark purple in parallel to a slight photocatalytic deactivation. The deactivation of Au/TiO_2 catalyst may be due to the saturation of the active sites.

The deactivated catalyst was easily recovered by centrifugation, and dried at 60 ℃ for 24 h. After recovery and heating, the catalyst regained over 90% of its activity.

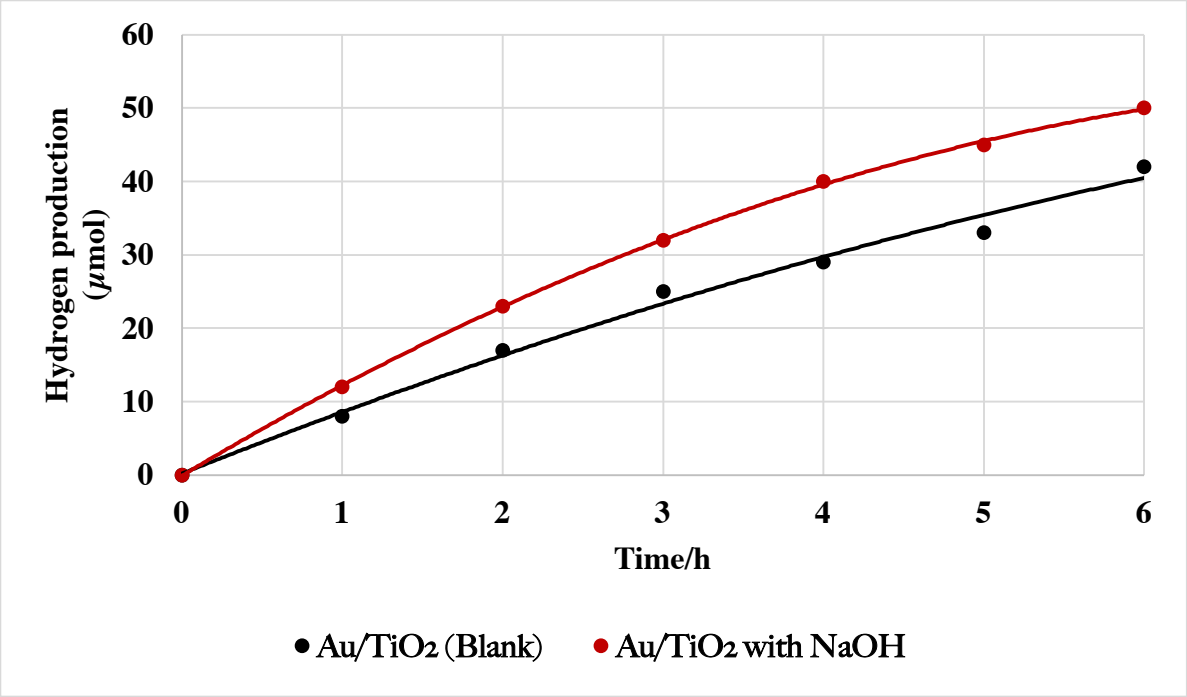

Figure 4.9. Hydrogen production with NaOH and without NaOH as blank.

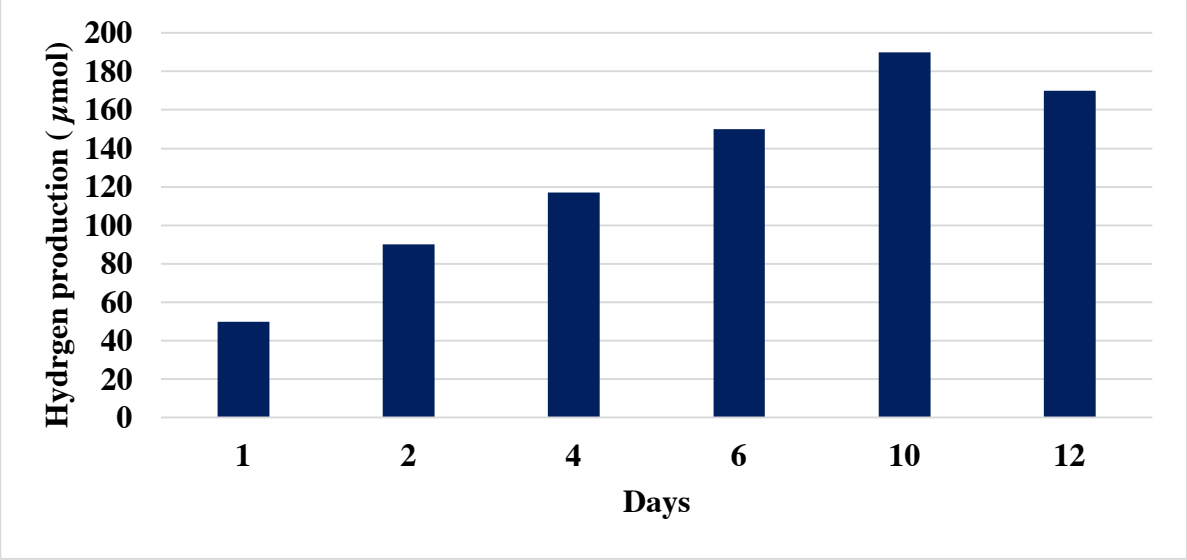

Figure 4.10. Long range hydrogen production with NaOH.

4.6 Effect of different amount of methanol

As mentioned previously, the role of sacrificial reagents such as alcohols and other organic materials is to enhance the photocatalytic activity and increase the volume of hydrogen production. Another feature is to reduce the extent of electron-hole recombination.[8,9,10] Bowker and coworkers have studied the effect of the addition of various amounts of methanol on 0.5%Pd-TiO_2. At low concentrations of methanol (micromoles), the amount of hydrogen production is very low but it is augmented with the increasing concentration of methanol. At a higher content of methanol, there was no significant increase in the volume of hydrogen production. [11]

To study the effect of methanol on hydrogen production, varying amounts of methanol were used Figure 4.11. The hydrogen production from pure water is almost zero, but with increasing methanol, hydrogen production augmented with parallel decomposition of the alcohol.

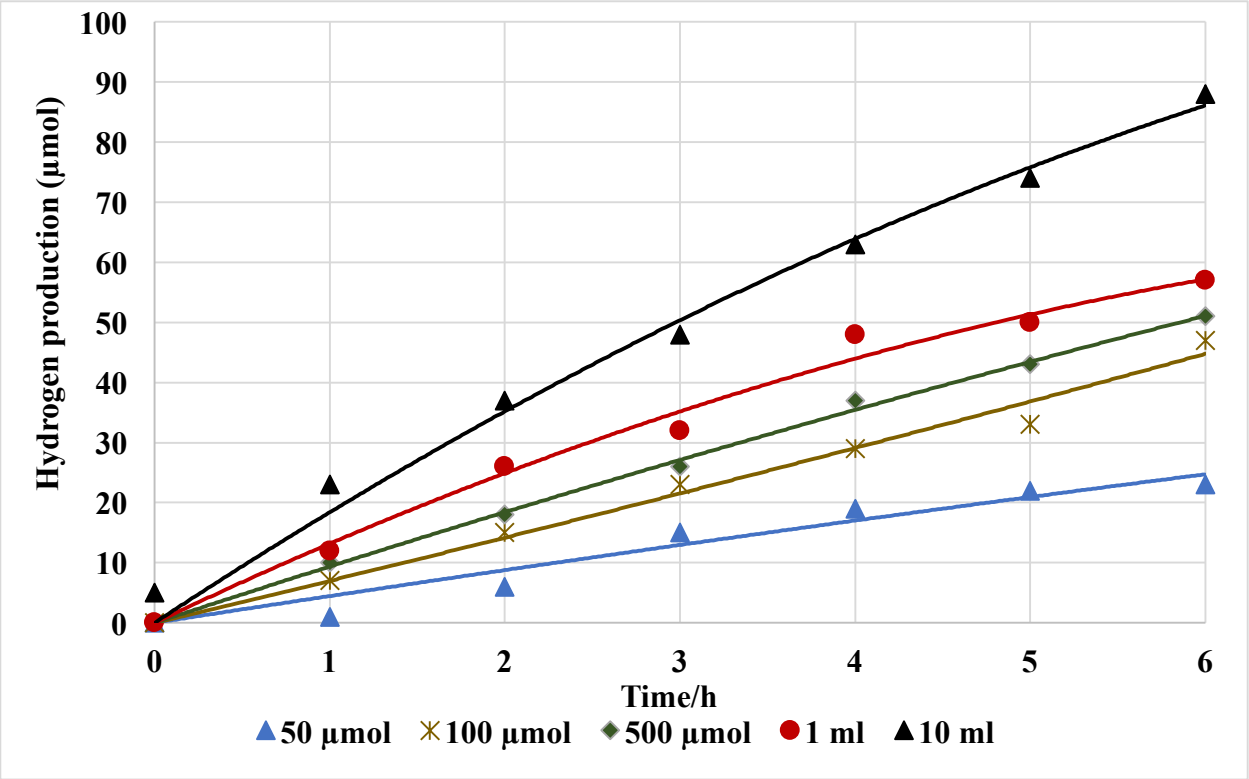

Figure 4.11. Hydrogen production at different volumes methanol.

4.7 Effect of 4%Au-TiO_2 catalyst mass

To determine the effect of the mass of the catalyst on hydrogen production, experiments were performed with masses varying between 50 mg to 250 mg. The conditions of the reaction were kept the same. Figure 4.12 shows the effect on hydrogen production.

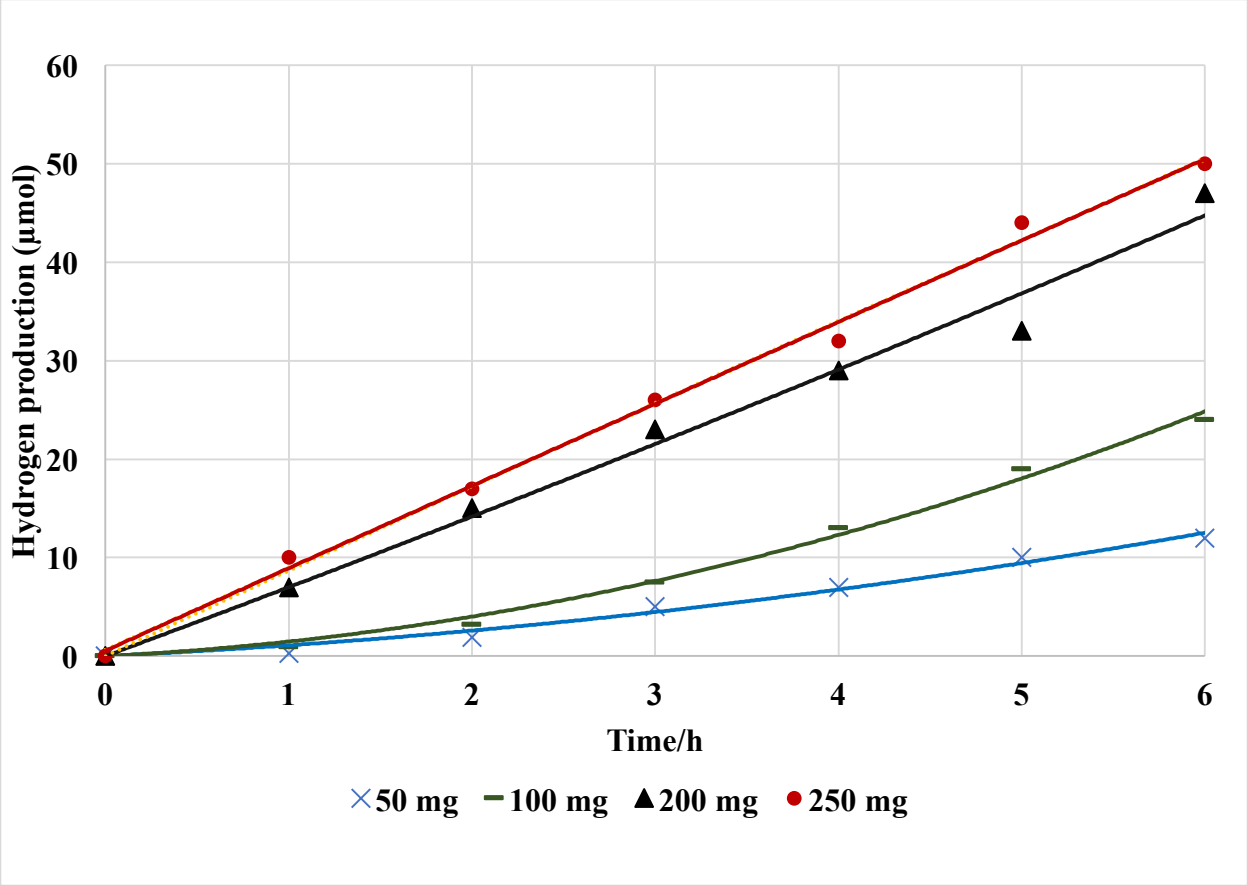

Figure 4.12. Hydrogen production at different 4 wt. %Au/TiO_2 masses.

4.8 Identification of by-products during the Photocatalytic Hydrogen Production over methanol/water mixture

Formaldehyde is one of the most elusive intermediate in the photo-oxidation of methanol due to its reactivity and intrinsic instability. During irradiation, samples were analyzed in an GC-FID to determine the concentration of methanol. Quantification of formaldehyde concentrations was carried out by a colorimetric procedure using Nash reagent.[13] The concentration was determined spectrophotometrically with a standard calibration curve. The experimental analyses were carried

out in triplicate to confirm the results. The data shown in Figure 4.13 gives the average values obtained from the three experiments.

As shown in Figure 4.13, a decrease in the concentration of methanol occurs during the reaction in parallel to the formation of formaldehyde. Similarly, the concentration of the initially formed formaldehyde decreases to yield carbon dioxide.

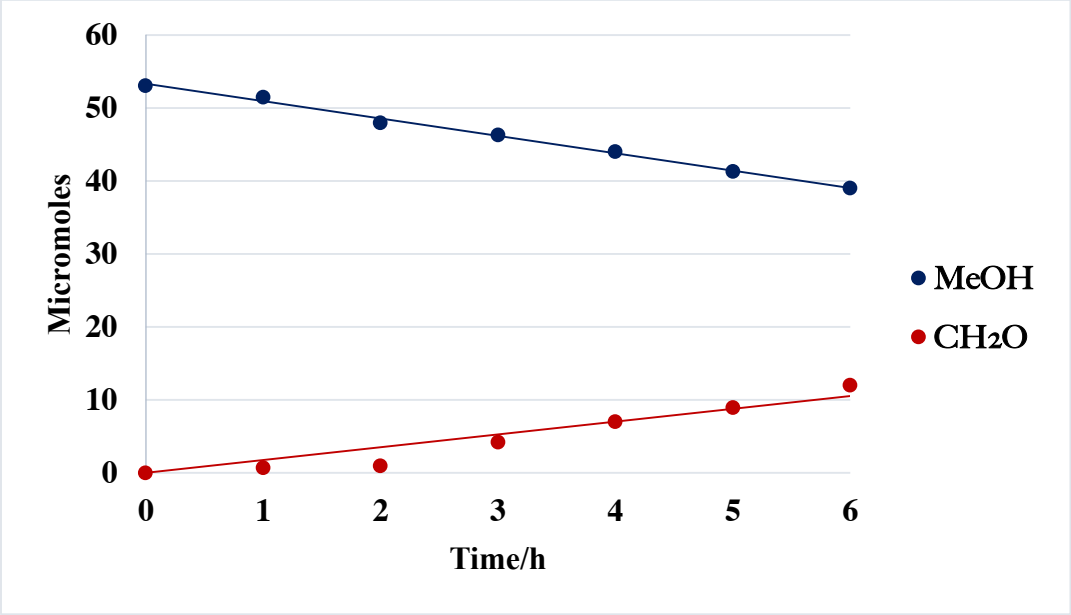

Figure 4.13. The concentration of methanol and formaldehyde during the photocatalytic hydrogen production. Reaction parameters: 100 µl MaOH,100 mL H_2O, 200mg 4 wt % Au/TiO_2

The formation of all these products can be regarded as a result of a multi-stage sequence each separated into steps.

First Stage

1) Without irradiation, adsorption of both the organic molecule (methanol) and water takes place on the surface of TiO_2.

$$\text{Organic Molecule}_{(l)} \xrightarrow{Au-TiO_2} \text{Organic Molecule}_{(ads)} \quad (4\text{-}1)$$

$$H_2O_{(l)} \xrightarrow{Au-TiO_2} H_2O_{(ads)} \quad (4\text{-}2)$$

2) During irradiation charge-separation takes place and photoreactions are initiated. Photons with appropriate energy excite the TiO_2 particles as described below.

$$h\nu \xrightarrow{Au-TiO_2} h^+ + e^- \quad (4\text{-}3)$$

3) Holes react with adsorbed OH^- hydroxyl ions on the surface of TiO_2 forming hydroxyl radicals OH•.

$$2H_2O_{(ads)} \xrightarrow{Au-TiO_2} H^+_{(ads)} + 2OH^-_{(ads)} \quad (4\text{-}4)$$

$$2OH^-_{(ads)} + h^+ \xrightarrow{Au-TiO_2} 2OH^{\cdot} \quad (4\text{-}5)$$

4) Gold nanoparticles immobilized on titanium dioxide act as electron reservoirs. At this point, protons remain adsorbed on the TiO_2 surface forming H• radicals, in turn, yielding H_2.

$$2H^+_{(ads)} + 2e^- \xrightarrow{Au-TiO_2} 2H^{\cdot} \quad (4\text{-}6)$$

$$2H^{\cdot} \xrightarrow{Au-TiO_2} H_{2(g)} \quad (4\text{-}7)$$

Second stage (photo-oxidation of methanol to formaldehyde)

The hydroxyl radicals formed during irradiation are consumed by the organic scavenger (methanol) forming formaldehyde.

$$CH_3OH + 2OH^{\cdot} \xrightarrow{Au-TiO_2} CH_2O + 2H_2O_{(l)} \quad (4\text{-}8)$$

with the overall reaction being:

$$CH_3OH_{(l)} \xrightarrow{Au-TiO_2} H_{2\,(g)} + CH_2O_{(ads)} \quad (4\text{-}9)$$

Third stage (Conversion of formaldehyde into formic acid)

During irradiation, hydroxyl radicals are consumed by the formaldehyde to form formic acid.

OH• radicals attack the adsorbed formaldehyde molecules resulting in the formation of adsorbed CHO anions as follows:

$$CH_2O_{(ads)} + 2OH^{\cdot} \xrightarrow{Au-TiO_2} HCOOH_{(ads)} + H_2O_{(ads)} \quad (4\text{-}10)$$

Fourth stage (Conversion of Formic Acid into Hydrogen and CO_2)

The hydroxyl radicals perform the final oxidation of formic acid to CO_2.

$$HCOOH + 2OH^{\cdot} \xrightarrow{Au-TiO_2} CO_{2ads} + 2H_2O \quad (4\text{-}11)$$

Overall equation:

$$HCOOH \xrightarrow{Au-TiO_2} H_{2\,g} + CO_{2\,g} \quad (4\text{-}12)$$

Figure 4.14. shows the formation of CO_2 as the final reaction product. One can observe that steady CO_2 photo-formation is due to the oxidation of the sacrificial agent. CO_2 gas was analyzed by GC-TCD and quantified using a calibration curve. As shown the amount of carbon dioxide formed was less than hydrogen. ESI-MS using deuterated water confirmed that H_2, HD and D_2 were produced thus indicating that both water and methanol were oxidized. Experiments using O^{18}-labelled water confirmed that the two oxygen atoms in CO_2 originated from both methanol and water oxygen atoms.

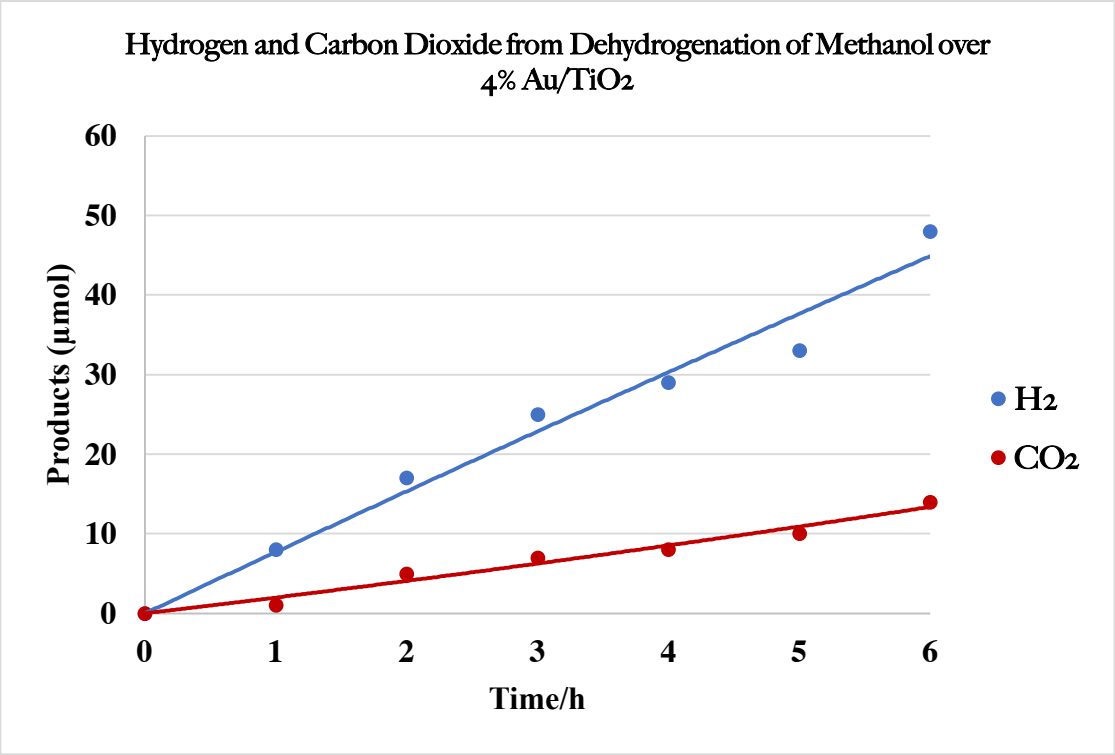

Figure 4.14. The amount of carbon dioxide generated from the dehydrogenation of methanol/water mixture via 4% Au/TiO_2

4.9 H_2 production from isopropanol/water mixtures over 4 wt. % Au/TiO_2 P25

Recent reports have shown the ability of other alcohols, such as ethanol and glycerol, to act as sacrificial agents in the photocatalytic hydrogen formation.[14,15,16]

Given the behavior of methanol for improving hydrogen production with 4 wt.% Au/TiO_2 photocatalysts, analyzing the behavior of other alcohols was the next obvious step. In this section, we describe the utilization of isopropanol as a sacrificial agent. Its dehydrogenation in presence of water by a Pt/TiO_2 photocalyst has been previously examined by Aitichou group, finding that the simultaneous presence of isopropanol and water was important for the reaction.[20] We have performed similar reactions by irradiating 4 wt.% Au/TiO_2 P25 in aqueous isopropanol with a Hg 400 W arc lamp at room temperature.

The comparative diagram reported in Figure 4.15. clearly indicates that the performance of isopropanol is inferior to methanol. Hydrogen production decreases with increasing carbon number of alcohols.

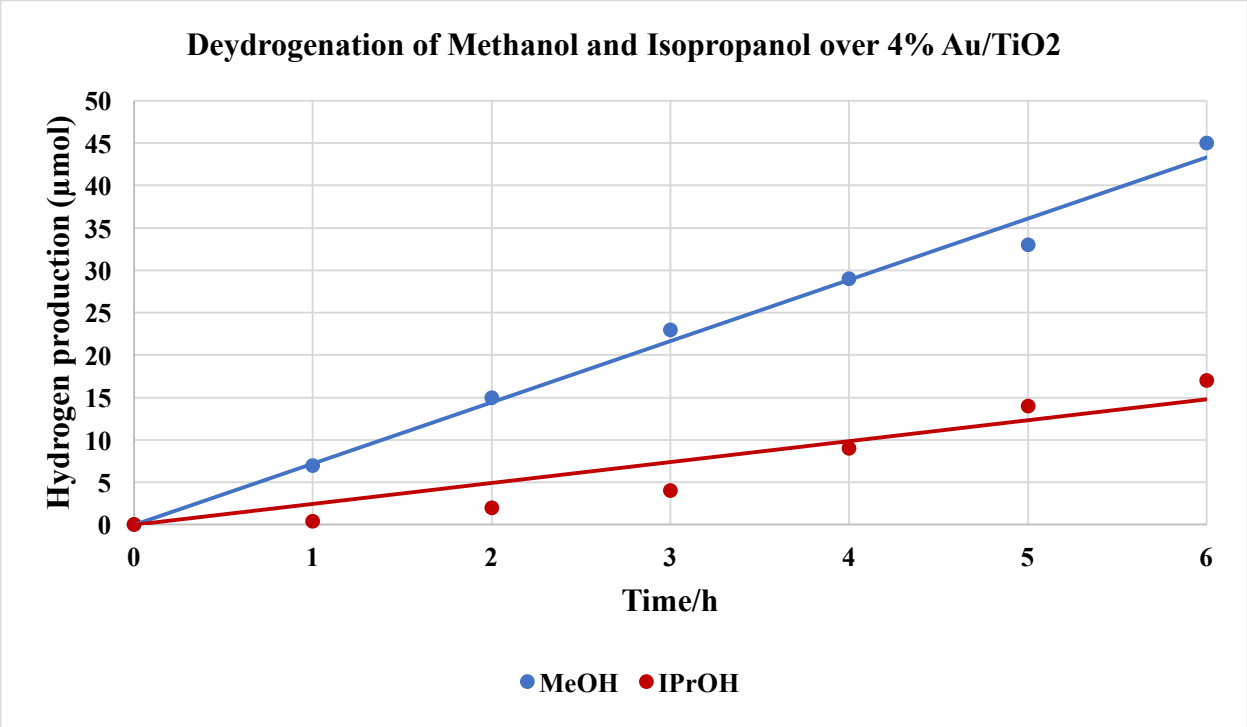

Figure 4.15. Hydrogen evolution from MeOH and IPrOH solution.

To assess the behavior of isopropanol during the photocatalytic decomposition, pure alcohol and various mixtures with water were irradiated in the presence of 100 mg of 4 wt.% Au/TiO_2. Table 4.1. reports the different reaction conditions.

Table 4.1. Various isopropanol water mixtures.

Reaction	**Isopropanol (ml)**	**Water (ml)**	**Photocatalysts**
A	50	0	No catalyst
B	50	0	200 mg 4 wt.% Au/TiO_2
C	45	5	200 mg 4 wt.% Au/TiO_2
D	25	25	200 mg 4 wt.% Au/TiO_2
E	5	45	200 mg 4 wt.% Au/TiO_2

The results of the photodecomposition are highlighted in Figure 4.16. The difference between hydrogen production from isopropanol with and without catalyst (A and B) clearly indicates that the catalyst is necessary. The addition of a small amount of water into the reaction mixture increases the productivity of hydrogen. However, the addition of larger amount of water has a detrimental effect on the production of hydrogen. These results indicate that the overall process is not a pure water splitting reaction.

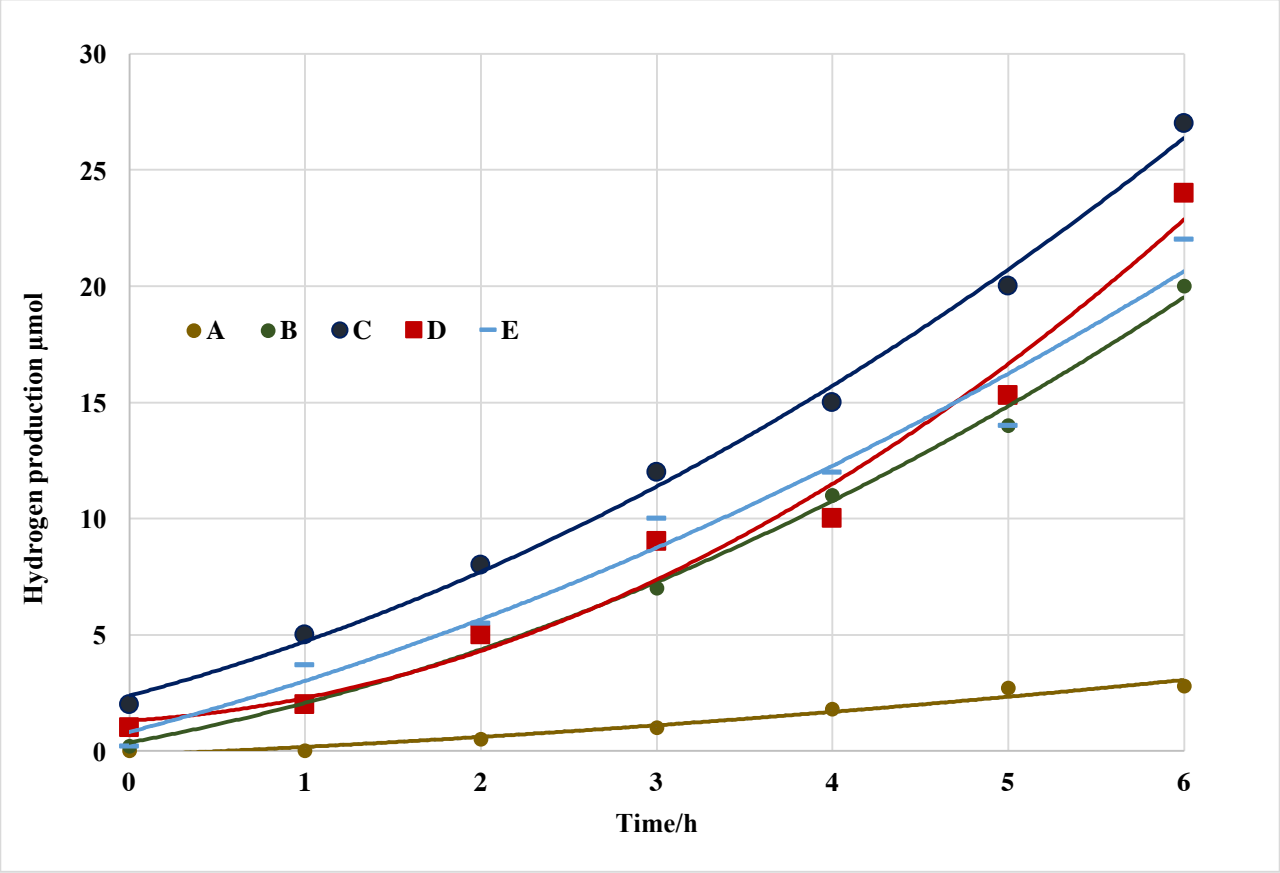

Figure 4.16. Different mixture of water/isopropanol over 200 mg 4 wt.% Au/TiO_2P25 with different isopropanol mixtures .

4.10 The effect of different TiO_2 supports on H_2 production from water/isopropanol mixture over 4 wt.% Au/TiO_2

This section illustrates the activity of the 4 wt. % Au on different TiO_2 phases such as TiO_2 P25 (70% anatae, 30% rutile), TiO_2 anatase, and TiO_2 rutile for hydrogen production from isopropanol /water mixtures. The aim of this study is to investigate the effect of the support on the photocatalytic production of hydrogen from isopropanol/water mixtures.

Figure 4.17. reports the amounts of hydrogen and acetone generated from isopropanol/water mixtures over three photocatalysts: 4 *wt.* % Au /TiO_2 anatase, 4 *wt.* % Au /TiO_2 rutile, and 4 *wt.* % Au /TiO_2 P25. In absence of catalyst, no hydrogen and acetone were formed. The comparison between the three systems clearly shows that Au/TiO_2 anatase is the most productive. Also of interest is that no carbon dioxide and other products were observed during the reaction implying that the photoxidation of acetone is not occurring and that the reaction is therefore selective.

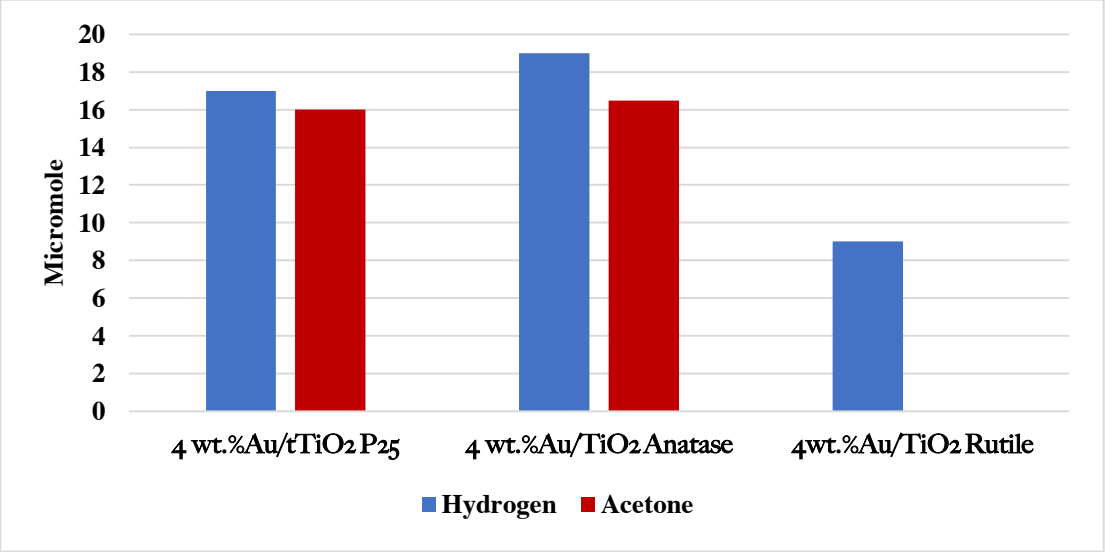

Figure 4.17. H_2 and acetone generation via 4 wt. %Au at different structures of TiO_2 in isopropanol /water mixtures Reaction condition: 100 μl isoprpanol ,100 ml water ,irradiation with UV 400 W Hg at RT.

4.11 The effect of bimetallic catalysts on the hydrogen production rate during the dehydrogenation of water/alcohols mixtures

As mentioned previously, there is common agreement in the literature that noble metals nanoparticles supported on TiO_2 are providing more efficiency for photocatalytic hydrogen production from alcohols such as methanol, ethanol and glycerol in the presence of water.[14] Bimetallic nanoparticles supported on TiO_2 such as Au-Pt, Au-Ag and Ag-Pt, Au-Pd have been investigated to tune the efficiency of the charge separation.[15,16] Recent studies showed that bimetallic Au-Pd and Au-Pt have an excellent photocatalytic activity for hydrogen production from ethanol and benzene.[16,17] Therefore, in this work, monometallic Au, Ag, and Pt and bimetallic Au/Ag and Au/Pt supported on titanium dioxide P25 (70% anatase and 30% rutile) were synthesized by sol immobilization.[18] These catalysts were tested to investigate their activities for photocatalytic hydrogen production for the dehydrogenation of methanol and isopropanol in the presence of water. The results are described below.

4.11.1 Monometallic catalysts for hydrogen production from alcohols /water mixture

Catalytic experiments were carried out in 250 ml quartz flask, with reaction mixtures containing 100 μl of alcohol (methanol or isopropanol), 100 ml of water and 200 mg of catalyst. The system was purged with argon for 20 min and irradiated for six hours. Samples for GC analysis were taken every 50 min.

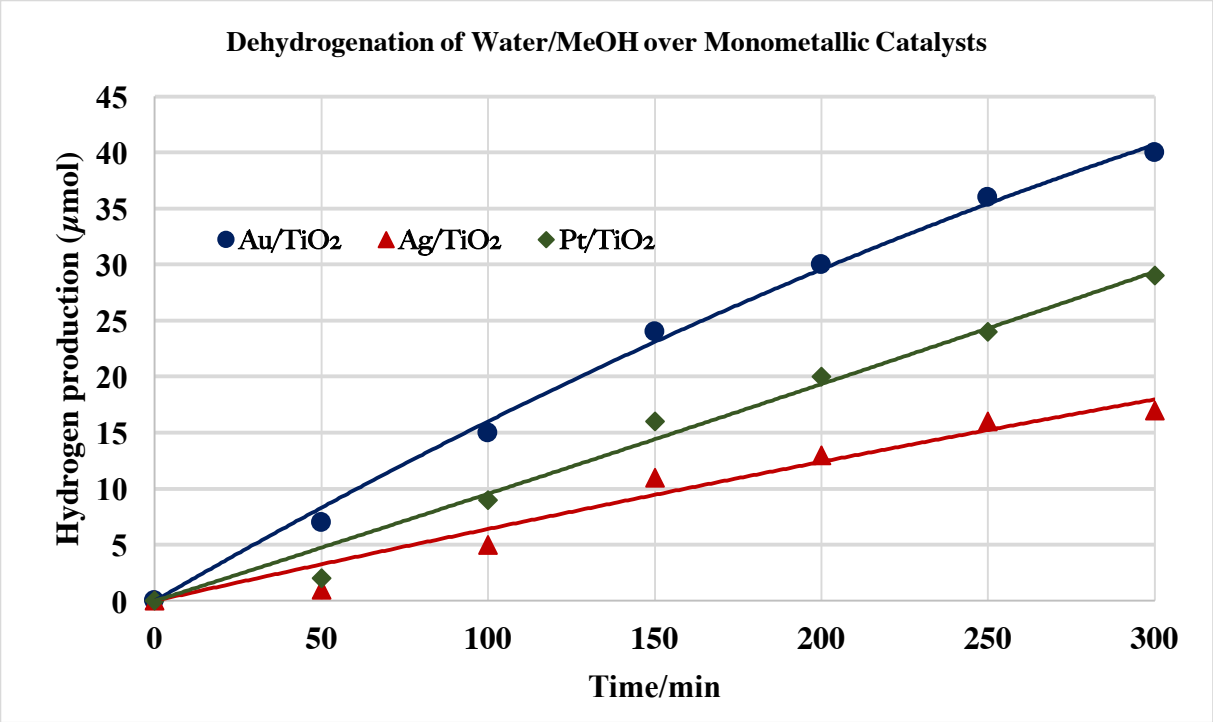

Figure 4.18. Hydrogen production from methanol /water mixture.

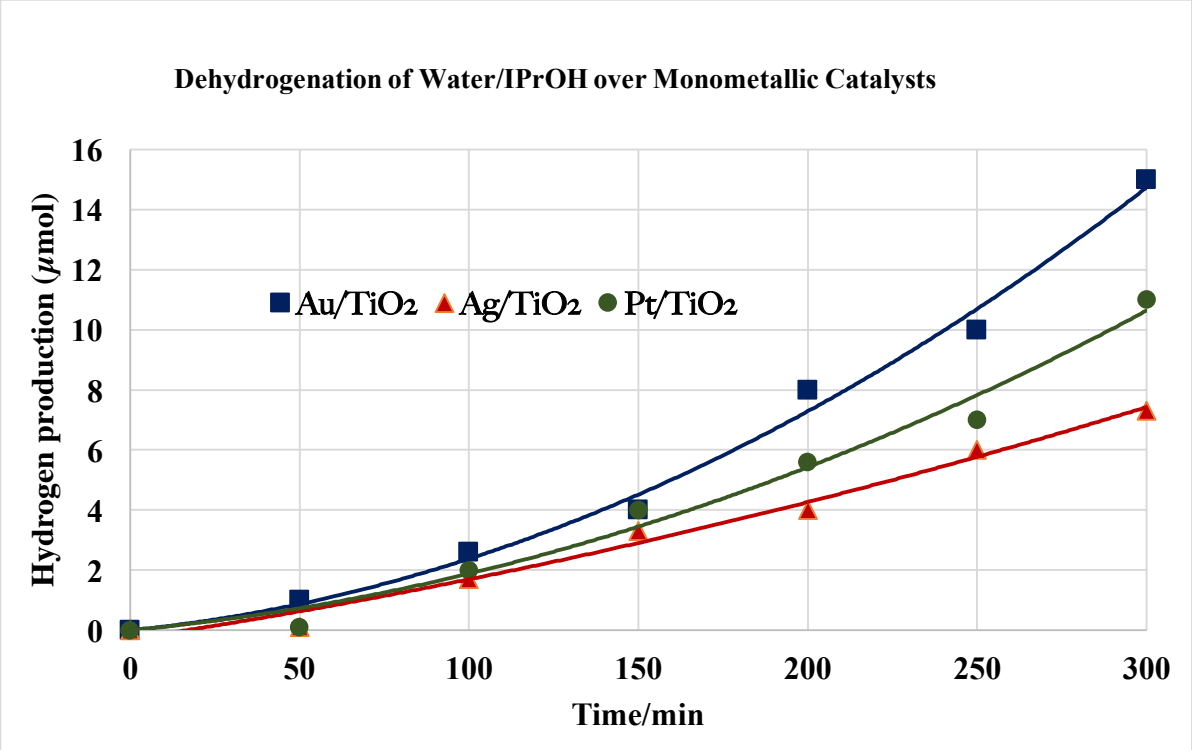

Figure 4.19. Hydrogen production from isopropanol/water.

Figures 4.18. and 4.19. show the amount of hydrogen produced by water/methanol and water/isopropanol solutions. The amount of hydrogen increased with time and independently on the catalyst used. Au/TiO_2 was more active in both systems while Ag/TiO_2 was the least active catalyst. These monometallic catalysts have a better activity for the hydrogen production from methanol in comparison to isopropanol. Nanoparticles of Au, Ag, and Pt supported by titanium dioxide prepared by sol immobilization were less active than the respective catalysts prepared via deposition/precipitation of urea.

4.11.2 Bimetallic catalysts for hydrogen production from alcohols /water mixture

Heterodimetallic catalysts , Au-Ag, and Au-Pt supported titanium dioxide P25 were synthesized via sol immobilization. In a standard preparation, a solution of $HAuCl_4.3H_2O$ was treated with polyvinyl alcohol(PVA) (PVA/Au-Ag = 1:2) followed by the addition of a solution of $NaBH_4$ (0.1M, $NaBH_4$/Au = 5:1) to form a sol. After stirring the solution for 30 min., a solution of $AgNO_3$ was added, followed by the addition of $NaBH_4$ (1:5). The resulting mixture was stirred for an additional 30 minutes. After sol formation and under vigorous stirring, titanium dioxide was added to the mixture (acidified to pH 1 by sulfuric acid). After 2 hours the slurry was filtered, the catalyst was washed with distilled water to remove soluble species such as Na or Cl, and the solid residue collected and dried at 120℃ overnight.

The experimental set up for photochemical experiments was as described in chapter 3.3.6. In a 250 mL quartz flask, 100 μL of alcohol (methanol or isopropanol), 100 mL of water and 200 mg of catalyst were added. These mixtures were purged with argon for 20 min and irradiated for six hours. Samples were taken every 50 min and analyzed by GC.

Figures 4.20 and 4.21 show the production of hydrogen from the photocatalytic dehydrogenation of methanol/water mixture by two different bimetallic nanoparticles: AuAg/TiO_2 and AuPt/TiO_2.

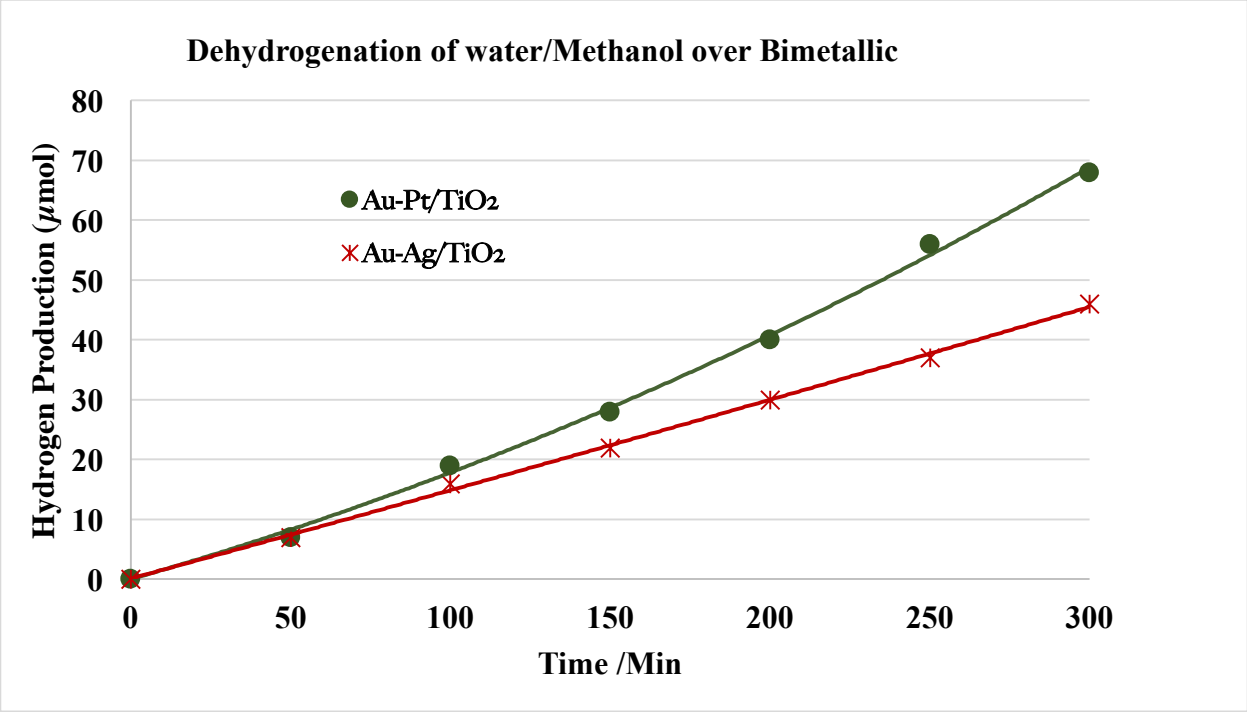

Figure 4.20. Hydrogen evolution from methanol/water mixture over bimetallic/TiO_2.

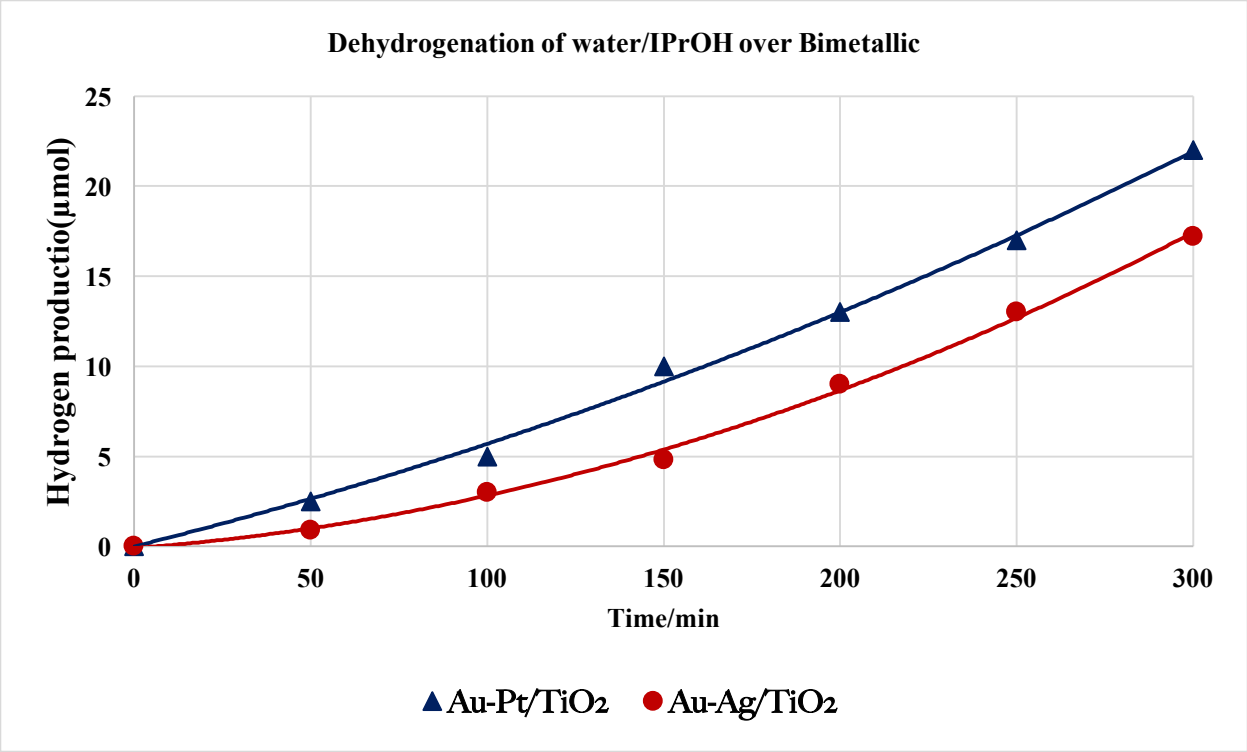

Figure 4.21. Hydrogen evolution isopropanol /water mixture over bimetallic/TiO_2.

In both reactions Au-Pt supported titanium dioxide showed a better activity for photocatalytic hydrogen production than Au-Ag supported titanium dioxide with 67 µmol and 22 µmol of methanol and isopropanol respectively. The good activity of Pt is due to its high density of near Fermi levels E_F and this electronic factor might have a role in charge separation.[24] By decreasing the charge-carrier recombination, as the distance between redox sites and charge formation sites minimizes.[26]

As shown previously, the rates of hydrogen production from the photocatalytic dehydrogenation of methanol/water samples were significantly higher than the rates from the dehydrogenation of isopropanol/water. Moreover, for the photocatalytic hydrogen production from alcohol/water mixtures, it is clearly evident that the amount of hydrogen obtained from

bimetallic systems is better than from the monometallic system. In the case of the Au-Pt/TiO_2 nanocomposite the hydrogen production increased up to 3 times for MeOH than with Au1/TiO_2 synthesized by deposition precipitation with urea. When Au-Ag/TiO_2 was used, the rate of hydrogen formation increased up to 2 times than that of Au/TiO_2. Clearly, the Schottky barrier at the junctions between the metal and TiO_2 decreases the recombination of photogenerated e^- and h^+ and the metal acts as an electron trap. The good activity of bimetallic AuPt/TiO_2 for hydrogen production results from the interaction between the Au and Pt. This interaction decreases the metal–hydrogen bond strength, thus facilitating the desorption of H_2 from the metal surface and enhances the electron trapping ability of metals nanoparticles. [21,25]

4.12 Conclusion

In this chapter, we have evaluated different parameters affecting the rate of hydrogen evolution during photocatalytic dehydrogenation of alcohol mixtures with water. The main conclusion of these studies can be summarized as follows.

- Among the different metal-supported titanium dioxide P25 (anatase 70%, and rutile 30%) obtained by deposition/precipitation with urea, the best catalyst was gold-supported titanium dioxide.
- The effect of different metals supported on titanium dioxide synthesized using a sol gel technique was tested to study the effect of the preparation method on the amount of hydrogen evolution. The best method for preparing Au supported TiO_2 appears to be deposition precipitation with urea.

- The effect of gold loading levels on titanium dioxide was examined finding that 2 wt. % Au /TiO_2 has a higher rate of hydrogen production compared to 1 and 4 wt. % .
- To compare the effect of different surface structures of titanium dioxide, anatase, rutile, and P25 (mixture of 70% of anatase and 30% rutile) were used for photocatalytic hydrogen production with 4% gold loading. The results indicated that anatase TiO_2 4% Au was the most active support compared to rutile and P25.
- The effect of alkaline conditions on the rate of hydrogen production was studied with NaOH indicating that the photocatalytic activity increased in alkaline mediums. Also, the reaction continued for more than ten days when base was added compared to several hours when reaction mixtures contained no base.
- Reactions with different volumes of methanol were probed. It was found that the volume of hydrogen evolution increased with increased volume of methanol.
- The quantity of 4% Au/TiO_2 catalyst was investigated to study the effect on the volume of hydrogen production. The optimum rate was obtained when 200 mg of 4% Au/TiO_2 was used.
- During the photocatalytic hydrogen production in presence of methanol, formation of formaldehyde was observed.
- The activity of 4% Au/TiO_2 with isopropanol as a sacrificial regent instead of methanol was also probed. The results showed that the volume of hydrogen production with isopropanol were inferior to the case of methanol.
- Photocatalytic hydrogen production from methanol and isopropanol were studied over monometallic Au, Ag, Pt supported on TiO_2 made by a sol immobilization method. It was found that a higher amount of hydrogen production was obtained when Au/TiO_2 was used

in both reactions. Also, the amount of hydrogen production was higher when methanol was used as a sacrificial reagent over all three monometallic photocatalysts. However, these monometallic Au, Ag and Pt have lower activity in terms of hydrogen production compared to 4 wt. % Au/TiO_2 synthesized by deposition precipitation with urea.

- The bimetallic nanoparticles Au-Ag and Au-Pt supported on titanium dioxide were prepared by sol immobilization technique. These bimetallic photocatalysts were tested to investigate their activity for hydrogen production with two different alcohols (methanol and isopropanol). Au-Pt $/TiO_2$ showed the greatest activity for hydrogen production in both reactions. Also, the results showed that bimetallic nanoparticles were more active than monometallic due to plasmatic absorption and efficient electron trapping.

4.13 References

(1) Zaleska, A. *Recent Patents on Engineering* **2008**, *2*, 157–164.

(2) Gärtner, F.; Losse, S.; Boddien, A.; Pohl, M.-M.; Denurra, S.; Junge, H.; Beller, M. *ChemSusChem* **2011**, *5*, 530–533.

(3) Oros-Ruiz, S.; Zanella, R.; López, R.; Hernández-Gordillo, A.; Gómez, R. *Journal of Hazardous Materials* **2013**, *263*, 2–10.

(4) Alenzi, N.; Liao, W.-S.; Cremer, P. S.; Sanchez-Torres, V.; Wood, T. K.; Ehlig-Economides, C.; Cheng, Z. *International Journal of Hydrogen Energy* **2010**, *35*, 11768–11775.

(5) Kennedy, J.; Jones, W.; Morgan, D. J.; Bowker, M.; Lu, L.; Kiely, C. J.; Wells, P. P.; Dimitratos, N. *Catalysis, Structure & Reactivity* **2014**, *1*, 35–43.

(6) Kmetykó, C.; Mogyorósi, K.; Gerse, V.; Kónya, Z.; Pusztai, P.; Dombi, A.; Hernádi, K. *Materials* **2014**, *7*, 7022–7038.

(7) Al-Azri, Z. H.; Chen, W.T.; Chan, A.; Jovic, V.; Ina, T.; Idriss, H.; Waterhouse, G. I. *Journal of Catalysis* **2015**, *329*, 355–367.

(8) Priebe, J. B.; Radnik, J.; Lennox, A. J. J.; Pohl, M.-M.; Karnahl, M.; Hollmann, D.; Grabow, K.; Bentrup, U.; Junge, H.; Beller, M.; Brückner, A. *ACS Catalysis* **2015**, *5*, 2137–2148.

(9) Sakata, T. *Journal of Photochemistry* **1985**, *29*, 205–215.

(10) Patsoura, A.; Kondarides, D. I.; Verykios, X. E. *Catalysis Today* **2007**, *124*, 94–102.

(11) Sakata, T.; Kawai, T. *Chemical Physics Letters* **1981**, *80*, 341–344.

(12) Al-Mazroai, L. S.; Bowker, M.; Davies, P.; Dickinson, A.; Greaves, J.; James, D.; Millard, L. *Catalysis Today* **2007**, *122*, 46–50.

(13) Dickinson, A.; James, D.; Perkins, N.; Cassidy, T.; Bowker, M. *Journal of Molecular Catalysis A: Chemical* **1999**, *146*, 211–221.

(14) Nash, T. *Biochemical Journal* **1953**, *55*, 416–421.

(15) Jiang, Z.; Zhu, J.; Liu, D.; Wei, W.; Xie, J.; Chen, M. *CrystEngComm* **2014**, *16*, 2384.

(16) Gallo, A.; Marelli, M.; Psaro, R.; Gombac, V.; Montini, T.; Fornasiero, P.; Pievo, R.; Santo, V. D. *Green Chem.***2012**, *14*, 330–333.

(17) Bowker, M.; Morton, C.; Kennedy, J.; Bahruji, H.; Greves, J.; Jones, W.; Davies, P.; Brookes, C.; Wells, P.; Dimitratos, N. *Journal of Catalysis* **2014**, *310*, 10–15.

(18) Su, R.; Kesavan, L.; Jensen, M. M.; Tiruvalam, R.; He, Q.; Dimitratos, N.; Wendt, S.; Glasius, M.; Kiely, C. J.; Hutchings, G. J.; Besenbacher, F. *Chem. Commun.***2014**, *5*, 12612–12614.

(19) Kennedy, J.; Jones, W.; Morgan, D. J.; Bowker, M.; Lu, L.; Kiely, C. J.; Wells, P. P.; Dimitratos, N. *Catalysis, Structure & Reactivity* **2014**, *1*, 35–43.

(20) Ichou, I.; Formenti, M.; Teichner, S. *Catalysis on the Energy Scene Studies in Surface Science and Catalysis***1984**, *2*, 297–307.

(21) Melvin, A. A.; Illath, K.; Das, T.; Raja, T.; Bhattacharyya, S.; Gopinath, C. S. *Nanoscale* **2015**, *7*, 13477–13488.

(22) Gallo, A.; Marelli, M.; Psaro, R.; Gombac, V.; Montini, T.; Fornasiero, P.; Pievo, R.; Santo, V. D. *Green Chem* .**2012**, *14*, 330–333.

(23) Kim, A.-Y.; Kang, M. *International Journal of Photoenergy* 2012, *2012*, 1–9.

(24) Hammer, B.; Nørskov, J. *Surface Science* **1995**, *343*, 211–220

(25) Gallo, A.; Marelli, M.; Psaro, R.; Gombac, V.; Montini, T.; Fornasiero, P.; Pievo, R.; Santo, V. D. *Green Chem.* **2012**, *14*, 330–333.

(26) Gołąbiewska, A.; Lisowski, W.; Jarek, M.; Nowaczyk, G.; Zielińska-Jurek, A.; Zaleska, A. *Applied Surface Science* **2014**, *317*, 1131–1142.

Chapter 5

Hydrogen Production from *p*-Formaldehyde and CO_2 photoreduction with Ir/ $\gamma - Al_2O_3$

5. Introduction

Formaldehyde is quite often encountered in multiple natural and artificial decomposition pathways of organic matter. In the chemical industry, it is used as a raw material for various purposes.[1] In recent years, the possibility of using this molecule for hydrogen production has been actively pursued. Prechtl *et al* , showed that para-formaldehyde solutions in water (6.7 wt% per unit) may be a source of H_2 and CO_2 under mild conditions.[2] In fact, a theoretical efficiency of 8.4 wt % of H_2 is possible from the reaction of equimolar amount of H_2O with CH_2O, thus placing formaldehyde among the most attractive hydrogen storing systems. So far only three homogeneous catalysts, [IrIII(Cp*)(4-(1*H*-pyrazol-1-yl-kN^2)benzoic acid-kC^3)(H_2O)]$_2SO_4$), [(Ru(p-cymene))$_2$(μ-Cl)$_2$Cl$_2$] and $Na_4Fe(CN)_6$ have been found for formaldehyde dehydrogenation in the presence of water along with a few heterogeneous catalysts.[1,2,3]

Bi *et al* have studied the decomposition of formaldehyde in alkaline solutions into hydrogen and formic acid under room temperature and atmospheric pressure.[4] This reaction has some obvious advantages with respect the homogeneous transformation reported above. It generates pure hydrogen with a stable production rate, the reaction works with both high and low concentrations of formaldehyde and the catalyst is easily recovered by filtration. The main drawback is that these nanoparticles tend to agglomerate into larger particles and which reduce the

catalytic activity. Hence, there is a need to develop a simple and effective strategy to prevent agglomeration for example by loading small noble metal nanoparticles.[4,5]

In 2014, the same group also reported that by using the impregnation-reduction process the metallic Ag nanocrystals are dispersed on the high specific surface area of γ-Al_2O_3 and this process reduces the possibility of Ag nanoparticle agglomeration.[6] Accordingly, Ag supported γ-Al_2O_3 catalysts have higher catalytic performance compared with unsupported Ag nanoparticles. By optimizing the reaction conditions such as temperature, amount of catalyst, concentrations of $CH_2O$and NaOH, the hydrogen formation rate over has been maintained for multiple hours without sign of decay.[6]

Figure 5.1. illustrates the possible mechanism of hydrogen formation over Ag/γ-Al_2O_3 catalysts in alkaline solutions. The mechanism is divided into 2 steps: (1) hydration of formaldehyde in water to methanediol, and (2) Ag/γ-Al_2O_3 catalyzed transformation to hydrogen and sodium formate in alkaline conditions.

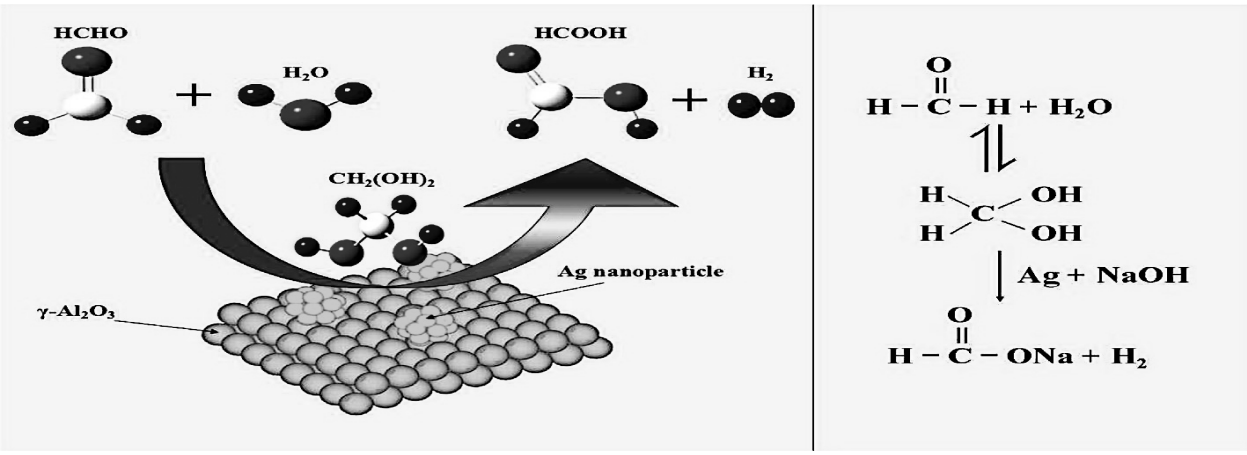

Figure 5.1. Schematic illustration of the hydrogen production from formaldehyde over Ag/ γ -Al_2O_3.[6]

The utilization of formaldehyde based systems as a true hydrogen storing system faces a major challenge. All the catalysts so far reported in the literature can produce hydrogen with good efficiency while affording CO_2, but the photo- or thermal reduction of carbon dioxide to restore the hydrogen storing molecules remain the limiting factor because of the high thermodynamic stability of CO_2. For this reason, it is important to selectively transform any of the intermediates of the oxidation of hydrocarbons or alcohols selectively to any intermediate product prior to CO_2. From this point of view, the Crabtree group has used several iridium catalysts to efficiently dehydrogenate methanol into formate, although some undesirable oxidation to carbonate is still observed.[7]

A novel and alternative way to take advantage of the versatility of formaldehyde for releasing hydrogen is to use it as an organic redox couple acting as a shuttling system during an overall water splitting catalytic cycle. In other words, one could dehydrogenate a hydrogen-rich molecule with an appropriate catalyst and form an oxidized species aside H_2 production. In a second step, and in the presence of the same or additional catalysts, the oxidized species may be deoxygenated and re-hydrogenated using water as hydrogen source. Overall this will complete an overall cycle of water splitting and regenerate the hydrogen-storing device.

To be successful, research in this direction should tackle selective and efficient dehydrogenation reactions of simple molecules (such as methanol or formaldehyde) to an oxidized species other than CO_2 (e.g. formic acid or formate). The hydrogenation reactions with water as the ultimate source of hydrogen may complete the cycle. This second step (also known as "reverse

combustion") is of course the most challenging. Other redox couples can also be considered for convenience reasons.

In our lab, we have previously shown that commercially available metal salts in alkaline solutions are very active for the selective formaldehyde dehydrogenation to formate (including iridium and ruthenium, among others). The benefit of these catalysts is the ability to work at room temperature without any external stimulus as the dehydrogenation is thermodynamically permissible.

In this line of thought, our lab has recently identified an inexpensive, light-switchable ferro-cyanide photo-catalyst for the selective dehydrogenation of *p*-formaldehyde to formate anion at room temperature.[3]

On a similar tune, the dehydrogenation of *p*-formaldehyde has been achieved with $IrCl_3$ as a homogenous catalyst while in alkaline conditions. This catalytic system was steadily producing hydrogen for over 1 year. Because of the high cost associated with Ir and the inconvenience of this homogenous catalyst to be recovered, there is an urgent need to transform the iridium homogeneous system into an heterogeneous one. This can possibly be achieved by doping or loading the iridium on semiconducting supports such as TiO_2 and Al_2O_3. Because Al_2O_3 supports have a large surface area it could effectively prevent metal nanoparticles agglomeration and can use the large contact area between catalyst and reactant to effectively enhance the catalytic activity for even more efficient hydrogen formation.[8,11] Also, the most important property of the iridium supported alumina as a heterogeneous catalyst is that the catalysts can be recovered by simple filtration.

5.1 Methodology

The list of chemicals which were used in these experiments is as follow: Paraformaldehyde, 37% formaldehyde solution was purchased from Sigma Aldrich, and γ -alumina supported catalyst (1% Ir/ γ-Al_2O_3) was purchased from Riogen. Sodium hydroxide was purchased from Sigma Aldrich. The reactions were performed in distilled water without any degassing and further purification. Iodine was purchased from Stream. Citric acid was purchased from Fisher Scientific. Sodium thiosulfate was purchased from Oakwood Chemicals. Acetic anhydride was purchased from VWR. Distilled water was used in all reactions.

5.2 Photoreactor Set-up

The experiments were carried out in a 250 ml Pyrex flask connected to a volumetric apparatus, and the standard amounts of catalyst (200 mg) Ir/ γ-Al_2O_3 was added a solution containing 33 mmol of *p*-FA and 150 mmol of NaOH. This solution was irradiated with a 400W Hg arc lamp and the gas phase sampled and analyzed every 10 minutes.

5.3 Analysis of Products

Hydrogen was collected in a volumetric apparatus and analyzed by GC. The concentration of methanol, identified by GC, was quantified by using a calibration curve. To determine the concentration of formate, a colorimetric procedure reported by Sleat and Mah was used.[10] 0.5 mL of the reaction mixture was added to 2 mL of 0.05% citric acid and 10% acetamide dissolved in a 1:1 mixture of isopropanol and water. 0.1 mL of 30% sodium acetate and 7 mL of acetic anhydride were added to test sample. The sample was mixed at room temperature and measured

spectrophotometrically at 510 nm. The concentration was determined using a standard calibration curve.

5.4 Results and Discussion

Dehydrogenation of *p*-formaldehyde via Ir/ γ-Al_2O_3 was performed under alkaline conditions. Several factors were examined to study their influence on the photocatalytic hydrogen production from formaldehyde.

The photocatalytic reactions were probed with and without Ir/ γ-Al_2O_3 catalyst. As shown in Figure 5.2, there is a very small amount of hydrogen formed during the blank reaction, whilst the addition of Ir/ γ-Al_2O_3 led to a substantial increase in hydrogen formation.

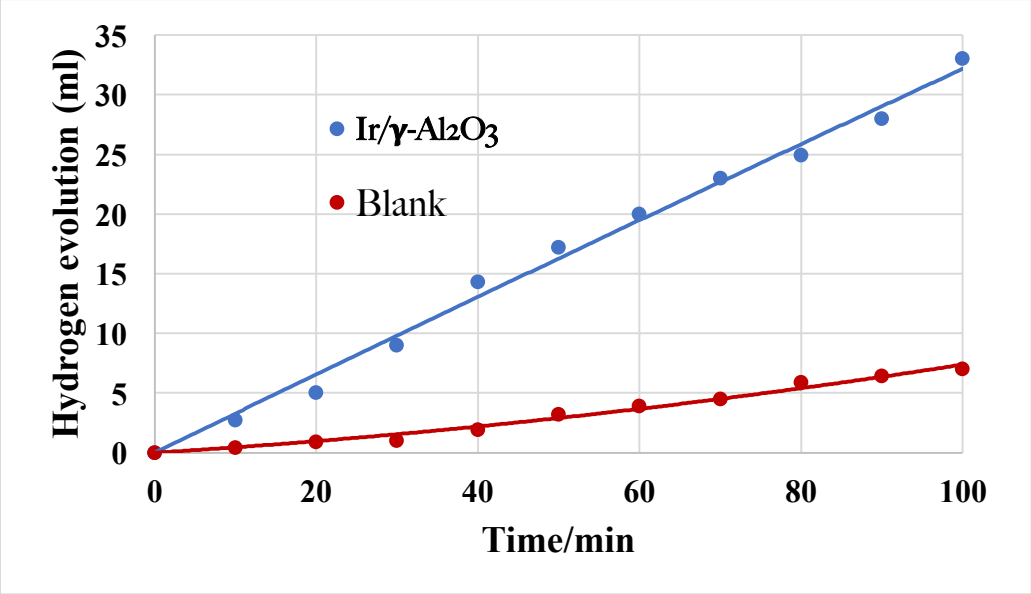

Figure 5.2. Hydrogen evolution from the dehydrogenation of p-formaldehyde/water mixture over Ir/ γ-Al_2O_3catalysts and with no catalysts (blank).

As a common problem with the usage of formaldehyde, when *p*-formaldehyde dissolves in 1M NaOH it is converted to methandiol. In turn, methanediol disproportionates into methanol and a formate anion, by the mechanism of the Cannizzaro reaction (equation 1). While consuming formaldehyde, the Cannizzaro reaction does not produce H_2 and is an unavoidable parasite process promoted by the alkaline conditions. Figure 5.3. shows the simultaneous formation of methanol and formate anion via the Cannizzaro reaction.

$$2\ CH_2O(l) + NaOH(aq) \rightarrow HCOONa\ (aq) + CH_3OH(l) \quad (1)$$

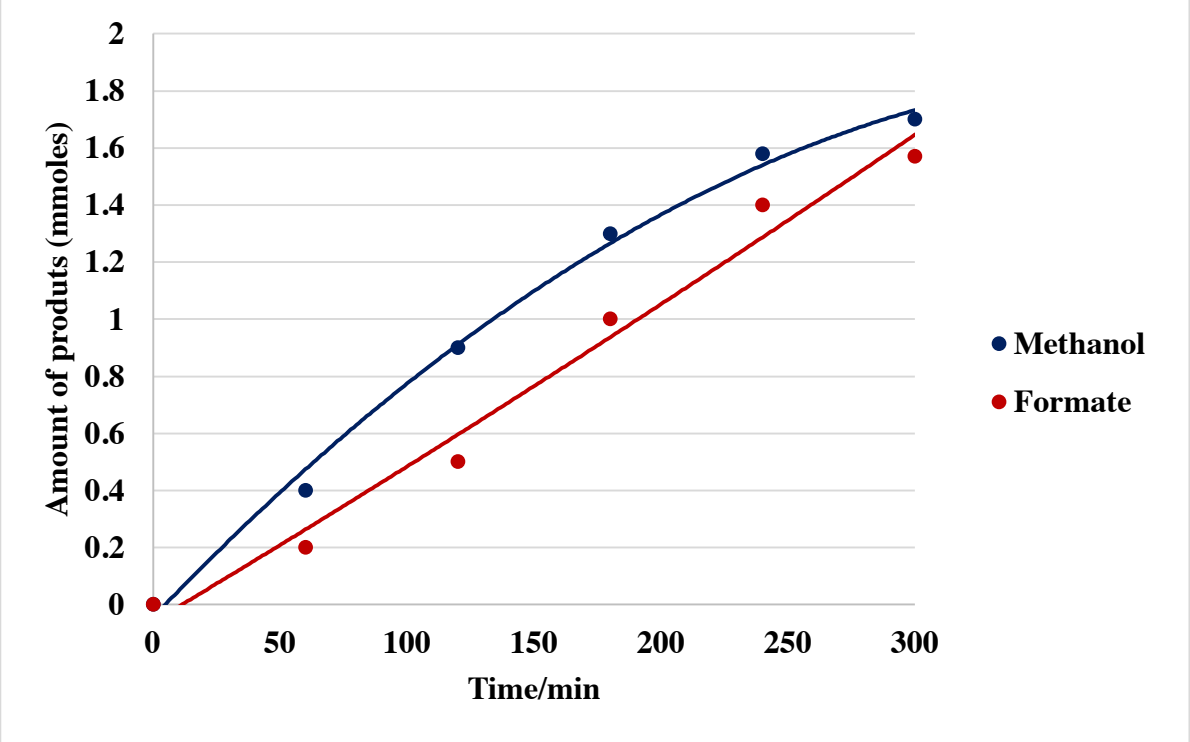

Figure 5.3. Cannizzaro reaction.

5.5 Study of the Influence of Parameters on the Dehydrogenation of *p* - formaldehyde over Ir/ γ-Al_2O_3

Among the different forms of alumina, γ-alumina (γ-Al_2O_3) is the most versatile for catalyst immobilization, having been used in many different applications such as hydrogenation and dehydrogenation of organic molecules.[11] The benefits of this catalyst can be ascribed to a favorable combination of crystalline properties such as surface area and pore volume, along with chemical, mechanical and thermal stability.[12] Transition metal-supported γ-Al_2O_3 have additional advantages such as allowing an easy recovery of precious metal and recycling of catalysts as well as providing a good distribution of active metals without sintering.[12]

Nanoparticles of Ir deposited over alumina, Ir/ γ-Al_2O_3, were used in this project to determine the activity of hydrogen production during the dehydrogenation of *p*-formaldehyde in alkaline solutions. Moreover, the effect of other variables such as NaOH concentration, formaldehyde concentrations, various amounts of Ir/ γ-Al_2O_3 catalyst, and different metal bases have been studied to determine their effects on the rate of hydrogen evolution.

5.5.1 Effects of NaOH concentration

Yingpu *et al* have studied the effect of NaOH on the rate of hydrogen production from *p*-formaldehyde solutions with Ag nanoparticles supported on γ-Al_2O_3.[5] The authors reported that the rate of hydrogen formation increases with increasing initial concentration of NaOH .[3,4].In the absence of NaOH, no hydrogen was formed, which means that NaOH is necessary for this reaction.[4,5] As shown, the volume of hydrogen increased from 4.7 ml to 68 ml when the concentration of NaOH changed from 0.25 M to 2.0 M. However, with increasing the

concentration of NaOH to 3 M, the rate of hydrogen production decreased to 45 ml. Therefore, a concentration of about 2M seems to be optimal.

The effect of NaOH concentrations on hydrogen production from *p*-formaldehyde over Ir/ γ-Al_2O_3has been examined and the result compared well to those of Ag/ γ-Al_2O_3 . With further increases in the concentration of NaOH, the amount of hydrogen decreased. This may be due to the competitive decomposition of formaldehyde through the Cannizzaro reaction (Figure 5.4.)

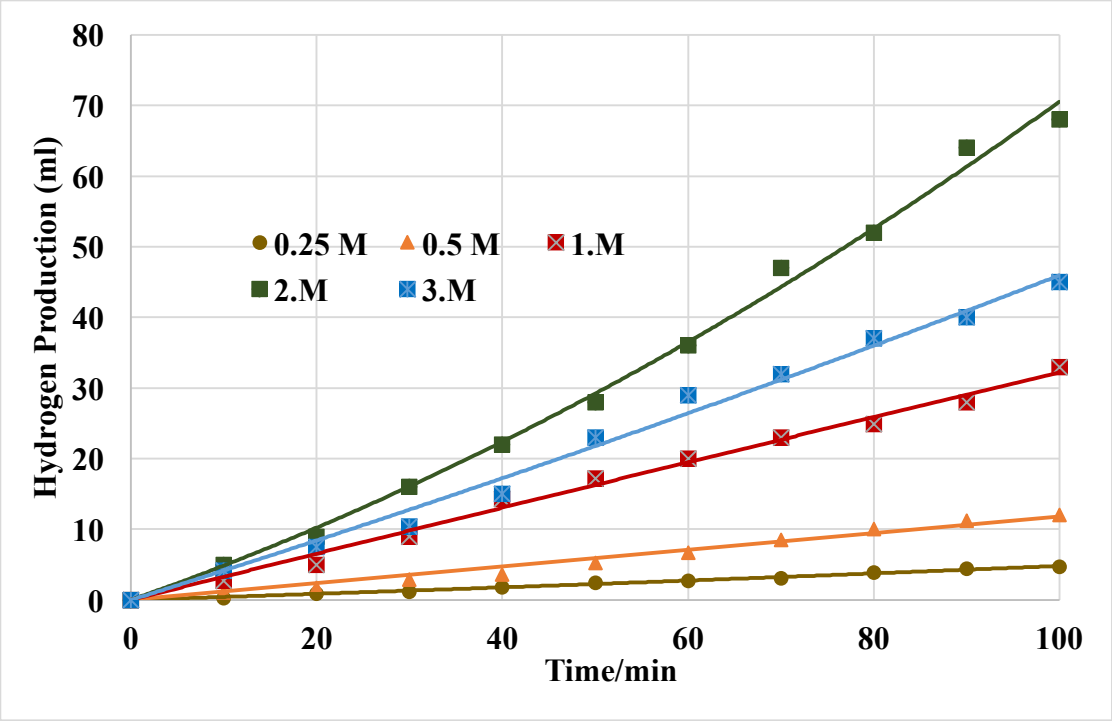

Figure 5.4. The effect of various NaOH concentrations on the volume of hydrogen evolution. Reaction conditions: Room Temperature, 1 g *p*-formaldehyde, 200 mg of Ir/ γ-Al_2O_3 catalysts.

5.5.2 Effects of HCHO concentration

The effect of different *p*-formaldehyde concentrations on hydrogen evolution over Ir/ γ-Al_2O_3 was investigated. The other parameters of these reactions were kept constant. Figure 5.5. indicates

that the rate of hydrogen production increased from 14 ml to 52 ml when the concentration of formaldehyde was changed from 16 mmol to 99 mmol. However, at higher loading of *p*-formaldehyde (115 mmol), the volume of hydrogen decreased to 46 ml. These results agreed with the observations of Yawen *et al.* and Yingp *et al.* [3,4] These authors outlined that the hydrogen volume decreased at higher concentration of formaldehyde (CH_2O) and sodium hydroxide (NaOH).

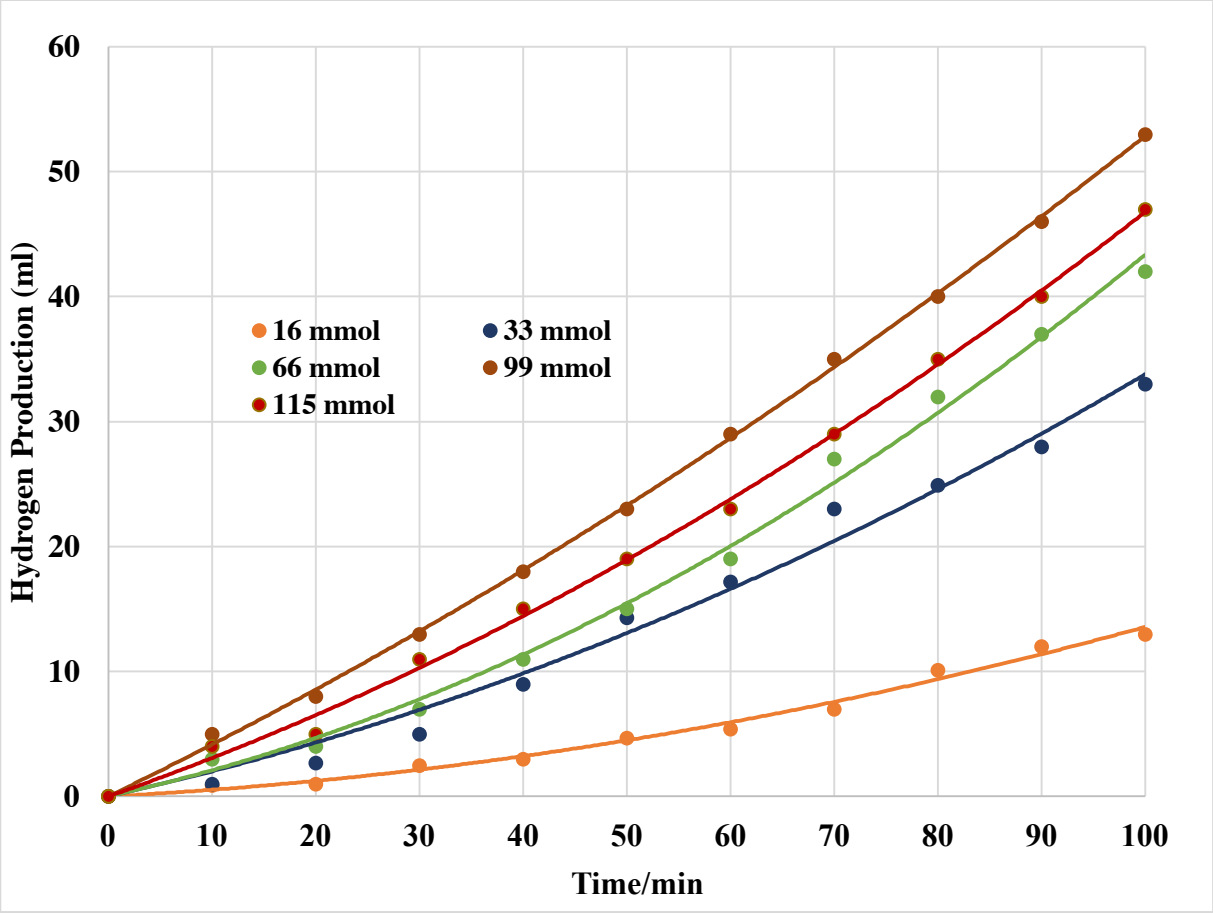

Figure 5.5. The effect of various CH_2O concentrations on the volume of hydrogen generation. Reaction conditions: RT, 150 mmol of NaOH, 200 mg of Ir/ γ-Al_2O_3.

5.5.3 Effects of different bases

The effect of using different bases such as KOH and $Ca(OH)_2$ instead of NaOH on the volume of hydrogen evolution from formaldehyde via Ir/ γ-Al_2O_3 was investigated. The reactions were performed with constant parameters. The results of these reactions are displayed in Figure 5.6. The highest rate of hydrogen production was obtained with NaOH. When $Ca(OH)_2$ is used as a base, no hydrogen was formed.

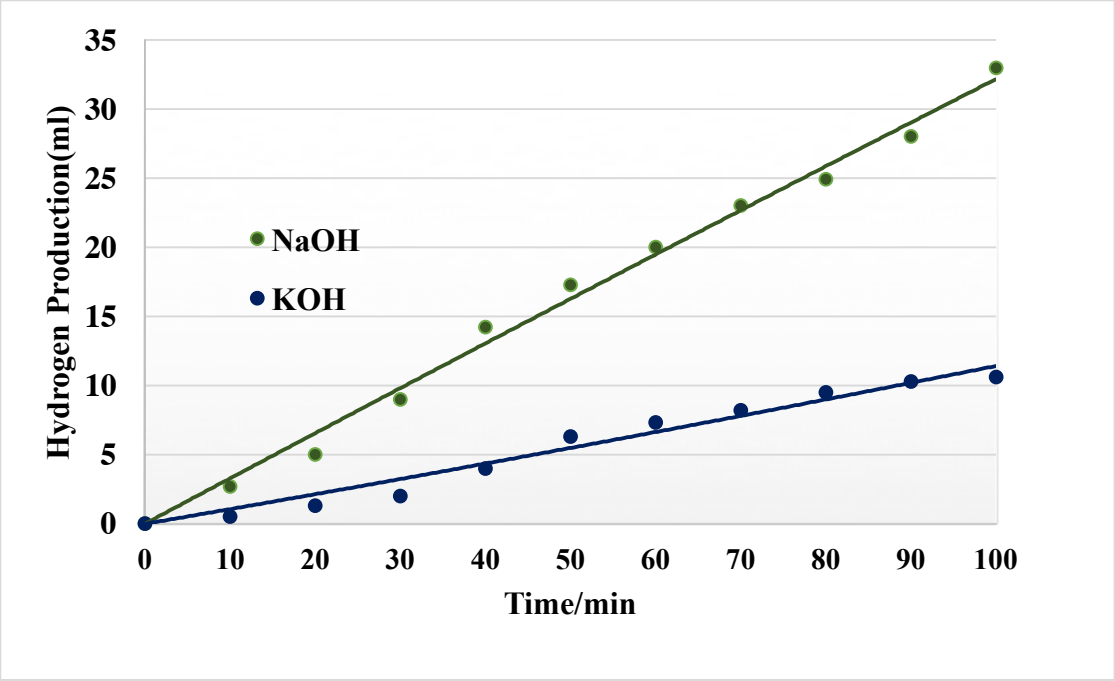

Figure 5.6. The effect of different bases on the rate of hydrogen formation. Reaction condition: RT, 150 mmol of base, 33mmol of CH_2O, 200 mg of Ir/ $\gamma - Al_2O_3$.

5.6 Photoreduction of CO_2 to Hydrocarbon Products

The most promising method to reduce CO_2 to fuels (hydrocarbons) is the use of photocatalysts in the presence of water as an electron source.[14] Recently, many semiconductor-based

photocatalystssuch as TiO_2, ZnO, ZrO_2, Fe_2O_3, WO_3, SnO_2 have been studied for the photocatalytic reduction of CO_2 and oxidation H_2O.[15,16,17,18] Table 5.1. lists the most popular photocatalysts

Table 5.1. Heterogeneous catalysts for photoreduction of CO_2 with water.

Photocatalysts	**Radiation Source**	**Major Products**	**Reference**
0.5 wt % Cu/TiO_2-SiO_2	Xe lamp (2.4 mW cm^{-2}, 250–400 nm)	CO and CH_4	19
$ZnGa_2O_4$	300 W Xe arc lamp	CH_4	20
Ag/$ALa_4Ti_4O_{15}$ (A = Ca, Ba and Sr)	400 W Hg lamp	CO, HCOOH, and H_2	21
I-TiO_2 nanoparticles	450 W Xe lamp	CO	22
$LiNbO_3$	Natural sunlight or Hg lamp (64.2 mW cm^{-2})	HCOOH	23
$Zn_{1.7}GeN_{1.8}O$	300 W Xe arc lamp	CH_4	24
Pt-TiO_2 thin nanostructured films	400 W Xe lamp	CO and CH_4	25
ZnO-based materials	8 W fluorescent tube (average intensity 7 mW cm^{-2})	CO, CH_4, CH_3OH, H_2	26
Pt/Cu/TiO_2	500 W Xe lamp	CH_4, CO	27

Ying *et al* have investigated a catalytic system based on Cu deposited on SiO_2 support.[19] This system displays an enhanced activity for photoreduction of carbon dioxide.[19] The major products

obtained of the photoreduction were CO and CH_4 with a Cu loading of 0.5 wt% determined to be the optimum.

Zhi *et al* have reported a new route for synthesizing mesoporous ZnGa2O_4 at room temperature, consisting of an ion-exchange process with a porous $NaGaO_2$ colloidal template as a precursor.[20] The pathway is generally versatile for synthesizing porous AB_2O_4-type materials. By using RuO_2 as co-catalysts, the mesoporous $ZnGa_2O_4$ shows good photocatalytic enhancement for reducing CO_2 into CH_4 under light irradiation due to strong gas adsorption and large specific surface area of the $ZnGa_2O_4$ photocatalyst.[20]

In 2011, Kudo *et al*. demonstrated that the BaLa4Ti_4O_{15} showed high photo-catalytic activity for CO_2 reduction with water as a hydrogen and electron donor.[21] Ag was the most active co-catalyst. The photocatalytic activity of catalyst was affected by the loading method of Ag. The liquid-phase chemical reduction was the most suitable method to load Ag particles on the surface of the $BaLa_4Ti_4O_{15}$ support. CO evolved on the Ag located at the edge of the lamellar particles of $BaLa_4Ti4O_{15}$.

In addition, Ying and co-workers have reported high photocatalytic activity for CO_2 photoreduction may be obtained over I-doped TiO_2 under visible light irradiation.[22] The efficiency of the reaction was greater than for non-doped TiO_2 due to the absorption of TiO_2 in the visible light region, facilitating charge recombination.

Dunn *et al.* have studied the photoreduction of CO_2 over $LiNbO_3$, and reported that this ferroelectric material is capable of reducing carbon dioxide to formaldehyde and formic acid.[23]

The use of a ferroelectric material for photo catalysis gives an interesting alternative to the standard semi-conducting materials. The enhancement in catalytic activity is due to inherent properties of the ferroelectric material such as spontaneous polarization.[23]

Zou *et al* have obtained 3D hierarchical architectures of Zn_2GeO_4 composed of closely packed nanorods, generated by the split crystal growth mechanism.[24] Nitridation of this material gave superstructures of a yellow $Zn_{1.7}$ GeN $_{1.8}$ O solid. When $Zn_{1.7}$ GeN $_{1.8}$ O was loaded with co-catalysts, higher conversion rate of CO_2 into CH_4 was obtained.

In 2012 Biswas and co-workers developed Pt-TiO_2 nanostructured films using versatile gas-phase synthesis which can be enlarged to industrial scale.[25] The Pt- TiO_2 films showed a good catalytic activity for photoreduction of CO to form of CH_4.[25] The high surface area and the properties of the 1D structure of the films and the efficient electron−hole recombination by the Pt NPs were considered as the main reasons for the good activity.

Serrano *et al.* have synthesized a variety of N- and Cu-modified ZnO photocatalysts for photoreduction of CO_2 with water under UV irradiation.[26] The authors indicated that N-doping ZnO did not show any important effect on the photocatalytic behavior of ZnO-based photocatalysts. The ZnO favored CO and H_2 production, but catalysts with Cu showed a good activity for CH_3OH production.

Wang *et al.* have prepared a core–shell-structured Pt-Cu_2O co-catalyst which promotes the photo-catalytic conversion of CO_2 with H_2O to CH_4 and CO.[27] It was proposed that the Cu_2O shell provides sites for activation and conversion of CO_2 in the presence of water, while the Pt core extracts the photogenerated electrons from TiO_2. The deposition of a Cu_2O shell on Pt enhances the reduction of H_2O to H_2, a competitive reaction with the reduction of CO_2.

A common major challenge in these studies is that most of photocatalysts are not active in visible light. As explained before, after absorbing light photo-generated holes in the VB of the photocatalyst oxidize H_2O. In addition, the photo-generated electrons in its CB forms products such as formic acid, formaldehyde and methanol by reducing carbon dioxide. The relation between the energy levels of the photocatalyst and the redox agent determines the type of reaction that takes place .[28] Figure 5.7. illustrates the conduction band and valence band potentials, and band gap energies of different semiconductor photocatalysts relative to the redox potentials of compounds involved in CO_2 reduction.[28]

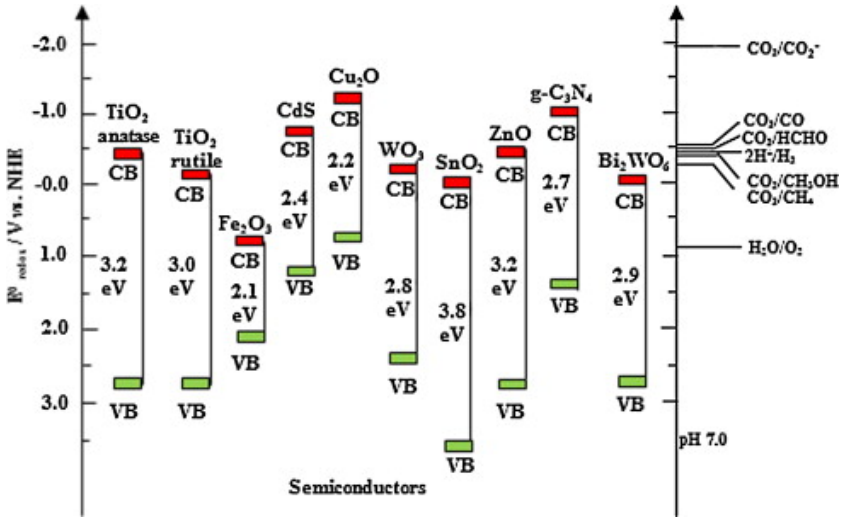

Figure 5.7. Conduction band and valence band potentials, and band gap energies of different semiconductor photocatalystss relative to the redox potentials of compounds involved in CO_2 photoreduction.[28]

Modified TiO_2 has been shown to be a promising candidate for hydrogen production and photoreduction of carbon dioxide because of the positive and negative redox potentials in the VB and CB, respectively. [29,30] In addition, alumina supported transition metals such as Ru, Ni have

been demonstrated to provide good heterogeneous catalyst for hydrogenating CO_2 to methanol. The authors of these studies have reported a diverse range of products formed from the photoreduction of CO_2, such as methane, methanol, carbon monoxide, methyl formate, formic acid, ethylene, ethanol and formaldehyde .[31,32]

The mechanism of photoreduction of CO_2 on the surface of photocatalysts varies from catalyst to catalyst. Equations 5-1 – 5-10 illustrate the pathway of CO_2 reduction over semiconducting materials. [33,34]

Oxidation of H_2O

$$SC \xrightarrow{hv < Eg} SC\,(h^+_{vb} + e^-_{cb}) \qquad 5\text{-}1$$

$$H_2O + h^+_{vb} \longrightarrow H_2O^+ \longrightarrow OH^{\cdot} + H^+ \qquad 5\text{-}2$$

$$OH^{\cdot} + OH^{\cdot} \longrightarrow H_2O + \tfrac{1}{2}\,O_2 \qquad 5\text{-}3$$

$$2H^+ + e^-_{cb} \longrightarrow H^{\cdot} + H^{\cdot} \longrightarrow H_2 \qquad 5\text{-}4$$

Photoreduction of CO_2

$$CO_2 + e^- \longrightarrow CO_2^- \qquad 5\text{-}5$$

$$CO_2 + 2H^+ + 2\,e^- \longrightarrow HCOOH \qquad 5\text{-}6$$

$$CO_2 + 2H^+ + 2\,e^- \longrightarrow CO + H_2O \qquad 5\text{-}7$$

$$CO_2 + 2H^+ + 4\,e^- \longrightarrow HCHO + H_2O \qquad 5\text{-}8$$

$$CO_2 + 2H^+ + 6\,e^- \longrightarrow CH_3OH + H_2O \qquad 5\text{-}9$$

$$CO_2 + 2H^+ + 8\,e^- \longrightarrow CH_4 + H_2O \qquad 5\text{-}10$$

5.7 Photocatalytic Reduction of Carbon Dioxide

We have studied the photoreduction of CO_2 in the presence of water using two different photocatalysts, Au/TiO_2 and $Ir/y\text{-}Al_2O_3$. Catalyst testing was performed with 400 W Hg lamp irradiation in quartz round bottom flasks in the presence of 1.0 M NaOH and 200 mg of catalyst. CO_2 was purged into photoreactor for 30 minutes. Samples were taken every hour, with the products analyzed by GC. The results indicated that Au supported TiO_2 is inactive for reducing CO_2 since only small quantity of sodium formate was formed. However, when the reaction was performed with $Ir/\gamma\text{-}Al_2O_3$ under UV irradiation, carbon dioxide was reduced to methanol. The amount of methanol produced as a function of time is presented in Figure 5.8. As shown, there is an increase in the amount of methanol followed by a sharp decrease. While formate was also formed, no other compounds such as methane or ethanol could be detected. In this reaction, a $HCOO^-$ intermediate is initially formed via transfer of a hydrogen atom from one molecule of water to carbon dioxide. Further hydrogen transfer leads to the formation of methanol.

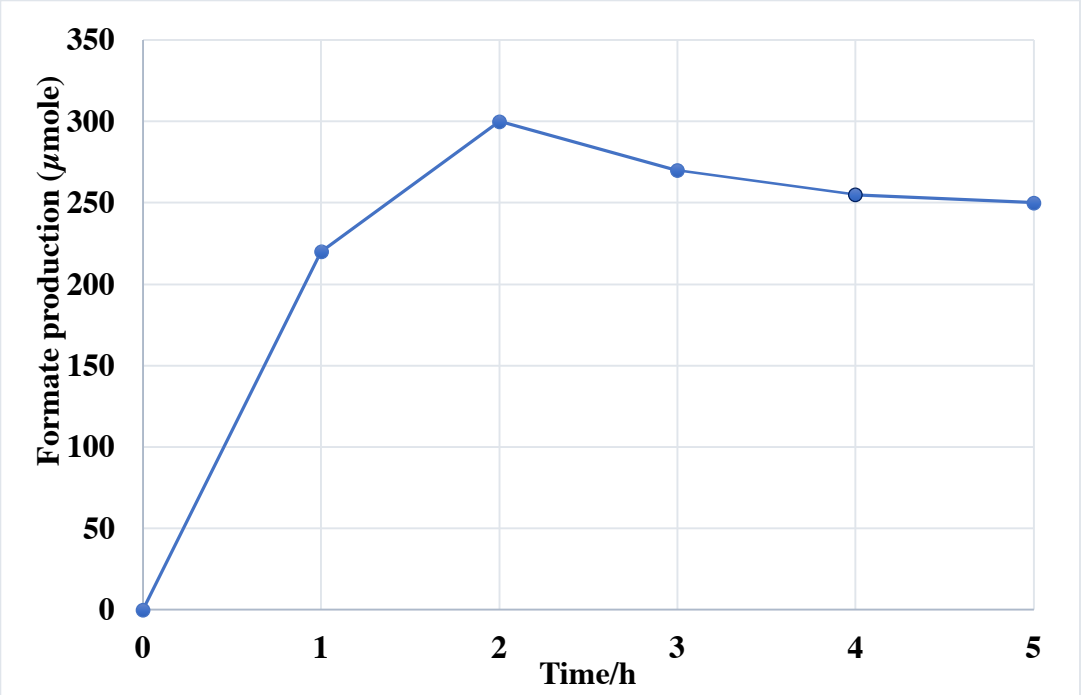

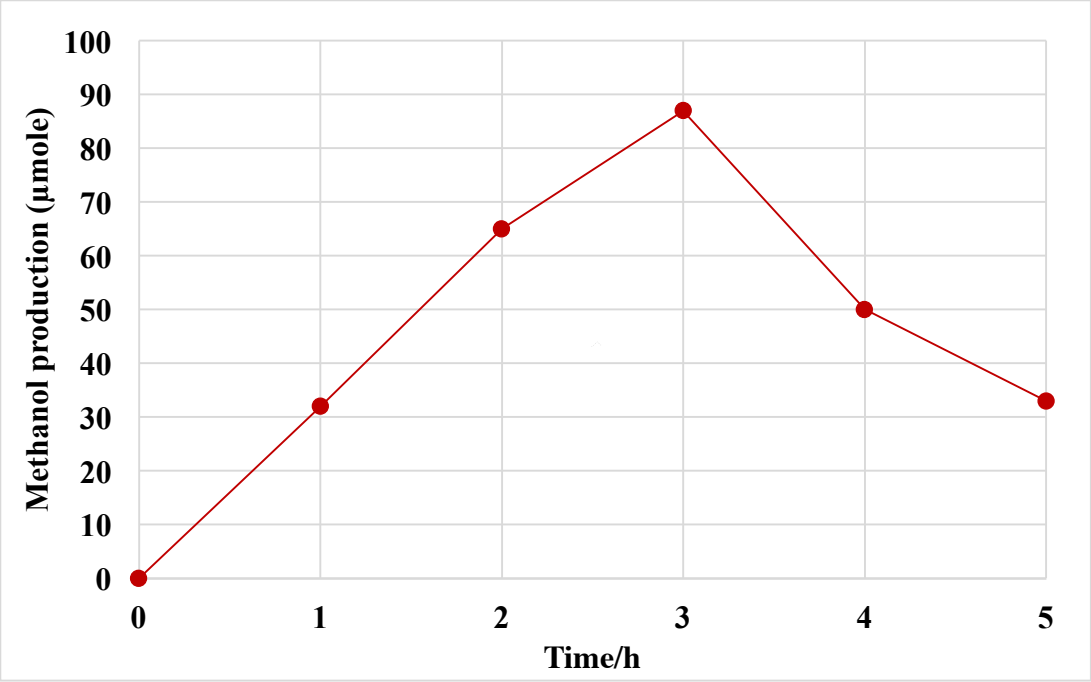

Figure 5.8. Methanol and formate formation from photocatalytic reduction of carbon dioxide and water over Ir/ γ −Al_2O_3.

5.8 Deactivation and Reactivation of Ir/ γ −Al_2O_3 Catalyst

The observed deactivation of the photocatalyst after five hours of reaction may be caused by the blocking of active sites, thus preventing further photocatalytic reaction. One possible reason is the saturation of the active sites with intermediate complex mixture formation. When the catalysts were observed to be deactivating, it was filtered, washed and dried in air at 60 ℃ for 24 h. After that, the catalyst once more afforded photoreduction of carbon dioxide with water forming both formate and methanol, albeit in lower quantity Figure 5.9.

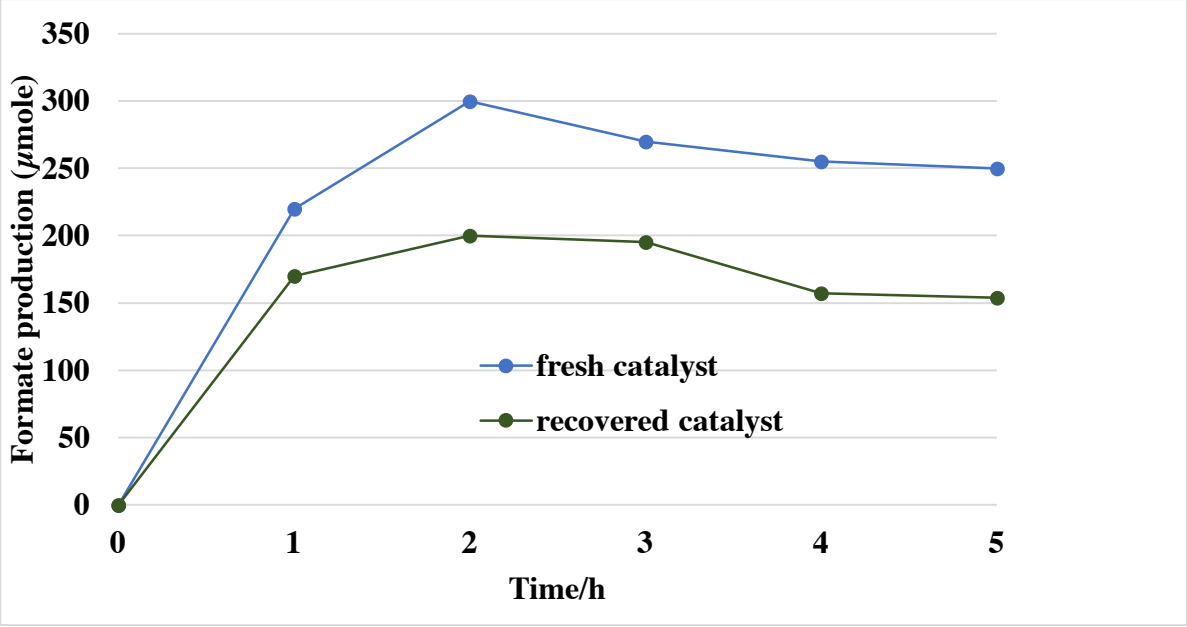

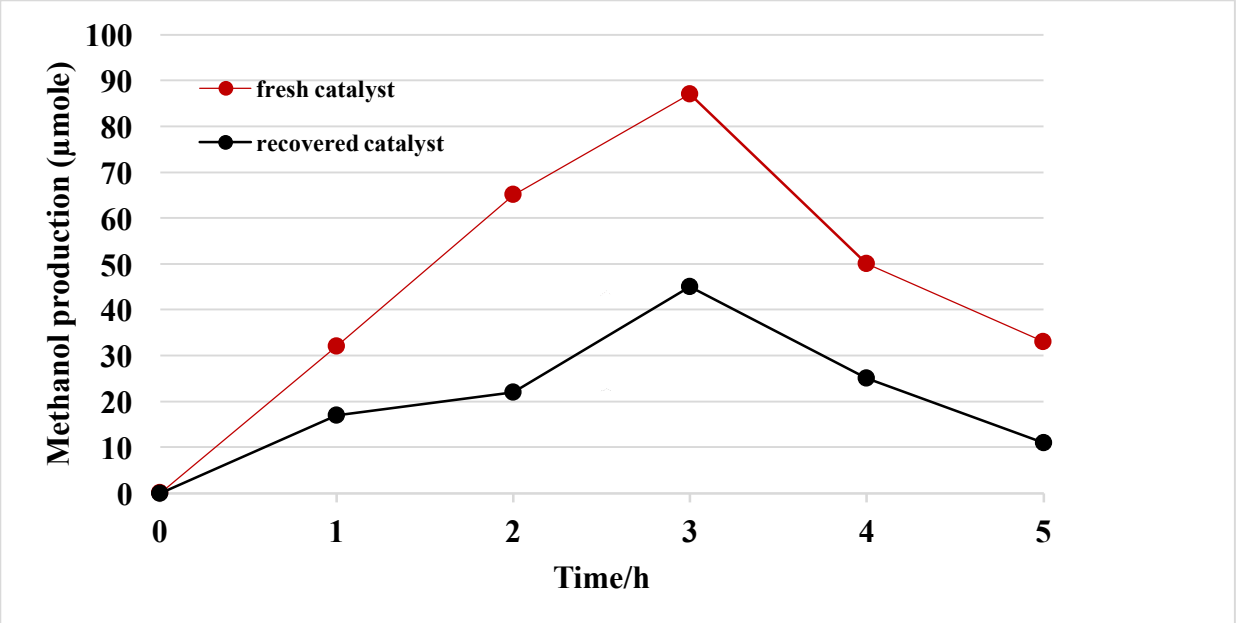

Figure 5. 9. Methanol and formate formation from photocatalytic reduction of carbon dioxide and water over recovery Ir/ γ −Al_2O_3 compare to fresh catalyst fresh Ir/ γ −Al_2O_3

5.9 Conclusion

In this chapter, the dehydrogenation of *p*-formaldehyde with γ −Al_2O_3 supported photocatalysts at room temperature and atmospheric pressure was studied. We found that Ir/ γ −Al_2O_3 catalysts display good catalytic activity for hydrogen production without deactivation.

The effects of different reaction conditions such as NaOH and CH_2O concentrations on the volume of hydrogen formed were analyzed. In addition, we have also observed an unprecedented photoreduction of CO_2 with H_2O towards hydrocarbon products. The results are summarized as follows:

- The rate of hydrogen evolution increased with increasing concentration of NaOH. After the concentration of NaOH was increased above 2 M, the rate of hydrogen decreased due to the competition with the Cannizzaro reaction.
- An increased amount of CH_2O also determines an increase of the volume of hydrogen evolution.
- KOH also was studied as a base to investigate its effects on the hydrogen production. The result showed that the NaOH was more effective than KOH in terms of hydrogen production
- $Ir/\gamma-Al_2O_3$ reduces CO_2 to methanol via intermediate formation of sodium formate.
- The deactivation and recovery of $Ir/\gamma-Al_2O_3$ was studied. Partial saturation of the active sites by adsorption of the by-products might be the main possible causes of deactivation.

5.10 References

(1) Suenobu, T.; Isaka, Y.; Shibata, S.; Fukuzumi, S. *Chem. Commun.*2015, *51*, 1670–1672.

(2) Heim, L. E.; Schlörer, N. E.; Choi, J.-H.; Prechtl, M. H. G. *Nature Communications* **2014**, *5*, 3621.

(3) Alderman, N. P.; Sommers, J. M.; Viasus, C. J.; Wang, C. H. T.; Peneau, V.; Gambarotta, S.; Vidjayacoumar, B.; Al-Bahily, K. A. *Dalton Transactions* **2017**, *46*, 49–54.

(4) Bi, Y.; Lu, G. *International Journal of Hydrogen Energy* **2008**, *33*, 2225–2232.

(5) Bojer, C.; Schöbel, J.; Martin, T.; Lunkenbein, T.; Wagner, D. R.; Greiner, A.; Breu, J.; Schmalz, H. *Polymer* **2017**, *128*, 65–70.

(6) Bi, Y.; Hu, H.; Li, Q.; Lu, G. *International Journal of Hydrogen Energy* **2010**, *35*, 7177–7182.

(7) Hu, H.; Jiao, Z.; Ye, J.; Lu, G.; Bi, Y. *Nano Energy* **2014**, *8*, 103–109.

(8) Sánchez, E. A.; Dangelo, M. A.; Comelli, R. A. *International Journal of Hydrogen Energy***2010**, *35*, 5902–5907.

(9) Peris, E.; Crabtree, R. H. *Iridium Complexes in Organic Synthesis* **2014***, 2,* 39–54.

(10) Cooley, R. B.; Dubbels, B. L.; Sayavedra-Soto, L. A.; Bottomley, P. J.; Arp, D. J. *Microbiology* **2009**, *155*, 2086–2096.

(11) Sleat, R.; Mah, R. a. *Appl. Environ. Microbiol***1984**, *47*, 884–885.

(12) Trueba, M.; Trasatti, S. P. *ChemInform* **2005**, *36*, 44-49

(13) Roy, S. C.; Varghese, O. K.; Paulose, M.; Grimes, C. A. *ACS Nano***2010**, *4*, 1259–1278.

(14) Wang, W.-N. *Aerosol and Air Quality Research* **2014**, *14*, 533-549

(15) Kumar, S. G.; Devi, L. G. *The Journal of Physical Chemistry A* **2011**, *115*, 13211–13241.

(16) Anpo, M. *Journal of CO2 Utilization* **2013**, *1*, 8–17.

(17) Kwak, B. S.; Kang, M. *Applied Surface Science* **2015**, *337*, 138–144.

(18) Nahar, S.; Zain, M.; Kadhum, A.; Hasan, H.; Hasan, M. *Materials* **2017**, *10*, 629.

(19) Li, Y.; Wang, W.-N.; Zhan, Z.; Woo, M.-H.; Wu, C.-Y.; Biswas, P. *Applied Catalysis B: Environmental* **2010**, *100*, 386–392.

(20) Yan, S. E. C.; Ouyang, S. X.; Gao, J.; Yang, M.; Feng, J. Y.; Fan, X. X.; Wan, L. J.; Li, Z.S.;Ye, J. H.; Zhou, Y.; Zou, Z. G. *Angewandte Chemie International Edition* **2010**, *49*, 6400–6404.

(21) Iizuka, K.; Wato, T.; Miseki, Y.; Saito, K.; Kudo, A. *Journal of the American Chemical Society* **2011**, *133*, 20863–20868.

(22) Zhang, Q.; Li, Y.; Ackerman, E. A.; Gajdardziska-Josifovska, M.; Li, H. *Applied Catalysis A: Genera* **2011**, *400*, 195–202.

(23) Stock, M.; Dunn, S. *Ferroelectrics***2011**, *419*(1), 9–13.

(24) Liu, Q.; Zhou, Y.; Tian, Z.; Chen, X.; Gao, J.; Zou, Z. *J. Mater. Chem.***2012**, *22*, 2033–2038.

(25) Wang, W.-N.; An, W.-J.; Ramalingam, B.; Mukherjee, S.; Niedzwiedzki, D. M.; Gangopadhyay, S.; Biswas, P. *Journal of the American Chemical Society* **2012,** *134*, 11276–11281.

(26) Núñez, J.; Víctor A. De La Peña Oshea; Jana, P.; Coronado, J. M.; Serrano, D. P. *Catalysis Today* **2013**, *209*, 21–27.

(27) Zhai, Q.; Xie, S.; Fan, W.; Zhang, Q.; Wang, Y.; Deng, W.; Wang, Y. *Angewandte Chemie* **2014,** *125*, 5888–5891.

(28) Xie, S.; Zhang, Q.; Liu, G.; Wang, Y. *ChemInform* **2016**, *47*(8).

(29) Gupta, S. M.; Tripathi, M. *Chinese Science Bulletin* **2011**, *56*, 1639–1657.

(30) Taziwa, R.; Meyer, E. *Pyrolysis***2017**.

(31) Kwak, J. H.; Kovarik, L.; Szanyi, J. *ACS Catalysis***2013**, *3*, 2449–2455.

(32) Garbarino, G.; Riani, P.; Magistri, L.; Busca, G. *International Journal of Hydrogen Energy* **2014**, *39*, 11557–11565.

(33) Yahaya, A.; Gondal, M.; Hameed, A. *Chemical Physics Letters* **2004**, *400*, 206–212.

(34) Maza, W. A.; Morris, A. J.; Mul, G. *Green Chemistry Series Green Photo-active Nanomaterials* **2015***, 1,* 202–239.

Chapter 6

Conclusions and Future work

6.1 Review of the project

The goal of this work was twofold as reflecting in the two main sections of this work: 1) the photocatalytic hydrogen production from water with different sacrificial reagents (methanol, isopropanol) by using various metals loaded on titanium dioxide and from p-formaldehyde with Au and $Ir/\gamma - Al_2O_3$. 2) The second part is a study on the photoreaction of carbon dioxide coupled with water oxidation over $Ir/\gamma - Al_2O_3$.

The photocatalytic dehydrogenation of methanol and isopropanol was obtained with metals supported on TiO_2 under UV light irradiation. In the case of methanol, the products were hydrogen, carbon dioxide and formaldehyde while hydrogen and acetone were obtained while using isopropanol. The rate of hydrogen production depends on several factors such as loading of metal, the type of titanium dioxide supports, concentrations of sacrificial reagents, preparation method of catalysts, loading of catalysts and types of metals.

In all reactions, Au supported TiO_2 synthesized by deposition precipitation with urea showed a greater activity compared to other metals. It was found that the amount of hydrogen produced over 4 wt. % Au/TiO_2 increased with increasing concentration of methanol. Mild alkaline conditions with 4 wt.% Au supported TiO_2 were found to be optimal for photocatalytic hydrogen production. In all reactions, hydrogen is released as a result of the dehydrogenation of alcohols.

When methanol is replaced by isopropanol, hydrogen and acetone are the only products detected. The hydrogen production was very low compared to that formed from the methanol / water mixture.

Mono and bimetallic transition metals supported on TiO_2 synthesized by sol immobilization were also tested. Bimetallic catalysts were found to have better activity when compared to monometallic catalysts. Au-Pt / TiO_2 shows the best activity for hydrogen production compared to Au-Ag / TiO_2.

In the second part of this thesis, photocatalytic production of hydrogen from *p*-formaldehyde in alkaline solutions using Ir/ $\gamma - Al_2O_3$ was investigated. The results show that Ir/ $\gamma - Al_2O_3$ has good activity for hydrogen production. In addition, $Ir/\gamma - Al_2O_3$ showed a good catalytic activity for CO2 reductionto methanol, while Au/TiO_2 was inactive.

6.2 Future work

- Various parameters were investigated which could affect the photocatalytic activity of 4 wt.% Au/TiO_2 catalysts for hydrogen production from alcohols/water mixtures. These effects include weight of metal loading, concentration of alcohols and TiO_2 structures. However, the impact of calcination temperature of catalysts and of particle size at a constant weight may also affect the activity of hydrogen production from water/alcohols mixtures. Further work is required to understand the mechanism of catalyst deactivation.
- Bimetallic noble metal supported TiO_2 materials need additional study to understand the mechanism of the reaction.
- The catalytic activity of Ir/ γ-Al_2O_3 should be further studied to understand the catalytic mechanism for both the hydrogenation and dehydrogenation reaction.

- In the deactivation process it is not yet clear which factors are responsible. Therefore, more work is recommended.